



universität
wien

DISSERTATION

Structural investigation of titin – α -actinin interactions in the
Z-disk context

Verfasser

Viktor Deineko

angestrebter akademischer Grad

Doctor of Philosophy (Ph.D.)

Wien, 2013

Studienkennzahl lt. Studienblatt: A 794 685 490

Dissertationsgebiet lt. Studienblatt: Molekulare Biologie

Betreut von: Dipl.Ing. Dr. Kristina Djinovic-Carugo



All the world is a very narrow bridge, and the most important thing is not to fear at all.

Reb Nachman of Breslov

Criticising others, giving them an unwelcome feeling, can be done by anyone. Uplifting them and giving them a good feeling - that takes a special gift and spending effort.

Reb Nachman of Breslov

A Jewish person needs to always look at the wisdom within everything in order that it will enlighten him so that he can come close to G-d through each thing. Because this wisdom is a great light and it will enlighten all his ways.

Reb Nachman of Breslov

Table of contents

ABSTRACT	vii
ZUSAMMENFASSUNG	xi
LIST OF ABBREVIATIONS.....	xv
1 INTRODUCTION.....	1
1.1 Types of muscles in the human body. Histological structure of muscle tissue	1
1.2 Sarcomere and its principal components	4
1.3 An outline of muscle contraction mechanism.....	6
1.4 Z-disk and its structure and function in the sarcomere.....	8
1.5 An overview of the Z-disk proteome	11
1.6 Domain composition of α-actinin	18
1.7 Domain composition of titin	23
1.8 The interaction between titin and α-actinin and its regulation by PiP2....	25
2 AIMS OF THE THESIS.....	33
3 MATERIALS AND METHODS	35
3.1 Chemicals.....	35
3.2 Kits	35
3.3 Enzymes	36
3.4 Molecular markers and other reagents.....	36
3.5 Buffers and stock solutions.....	36
3.6 Antibiotics.....	39
3.7 Bacterial growth media	40
3.8 Expression plasmids.....	44
3.9 <i>E.coli</i> strains and theirs genotypes.....	45

3.10	Electrophoresis and enzymatic manipulation of DNA	45
3.11	DNA sequencing	46
3.12	Coding DNA sequence of human titin Z-repeats.....	47
3.13	Translation of cDNA sequence of human titin Z-repeats	47
3.14	The list of primers	48
3.15	Preparation of the chemically competent <i>E.coli</i> cells.....	52
3.16	Transformation of the chemically competent <i>E.coli</i> cells	52
3.17	Protein overexpression in <i>E.coli</i>	52
3.18	Size-exclusion chromatography/analytical size-exclusion chromatography	54
3.19	Protein identification.....	54
3.20	Protein electrophoresis	54
3.20.1	Protein electrophoresis equipment.....	54
3.20.2	SDS-PAGE (gradient gel, 4%-20%).....	55
3.20.3	SDS-PAGE (Tris-Tricine)	55
3.20.4	Native-PAGE	56
3.20.5	Protocol for staining gels with “safe-stain”	57
3.20.6	Protocol for silver staining of the gels	58
3.21	Concentration of the purified proteins	59
3.22	Storage of the purified proteins.....	59
3.23	Protein dialysis	60
3.24	Measurements of protein concentration.....	60
3.25	Routine calculation of protein parameters	60
3.26	Static light scattering.....	61
3.27	Circular dichroism measurements.....	61
3.28	Analytical ultracentrifugation	62
3.29	Protein crystallization experiments.....	63

3.30 Small angle X-ray scattering (SAXS).....	63
4 RESULTS AND DISCUSSION	65
4.1 Gene amplification and protein constructs	65
4.2 Protein over-expression.....	66
4.3 Co-transformation/co-expression experiments	67
4.4 Recombinant protein purification	68
4.5 Size-exclusion chromatography and static light scattering experiments.....	76
4.6 Far-UV circular dichroism spectroscopy of titin Z-repeats and α -actinin EF-hands	80
4.7 The complex of α -actinin Δ and Zr.1-2-3	84
4.8 Characterization of titin/ α -actinin complexe by small angle X-ray scattering	87
4.9 Reconstruction of complexes of α -actinin and myopalladin	91
5 CONCLUSIONS AND FUTURE PERSPECTIVES.....	95
REFERENCES	101
CURRICULUM VITAE.....	123

Acknowledgements

I would like to acknowledge Dr. Matthias Wilmanns for recruiting me in frame of EMBL International PhD program to perform research in his group during 42 months.

I would like to sincerely acknowledge prof. Dr. Kristina Djinović-Carugo (Max Perutz Laboratories, University of Vienna) for supervision and support during my studies.

I would like to acknowledge Dr. Gerlinde Aschauer (University of Vienna) for her kind assistance in document preparation for university registration and thesis defense.

I would like to express my gratitude to Dr. Dmitri Svergun and Dr. Petr Konarev for their support during SAXS experiments.

I would like to express my cordial gratitude to following people from EMBL-Hamburg who provided assistance and advice during preparation of the thesis manuscript: Dr. Arjen Jakobi, Dr. Eike Schulz, Dr. Cy Jeffries, Dr. Petr Konarev.

*Hamburg,
September 2013*

V.Deineko

Copyright acknowledgement

I would like to make following statement regarding used sources as it is recommended by the “Statutory Order Regarding Formal Requirements when Submitting Scientific Papers” of the University of Vienna:

I endeavoured to ascertain the copyright holders of all illustrations and secure their consent to the utilisation of their illustrations in the present paper. If, in spite of my efforts, a copyright infringement should have occurred, I kindly request the relevant parties to contact me.

Abstract

The *sarcomere* is often described as a contractile unit in the striated muscle fibers. This unit is repeated along the length of the fiber and limited by the Z-disks from both sides. Within the sarcomere the chemical energy of ATP is converted into mechanical contraction through the sliding motion of thin and thick filaments relatively to each other. Three main filament systems present in the sarcomere are thin F-actin filaments, thick myosin filaments and titin filaments. Actin and myosin represent the core of contractile machinery, whereas titin plays a role of a molecular ruler.

The detailed studies of the sarcomere reveal a great level of complexity commensurate with the functions it performs. Precise coordination of all processes in space and time, strict regulation of individual components, as well as flexibility and robustness are all key features of muscle cells. The order is largely enabled by the anchoring of all sarcomeric filaments into the molecular grids of the Z-disk and the M-band. The thin filaments from adjacent sarcomeres are cross-linked by α -actinin into the small square lattice in the Z-band. The thick myosin filaments are interconnected at the M-band into a lattice with 6-fold symmetry. Since a long time, the M-band has been a research target of many scientists, whereas the Z-disk has remained largely unexplored until now. The details of forming and functioning of the Z-band macromolecular grid are of particular interest. The present study was focused on two structural proteins (titin and α -actinin), which build the Z-disk lattice in conjunction with the F-actin.

The following results were obtained in the present work:

- 1) Several isoforms of titin Z-repeats (Zrs) were isolated from human striated muscle cDNA libraries. These isoforms contain different arrays of titin repeats: four and six repeats are found in skeletal muscles, and seven repeats are found in cardiac muscle.
- 2) Using the seven repeat isoform as a basis, a protein constructs toolkit was created. This toolkit includes both separate repeats (peptides) and various combinations of interacting and non-interacting Z-repeats, completely covering the corresponding region of titin.
- 3) A protocol for the reconstitution of titin – α -actinin complexes was developed. It included both protein co-expression in the “rare-codon” optimized *E.coli* strain and several consequent purification steps. Immobilized metal affinity chromatography (IMAC) and size-exclusion chromatography (SEC) were employed for the purification of the complexes. Ion-exchange chromatography was utilized either as a polishing step or as an intermediate step preceding SEC. This approach allowed the removal of both contaminating bacterial proteins and degradation products.
- 4) The following “single-domain” complexes were reconstituted: EF-hands 1-4 plus Zr.1; EF-hands 1-4 plus Zr.7; EF-hands 3-4 plus Zr.1; EF-hands 3-4 plus Zr.7; EF-hands 1-4 plus Zr. 1-2-3; EF-hands 1-4 plus Zr. 5-6-7.
- 5) The molecular weights of single EF-hands domains 1-4 and 3-4 as well as of the reconstituted complexes were estimated by static light scattering coupled with analytical size-exclusion chromatography. The obtained data suggest a 1:1 stoichiometry of the components in the reconstructed complexes. These findings are in good agreement with the data available

in the literature (Atkinson *et al.*, 2001; Joseph *et al.*, 2001). We further confirmed by this that only EF-hands 3-4 of α -actinin are able to interact with titin Z-repeats. The binding sites are present only at Zr. 1 or 7.

- 6) The secondary structure content of EF-hands domains was analyzed by circular dichroism spectroscopy. It was shown that these domains contain mainly α -helical elements. It was also shown that the percentage of α -helices had significantly increased upon interaction with the Z-repeats.
- 7) The analysis of the large titin – α -actinin complexes further confirmed the 1:1 stoichiometry of the binding components.
- 8) A number of reconstituted complexes, as well as EF-hands domain 1-4, EF-hands domain 1-2 and EF-hands domain 3-4 were characterized by small-angle X-ray scattering (SAXS). Overall parameters (radius of gyration, maximum size of the particle, molecular mass) and low resolution shapes of the molecular assemblies were determined. The SAXS data were in good agreement with the results of the biophysical experiments. Moreover, clear difference between EF-hands domain 1-2 and EF-hands domain 3-4 was found. It was also shown that maximum size of the complexes is smaller than distance between the Z-disk layers.

In summary, a number of titin Z-repeat constructs was created. These constructs, together with single EF-hands domains and truncated α -actinin 2, present a complete toolkit to study interactions of given muscle proteins. The protocols for the reconstitution and purification of titin– α -actinin complexes were successfully established. The complexes obtained by the developed protocols were stable and homogeneous. They were used for further characterization using available state-of-the-art biophysical methods.

The body of data, obtained as a result of the present research work, does not support the idea that sole titin Z-repeats can act as the regulators of the Z-disk thickness in determining the number of its layers. It is possible to suggest that the primary role of titin/ α -actinin interactions is to robustly integrate titin within the Z-disk macromolecular grid. Taking into account the functions of titin in the sarcomere it is clear that this protein must be positioned with the high level of precision and tightly fixed at both amino- and carboxy-termini. The studied interaction of Z-repeats and α -actinin EF-hands is one of the mechanisms responsible for anchoring and correct positioning of titin N-terminus within F-actin – α -actinin scaffold.

Zusammenfassung

Das *Sarkomer* wird häufig als kontraktile Einheit der gestreiften Muskelfasern beschrieben. Es ist in Längsrichtung der Muskelfaser hintereinander gereiht und wird an beiden Seiten durch die sog. Z-Scheiben begrenzt. Innerhalb des Sarkomers wird durch die Gleitbewegung der dünnen und dicken Filamente gegeneinander chemische Energie in Form von ATP, in eine mechanische Kontraktion umgewandelt. In den Sarkomeren gibt es drei Filamentsysteme: dünne F-Actin Filamente, dicke Myosin- sowie Titinfilamente. Actin und Myosin stellen den Kern der kontraktile Maschinerie dar, während Titin die Rolle eines molekularen Maßbandes spielt.

Entsprechend der Funktion des Sarkomers haben detaillierte Untersuchungen seine ausgesprochen hohe Komplexität gezeigt. Muskelzellen sind durch genaue zeitliche und räumliche Koordination, strikte Regulation der Einzelkomponenten sowie Flexibilität und Robustheit charakterisiert. Dieser hohe Ordnungsgrad wird weitgehend durch die Verankerung aller Sarkomerfilamente in den molekularen Strukturen der Z-Scheiben und M-Bändern möglich. So sind die dünnen Filamente von gegenüberliegenden Sarkomeren durch α -Actinin mit kleinen quadratische Muster in der Z-Scheibe quervernetzt. Die dicken Myosinfilamente hingegen sind mit den M-Bändern zu einem Gitter mit 6-facher Symmetrie verbunden.

Bereits seit langem sind die M-Bänder Forschungsgegenstand vieler Wissenschaftler, wohingegen die Z-Scheiben bisher weitgehend unerforscht sind. Hier sind die Details über die Ausbildung und Funktionsweise der molekularen Strukturen der Z-Scheiben von besonderem Interesse. Die vorliegende Studie hat sich auf zwei Strukturproteine konzentriert, die zusammen mit F-Actin das Gitter der Z-Scheiben aufbauen.

Als Ergebnis wurden folgende Ziele erreicht:

- 1) Mehrere Isoformen der sog. Titin Z-Repeats (kleine sich wiederholende Motive im N-terminalen Bereich von Titin) wurden aus cDNA Datenbanken menschlicher gestreifter Muskelzellen isoliert. Diese Isoformen enthalten eine unterschiedliche Anzahl an Titin Repeats: so findet man Titin mit vier und sechs Repeats in Skelettmuskeln hingegen sieben Repeats im Herzmuskelgewebe.
- 2) Auf Grundlage der Isoform mit sieben Repeats wurde eine Proteinkonstrukt Datenbank erzeugt. Diese Datenbank enthält sowohl separate Repeats als auch verschiedene interagierende und nicht-interagierende Motive, die die gesamte Region in Titin abdecken.
- 3) Ein Protokoll für die Rekonstitution von Titin- α -Actinin Komplexen wurde entwickelt. Dazu wurden zunächst beide Proteine in *E. coli* Stämmen mit erweiterter Codon Nutzung co-exprimiert. Nachfolgend wurde der Komplex über mehrere Reinigungsschritte isoliert. Hier kamen Affinitätschromatographie mittels immobilisierte Metallionen (IMAC) sowie Größenausschlusschromatographie (SEC) zum Einsatz. Ionenaustauschchromatographie wurde entweder als Zwischenschritt vor der SEC oder als finaler Politturschritt eingesetzt. Dieser Ansatz erlaubt sowohl die Entfernung von bakteriellen Proteinen als auch von Abbauprodukten des Zielproteins.
- 4) Die folgenden Einzeldomänen Komplexe wurden rekonstituiert
 - EF-Hände 1-4 plus Zr.1
 - EF-Hände 1-4 plus Zr.7
 - EF-Hände 3-4 plus Zr.1

EF-Hände 3-4 plus Zr.7

EF-Hände 1-4 plus Zr.1-2-3

EF-Hände 1-4 plus Zr.5-6-7

- 5) Das Molekulargewicht der Einzeldomänen EF-Hände 1-4 und 3-4 sowie das der rekonstituierten Komplexe wurde durch SEC gekoppelte statische Lichtstreuung (SLS) ermittelt. Die Daten legen eine 1:1 Stöchiometrie der Komponenten innerhalb der Komplexe nahe. Ergebnisse die gut mit den Literaturwerten übereinstimmen. Die ausschließliche Wechselwirkung der EF-Hände 3-4 von α -Actinin mit Z-Repeats von Titin kann als gegeben angesehen werden. Die Bindungsstellen sind nur in Zr.1 oder 7 vorhanden.
- 6) Der Sekundärstrukturanteil der EF-Hände wurde mittels Cirkulardichroismus analysiert. Hier konnte gezeigt werden, dass diese Domänen hauptsächlich α -helicale Bereiche enthalten und sich dieser Anteil durch Wechselwirkung mit den Z-Repeats noch deutlich erhöht.
- 7) Die Analyse des großen Titin- α -Actinin Komplexes bestätigte die 1:1 Stöchiometrie der Komponenten.
- 8) Eine Anzahl an rekonstituierten Komplexen sowie EF-Hände 1-4, EF-Hände 1-2 und EF-Hände 3-4 wurden mittels Kleinwinkelröntgenstreuung (SAXS) charakterisiert. Hiermit wurden Parameter wie der Gyrationradius, die maximale Partikelgröße, das Molekulargewicht und die Gesamtform der Komplexe bestimmt. Die SAXS-Daten stimmen gut mit den Ergebnissen der biophysikalischen Charakterisierung überein. Darüberhinaus konnten klare Unterschiede zwischen den EF-Hände 1-2 und den EF-Hände 3-4 festgestellt werden. Außerdem wurde gezeigt, dass die maximale Größe der Komplexe kleiner ist als der Abstand zwischen den Schichten von zwei Z-Scheiben.

Zusammenfassend wurde eine Anzahl an Titin Z-Repeat Konstrukten erzeugt. Diese Konstrukte stellen zusammen mit einzelnen EF-Hand Domänen und verkürztem α -Actinin eine komplette Datenbank dar um die Wechselwirkung von Muskelproteinen zu untersuchen. Die Protokolle für die Rekonstitution und Reinigung der Titin- α -Actinin Komplexe wurden erfolgreich etabliert. Die mit diesem Protokoll erhaltenen Komplexe sind sowohl stabil als auch homogen und wurden für die weitere Charakterisierung mit modernsten biophysikalischen Methoden herangezogen.

Die in dieser Studie erhobenen Daten stützen nicht die These, dass Titin Z-Repeats als Regulatoren der Z-Scheiben Dicke agieren und die Anzahl seiner Schichten bestimmen.

List of abbreviations:

6His-tag	hexahistidine tag for the affinity purification
Å	Angstrom, 1×10^{-10} meters
ABD	actin-binding domain
ADP	adenosine-5'-diphosphate
ATP	adenosine-5'-triphosphate
AUC	analytical ultracentrifugation
β-ME	β-mercaptoethanol
CaM	calmodulin-like domain
CD	circular dichroism
CH	calponin homology domain
Da	Dalton, a mass of $\frac{1}{12}$ of a carbon atom
DLS	dynamic light scattering
cDNA	complementary DNA
DNA	deoxyribonucleic acid
DNAse	deoxyribonuclease
dNTP	2'-deoxynucleoside 5'-triphosphate
DTT	dithiothreitol
<i>E.coli</i>	Escherichia coli
EDTA	ethylene-diamine-tetra-acetic acid
EM	electron microscopy
FnIII	fibronectin type 3-like domain
g	gram
HCl	hydrochloric acid

IEX	ion exchange (chromatography)
Ig	Immunoglobulin-like domain
IMAC	immobilized metal ion affinity chromatography
IPTG	isopropyl- β -D-thiogalactoside
kDa	KiloDalton= 10^3 Dalton
kb	kilobase, 1000 DNA bases
LB	lysogeny broth
L	liter
MALDI-TOF	matrix-assisted laser desorption/ionization – time-of-flight
MCS	multiple cloning site
MDa	MegaDalton, 10^6 Dalton
μ g	microgram, 10^{-6} gram
mg	milligram, 10^{-3} gram
ml	milliliter, 10^{-3} liter
μ l	microliter, 10^{-6} liter
μ m	micrometre, 10^{-6} metres
ms	millisecond, 10^{-3} second
MW	molecular weight
Ni-NTA	nickel-nitrilotriacetic acid
nm	nanometer
NMR	nuclear magnetic resonance
OD _{600nm}	optical density at the wavelength of 600 nm
OD _{280nm}	optical density at the wavelength of 280 nm
PCR	polymerase chain reaction
PiP2	phosphatidylinositol 4,5-bisphosphate
PDB	Protein Data Bank
SAXS	small angle X-ray scattering

SDS-PAGE	sodium dodecyl sulfate polyacrylamide gel electrophoresis
SEC	size-exclusion chromatography (<i>syn.</i> gel filtration)
SOB	super-optimal broth
SOC	super-optimal broth with catabolic repressor
SR	spectrin-like repeat
rpm	revolutions per minute
RT	room temperature, 298.15 K
TAE	Tris-acetate-EDTA buffer
TBE	Tris-borate-EDTA buffer
TB	“terrific broth”
TCEP	tris(2-Carboxyethyl)-Phosphine Hydrochloride
TEV protease	Tobacco etch virus protease
Tricine	N-[2-Hydroxy-1,1-bis(hydroxymethyl)ethyl]glycine
Tris	tris-(hydroxymethyl)-aminoethane (IUPAC name 2-Amino-2-hydroxymethyl-propane-1,3-diol)
UV	ultraviolet light
ZASP	Z-band alternatively spliced protein
Zr.	Z-repeat of titin

1 Introduction

1.1 Types of muscles in the human body. Histological structure of muscle tissue

Muscular tissue is one of the most abundant in human body. On average, muscles account for 38–55 % of body weight for males and 28–39 % for females. Force generation and body shape support are the main functions of the muscular tissue. The malfunction of muscles due to inherited diseases or acquired pathologies can lead to severe health distortions, some of which are lethal (for instance, Duchenne muscular dystrophy and similar myopathies).

Muscle tissue can be divided into the following classes: **a)** smooth or ‘involuntary’ muscles, **b)** striated skeletal or ‘voluntary’ muscles and **c)** striated cardiac muscle (*syncytium*). Smooth muscles are innervated by the autonomic nervous system and possess the same basic structure and spindle-like shape in various organs. Smooth muscles are found in the walls of gastrointestinal tract, blood vessels and lymphatic vessels, the bronchial tree, uterus, the bladder, etc. and are involved in maintenance of organ shape and slow motility (for example, the peristaltic motions of intestines). Striated skeletal muscle tissue is organized into more than 600 muscles of variable shape and size (Spalteholz, 1903). For instance, the longest muscle in human body, *m. sartorius* or tailor’s muscle (found in the lower extremities), is 40 cm in length whereas *m. stapedius* in the ear is only 5 mm long. Despite such notable differences, all striated muscles have similar architecture. They are composed of elongated, multi-nucleated cells known as myocytes (or muscle fibre). These cells form separate bundles (*fascicles*) that are wrapped in elastic connective tissue. The fascicles are placed into the fibrocartilage envelope, which is attached to the bones by collagen

tendons. The multi-nuclearity of myocytes originates from the processes of development when a number of myoblasts merges to form a single myofiber. Within each myocyte the cytoskeletal components form a highly ordered structure that is observed as a characteristic striation pattern under conventional light microscope using hematoxylin/eosin tissue staining. The basis of this higher-organisation originates from the multiple repetitions of *sarcomeres* – elementary contractile units of a muscle fiber.

Finally the last major grouping of muscle tissue is striated cardiac muscle. This type of involuntary muscle forms walls and septums of the heart (*myocardium*). Cardiomyocytes possess a fine striation pattern, similar to that of skeletal muscle fibres. However, the cells often appear branched, in contrast to skeletal tissue. All cardiomyocytes are connected with each other by highly specific structures known as intercalated disks. This type of organisation enables both the rapid propagation of electrical impulses from pacemaker (*the sinoatrial node*) and the coordinated transmission of the contractile force to maintain a regular heart rhythm.

Despite its anatomical diversity, muscle tissue carries out similar functions in different organs and parts of the body and indeed shares many ‘variations on a theme’ with respect to performing contractile events. For example all muscle cells contain a number of long, parallel fiber-like structures named myofibrils. The myofibrils are enclosed in a common outer cellular membrane (*sarcolemma*). Every myofibril contains *myofilaments* – protein assemblies, responsible for the generation of the contractile force. These assemblies consist of thin filaments which are made of polymerized actin, tropomyosin and the regulatory protein troponin; and thick filaments which are mainly comprised of myosin and titin. The interactions of actin and myosin create contractile force in all muscle cells, but it is the unique and often subtle differences between these

proteins and their interactions with accessory proteins (for example myosin binding protein C) that help confer a level of regulation or ‘fine tuning’ unique to each muscle type.

In brief, there are 3 types of muscle tissue in human body: smooth, striated skeletal and striated cardiac. The striated muscles possess a complex, multilevel architecture: muscle => fascicles => myocytes => myofibrils => myofilaments. Two of most abundant proteins of muscle cells, namely actin and myosin, are responsible for the generation of contractile force in both smooth and striated muscles.

1.2 Sarcomere and its principal components

The *sarcomere* is defined as a contractile unit of a myofibril, which repeats along the myofibrils' length and is limited by Z-disks on both sides. The length of sarcomeres typically varies from 1.5 μm to 3.5 μm and their arrangement results in characteristic striation pattern (dark/light bands of alternating thin and thick filaments (**Fig.1**)). Several features within the sarcomere can be distinguished and identified (**Fig.2**). Thin dark lines that traverse the sarcomere across its width are called Z-disks or Z-lines (German *Zwischenscheibe*) that effectively define sarcomere length. Z-disks are exceptionally complex multi-component protein super-assemblies that are involved in the mechanical stability, 'mechanosensation' and mechanical transduction of sarcomeres as well as acting as anchor-points for thick and thin filaments, and conduits for intracellular signaling events (Knöll *et al.*, 2011). The Z-disk is surrounded by a light area called I-band (*isotropic* band). The thin filaments of actin can be found in this region of the sarcomere.

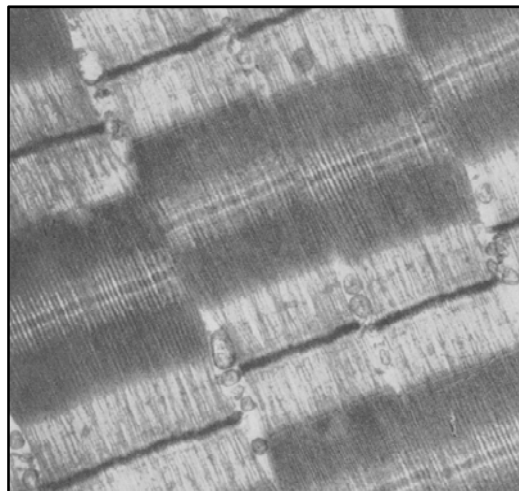


Figure 1. A low-magnification electron micrograph of striated muscle tissue specimen (rabbit psoas, $\times 27\,000$). Image credit: Huxley, 1961.

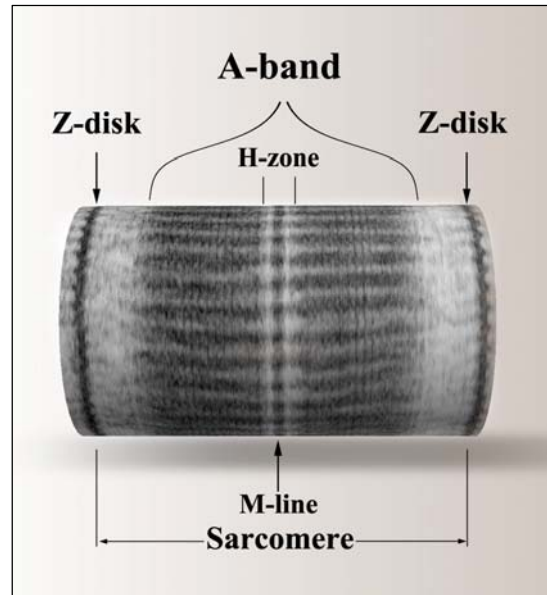


Figure 2. The sarcomere and its parts. The I-bands, adjacent to the Z-disks, are not labelled on the image. Image credit: EM micrograph by Dr. P. Luther (www.sarcomere.org), rendition by V. Deineko.

The A-band (or *anisotropic* band) is located next to the I-band. The length of the A-band is equal to the average length of thick (myosin) filaments. The A-band is divided into equal halves by the so-called H-zone (German *heller*). In this zone, myosin is not superimposed by actin. Finally, the M-band (German *Mittelscheibe*) is located in the middle of the H-zone. The M-band is made of cross-linking proteins, which create a spatial lattice (seen as a hexagonal in filament cross-sections). The presence of ~6 sub-bands can be observed in the M-band by high-resolution electron microscopy imaging of longitudinal myofibril sections. Bipolar myosin filaments are located in the A-band. Actin filaments span from the Z-disk to the A-band. In the process of muscle contraction, the length of the A-band remains the same, whereas the I-bands become shorter. This makes the Z-disks move towards each other and decreases the overall length of the sarcomere.

The other main proteins found within muscle sarcomeres are titin, nebulin and obscurin (Kontrogianni-Konstantopoulos *et al.*, 2009). Titin, the largest muscle protein, spans from the Z-disk to the M-band and is fixed within macromolecular scaffolds at both ends. The molecular mass of titin can reach ~3,7 MDa for the un-spliced protein. It plays an important role as a molecular “ruler”, or scaffold, which helps to define the placement of other sarcomeric proteins during muscle contraction (Trinick, 1996). Titin provides elasticity to the sarcomere during muscle relaxation and participates in intracellular signaling. Titin can make up as much as 9% of the entire myofibril mass. Two other giant proteins of MW≈800 kDa each, namely nebulin and obscurin, can also be found in the sarcomere. Nebulin is located along other filaments and obscurin can be found at the Z-disks and M-bands. It is suggested that nebulin acts as a docking platform for other proteins, whereas obscurin may participate in the processes of myofibril assembly (Kontrogianni-Konstantopoulos *et al.*, 2009; Witt *et al.*, 2006).

1.3 An outline of muscle contraction mechanism

The process of muscle contraction is comprehensively described by the theory of sliding filaments. This theory was first established in 1954 (Huxley & Niedergerke, 1954; Huxley & Hanson, 1954) and subsequently developed by others. In brief, protein tropomyosin is bound to F-actin and another protein, called troponin, is bound to tropomyosin. All three proteins make up the thin filament. When Ca^{2+} ions are released from the sarcoplasmic reticulum (e.g., after an impulse is received from a neuron) the calcium ions bind to troponin, causing it to change conformation.

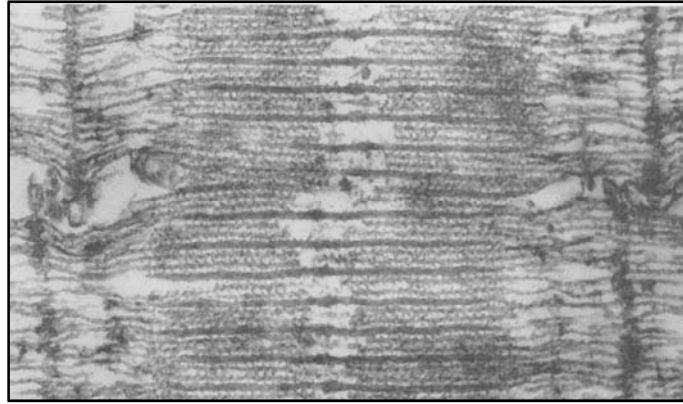


Figure 3. Arrangement of actin (thin) and myosin (thick) filaments in the sarcomere, as seen on electron micrograph (rabbit psoas, $\times 150\ 000$). The Z-disks are seen as dark lines, perpendicular to the filaments. Image credit: Huxley, 1961.

These structural rearrangements of troponin lead to a displacement of tropomyosin on F-actin that, in turn, exposes myosin binding sites. Consequently, myosin heads – or “the motors” responsible for force generation – that are otherwise blocked from accessing the thin filament in a Ca^{2+} -off state – become capable of accessing F-actin to impart force and thus perform contraction. This stage is called the “pre-processing”.

During process of the movement, adenosine triphosphate (ATP) binds to the myosin head. ATP is hydrolysed upon binding and the released energy activates myosin. The activated myosin attaches itself to its binding site on the actin filament. ADP is released upon binding; myosin returns into its low-energy state and pulls the thin filament (“*stroke*”). The myosin head can be further detached from the actin if a new molecule of ATP binds to it, and the entire cycle can be repeated (the Lymn–Taylor Cycle, Lymn & Taylor, 1971). The simultaneous pulling movement of numerous myosin heads leads to the shrinkage of the I-band and to the contraction of the entire sarcomere. The displacement of the thick filaments can be observed during the process of contraction. The giant protein titin helps to correctly position filaments within the sarcomere in order to

distribute the tensile force evenly, and provides passive stiffness during relaxation (Granzier *et al.*, 1997).

To sum up, there are many proteins in muscle sarcomeres that are important for the maintenance of muscle contraction, but it is the interaction between actin and myosin of the thin and thick filaments, respectively, that is primarily responsible for force generation. The chemical energy, released during the hydrolysis of ATP by myosin heads is converted into mechanical energy upon interacting with F-actin. Troponin and tropomyosin play an important role during the preprocessing – or activation of the thin filament – prior to contraction and help ensure the thin filament can respond to Ca^{2+} signaling mechanisms (Geeves and Holmes, 2005). Besides that, a number of other sarcomeric proteins help to correctly position thick and thin filaments within spatial grids of the Z-disk and the M-band. They act as both scaffolds and mechanical accessories that help both to distribute the contractile force, and to maintain the integrity of the sarcomere.

1.4 Z-disk and its structure and function in the sarcomere

As it was mentioned before, the sarcomere is clearly defined by its boundaries, the Z-disks. It was also shown that during contraction, the Z-disks move towards each other as the sarcomere shortens during contraction. This phenomenon is possible because F-actin filaments from adjacent sarcomeres are tightly interconnected by α -actinin into a macromolecular grid within the Z-line. This connection imparts the necessary order and rigidity to the entire sarcomere structure. Due to the crucial role of the Z-disk macromolecular scaffold in sarcomere functioning, the key Z-disk structural proteins, namely *titin* and α -*actinin*, were selected as a target of further investigation for this thesis. The

attention of many researchers is still focused on the thin and thick filaments as force-generating molecular motors, and the M-band and its components are also actively explored. In contrast, the Z-disk still remains to a large extent “*terra incognita*” due to extreme complexity of its structure, assembly, regulation and function. This is yet another reason for performing the thesis work in the tantalizing field of Z-disk biology. An outline of Z-disk structure, as well as its protein composition and role in health and disease, will be given below as the necessary background for understanding of the thesis topic.

The Z-disk is a unique macromolecular scaffold that performs various roles within myofibrils. It plays a role of interface between adjacent sarcomeres, serves as a point of signal perception and fibril remodeling. The Z-line is simultaneously involved both in the transmission of tensile forces along the myofibril (axial forces) and in the preservation of cytoskeleton structure against possible distortions (lateral forces). The Z-disk is usually seen as dense dark band on longitudinal sections of myofibrils, and its thickness depends on the type of muscle tissue. For example, in fast muscles it is approximately 50 nm thick, whereas in slow muscle the width can be ~100–140 nm. Particularly wide Z-disks can be found in the cardiac tissue (> 400 nm). They are called Z-bodies. The thicker the Z-line is, the more overlapping are thin filaments. The average overlap of F-actin filaments is ~22–25 nm (Luther, 2000). Extremely wide Z-disks (nemaline bodies or Z-crystals) can be also observed in case of so-called congenital nemaline myopathy.

When myocyte cross-sections are observed at high magnification in the electron microscope, one can notice a highly ordered three-dimensional structure of the Z-disk (Goldstein *et al.*, 1982; Goldstein *et al.*, 1986; Goldstein *et al.*, 1990).

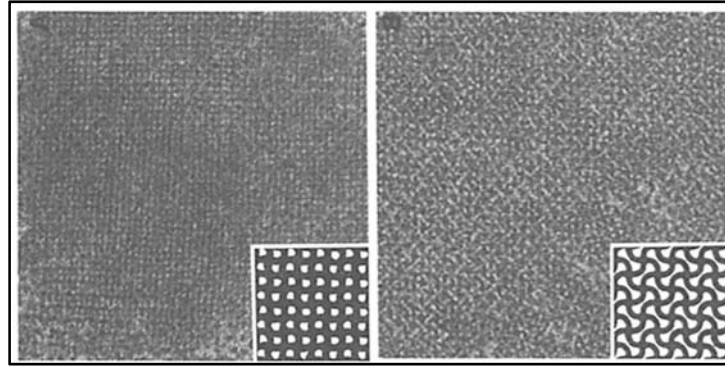


Figure 4. Electron micrographs of the Z-disk cross-sections. The image on the left shows the Z-disk grid during relaxation (“small square”); the image on the right shows the lattice during muscle contraction (“basket-weave”). Image credit: Goldstein *et al.*, 1988.

Moreover, by examining specimens of muscle tissue either in rigor or relaxation, it is possible to conclude that the Z-line can exist in two distinct states: **a)** small square (**ss**) lattice and **b)** basket-weave (**bw**) lattice (**Fig.4**). The average dimensions of the **ss** lattice are 20 nm, the **bw** state is characterized by ~20 % increase of the distances between filaments (24 nm on average). The **ss** appearance is associated with the relaxed state of the muscle and **bw** is observed predominantly during tetanic contraction (Goldstein *et al.*, 1991, Goldstein *et al.*, 1990). It was also suggested that the **bw** state of Z-disk lattice might be dependent on the Ca^{2+} ions, which are present during contraction (Goldstein *et al.*, 1989). By examining longitudinal sections through the Z-disk, it can be noticed that the latter has a complex “zigzag” appearance. These patterns are due to Z-links, which join F-actin filaments from the neighboring sarcomeres. It is generally accepted that these Z-links are composed of antiparallel α -actinin dimers (Takahashi and Hattori, 1989; Luther, 2009).

It appears that the entire Z-disk consists of an even number of layers. The minimum observed number of layers is two (example: fish fast muscle) and the maximum number is six in slow muscles of mammals. It was also noticed that

the number of layers and the Z-disk thickness may vary even within the same sarcomere (Luther *et al.*, 2003). The thickness of one layer is approximately 19 nm and the layers have a rotation of $\sim 90^\circ$ relative to each other. One can observe a pair of α -actinin links coming from opposite sides of the actin fiber and connecting it to two antiparallel fibers. The question about the exact mechanism that defines the number of layers in the Z-disk has yet to be answered. More than a decade ago a hypothesis was proposed, claiming that a unique 45-residue motif in the N-terminal part of titin located in the Z-disk could be involved in organizing of Z-disk. This hypothesis will be described in more detail below.

Due to recent discoveries, the Z-disk is currently regarded as one of the most complex macromolecular assemblies known. Such a dramatic change in perception was possible because of the rapid development of high-throughput methods of molecular biology. Now it is clear that the Z-disk performs not solely a structural role, but it is also involved in mechanosensing and signaling. According to the NCBI databases, more than 200 proteins or gene products can be found within the Z-disk (Knöll *et al.*, 2011). While describing the entire Z-disk proteome is far beyond the scope of the present introduction, nonetheless, the main protein groups will be mentioned. The emphasis, however, will be put on the structure and function of titin and α -actinin – the targets of this thesis.

1.5 An overview of the Z-disk proteome

With new discoveries of new Z-disk proteins it became clear that the Z-line is not only a robust macromolecular scaffold capable of transmitting axial forces during sarcomere contraction. It appears that many of the Z-disk components are involved in signal sensing and transduction. It was shown that the Z-line takes part in the sensing of force load and is involved in the process of physiological

hypertrophy. Moreover, the protein turnover in the Z-disk is regulated by its own, ubiquitin-dependent, degradation pathways. These more recent observations further emphasise the extreme complexity of this unique macromolecular assembly.

All Z-disk proteins can be roughly divided into the following functional categories: **1)** structural proteins; **2)** proteins involved in signaling; **3)** proteins involved in degradation pathways (including ubiquitin-ligases) and **4)** components of costamere¹ protein complexes (Frank, 2006). The other classification (Knöll *et al.*, 2011) divides all Z-disk proteins into central or ‘core’ proteins, and transversal or ‘partial’ proteins depending on their location.

The group of structural proteins of Z-disk includes the following members: actin, CapZ (actin-capping protein), titin, α -actinin, nebulin/nebulette, obscurin, γ -filamin (filamin C), myosin II.

Actin is an extremely abundant protein, which is expressed in different types of tissues. It takes part in processes of cell migration, motility and contraction. Actin exists in two forms: a globular monomeric form, or G-actin and filamentous F-actin, the overall structure of which can be described as a twisted parallel helix. Two distinct isoforms of actin can be found in striated muscles: **a)** skeletal actin and **b)** cardiac actin. They are encoded by different genes. The ratio between isoforms depends on the type of muscle fiber and the stage of muscle development. F-actin filaments from neighboring sarcomeres are interconnected within the Z-disk. Mutations in cardiac actin may cause such diseases as either hypertrophic or dilated cardiomyopathy, whereas mutations in skeletal actin can result in myopathy, arthrogryposis and other dystrophic conditions.

¹ Costameres – components of striated muscle cells. They are macromolecular assemblies, aligned with Z-disks and located under sarcolemma. They connect cell membrane with the sarcomere

The actin-capping protein, CapZ, is a dimer formed by α - and β -subunit. This protein interacts both with actin (at the "barbed end" (Clark *et al.*, 2002)) and α -actinin, and provides an additional Z-disk anchor for thin filaments (Schafer *et al.*, 1995; Schafer *et al.*, 1996). It is also involved in regulation of the actin dynamics.

Nebulin is a large structural protein (MW \approx 600-900 kDa, depending on isoform) expressed specifically in muscle tissue. This protein is composed of a large number of repetitive "nebulin" motifs and has a SH3 domain at the very C-terminus. It interacts with actin filaments and titin. Nebulin is suggested to play the role of a molecular ruler (similar to titin), regulating the width of the I-band (Kruger *et al.*, 1991). There is a smaller cardiac-specific isoform of nebulin, called nebulin. The role of this protein remains unclear. The distortions in nebulin function can lead to the development of nemaline myopathy.

The giant elastic protein titin (\sim 3,7 MDa) spans from the Z-disk to the middle of the sarcomere (M-line). The domain composition and, hence, molecular properties of titin vary along its length (Granzier and Labeit, 2005). An I-band portion of titin provides necessary elasticity during sarcomere relaxation, whereas the Z-disk part is non-extensible and provides additional support for the macromolecular scaffold. In general, titin acts as a molecular ruler and docking platform, defining the location of other sarcomeric proteins (Granzier and Labeit, 2007). It also participates in numerous signaling pathways due to its unique force-activated kinase domain (Krüger and Linke, 2011). Mutations in titin cause a number of myopathies ("titinopathies"), for example, hereditary myopathy with early respiratory failure is linked to the mutation in the kinase domain of titin (Hackman *et al.*, 2003; Kostin *et al.*, 2000; Matsumoto *et al.*, 2005).

Telethonin (titin-capping protein, t-cap) is a small 19 kDa Z-disk protein. It binds Z1-Z2 domains of titin into an antiparallel sandwich complex, anchoring the N-terminus of titin within the Z-disk (Mues *et al.*, 1998). This is one of the most robust protein-protein interactions known (Zou *et al.*, 2006). Furthermore, telethonin interacts with a number of other proteins, like minK (potassium channel subunit β), small ankyrin 1, muscle ring fingers-E3 ligases, calsarcin 1 etc. Telethonin links the Z-disk with the T-tubular system and participates in numerous signaling cascades. Mutations in telethonin can cause such severe distortions as dilated cardiomyopathy, limb-girdle muscular dystrophy type 2G, to name a few.

γ -filamin or filamin C is a muscle-specific isoform of filamin, which has actin-binding and cross-linking functions. It interacts with calsarcins, myotilin (van der Ven *et al.*, 2000), γ - and δ -sarcoglycans (Thompson *et al.*, 2000).

Obscurin is a yet another giant protein found in striated muscle cells. It has a molecular mass of ~900 kDa and is composed of Ig-like and Fn-like domains. It also has a pair of unique domains at the C-terminus. It was shown that obscurin interacts with N-terminal domains Z9-Z10 of titin (Sanger and Sanger, 2001) and with ankyrin 2. It was proven recently that obscurin plays an important role in the processes of myofibrillogenesis, particularly in formation of M-lines (Kontrogianni-Konstantopoulos & Bloch, 2005; Borisov *et al.*, 2006). More functions and interacting partners of obscurin are yet to be discovered.

The cohort of proteins involved in Z-disk signaling includes such members as myotilin, myopalladin, PDZ/LIM proteins, actinin-associated LIM proteins, ZASP/Cypher, Enigma. They interact with structural components of the Z-disk and are involved in mechanosensing and signal transduction (Frank & Frey, 2011).

The ~57 kDa muscle protein myotilin localizes within the Z-disk, where it interacts with α -actinin. Other myotilin partners include such proteins as actin, caldesmon 1 and 2 γ -filamin. Mutations in myotilin gene can be the cause for muscle dystrophy (Selcen *et al.*, 2004).

The 145 kDa protein myopalladin belongs to relatively recent discoveries in the field of Z-disk biology (Bang *et al.*, 2001). It interacts with cardiac ankyrin repeat protein, nebulin and α -actinin. Myopalladin is involved in the fine regulation of myofibrillogenesis. Besides that, it can also be involved in transforming mechanical strain signal from titin I-band part into activation of gene transcription.

All members of the enigma family of muscle proteins contain the N-terminal PDZ domain and zinc-binding LIM domains at their carboxy-terminus. This family includes the following members: enigma (Guy *et al.*, 1999), ENH (Kuroda *et al.*, 1996) and cypher (Zhou *et al.*, 2001). The later is also known as ZASP or Oracle. All these proteins are localized at the Z-disk. They are interaction partners of protein kinases type C (PKC) and take part in signaling pathways. ZASP was also shown to interact directly with α -actinin. Gene knock-out animals deficient in enigma proteins usually develop severe pathological phenotypes (for example, congenital myopathy and postnatal death). The distortion of Z-disk architecture is clearly visible in knock-out mice tissue specimens under EM.

Significant portion of Z-disk proteins belong to the so-called LIM/PDZ protein family. PDZ domains are ~90 residues long. They are involved in the mediation of protein-protein interactions. Proteins with PDZ-domains are usually assembled in large, multi-subunit complexes, and play a role in signal transduction.

Another protein which interacts with α -actinin 2 is a muscle LIM protein (MLP). Other interaction partners of MLP are telethonin, calcineurin, β -spectrin. This protein plays a role during processes of muscle differentiation and is involved in the process of mechanosignalling. The mutations in MLP were observed in different forms of cardiomyopathy.

Protein kinases type C are members of the serine/threonine kinase family and are typically divided into Ca^{2+} sensitive, Ca^{2+} insensitive and atypical classes (Newton, 1995). It has been shown that protein kinase C ϵ is expressed at the Z-disk and can be translocated into the nucleus under mechanical stress conditions. Apparently, it is involved in processes of remodeling and physiological hypertrophy of myofibrils in response to the force loads (Newton & Messing, 2010; Russell *et al.*, 2010).

The recently discovered muscle protein melusin is involved in myofibrillar remodeling. It is located at the Z-disk/costameres where it interacts with cytoplasmic domain of β 1-integrin. Melusin is an integral part of integrin-related mechanosensing pathway (Brancaccio *et al.*, 2003; De Acetis *et al.*, 2005).

Calcineurin and its modulators calsarcins are important proteins, involved in regulation of cardiac hypertrophy. Calcineurin is a serine/threonine phosphatase that consists of catalytic and regulatory subunits. The primary targets of calcineurin are transcription factors NFAT (Crabtree & Olson, 2002). Upon dephosphorylation, these transcription factors are translocated into the nucleus where they activate hypertrophic gene cascade.

Calsarcins (calcineurin-associated sarcomeric proteins) are muscle proteins located in the Z-disk. The calsarcin family includes three isoforms that are expressed in different types of muscle fibres (Frey *et al.*, 2000). Their interaction partners include telethonin/T-cap, α -actinin, γ -filamin and calcineurin. They

modulate calcineurin-dependent signal transduction by inhibiting the activity of this phosphatase.

A number of proteins located in the costamere provide an interface between the extracellular matrix and the cytoskeleton, and connect the scaffold of the Z-disk with the plasma membrane. Costamere proteins also take part in mechanosensing and signal transduction. For instance, a 52 kDa protein desmin (Lazarides and Hubbard, 1976; Small and Sobieszek, 1977) interacts with structural proteins nebulin and spectrin, with ankyrins and with protease calpain-3. Transmembrane proteins integrins (Ross and Borg, 2001; Ross, 2004) have focal adhesion kinase, integrin-linked kinase and calreticulin bound to their cytoplasmic domain. Such interactions allow transformation of mechanical signals into chemical signals and the consequent activation of signaling pathways.

This short review of Z-band proteome emphasizes the extreme structural and functional complexity of Z-disk that in itself comprises a macromolecular assembly unique to muscle cells. Scaffolding, mechanosensing, signal transduction – all these functions are performed by dozens of various proteins in a highly coordinated and interdependent manner. Mutations or malfunctions in any of the Z-disk proteins lead to severe myopathies with characteristic phenotypes. A majority of Z-disk proteins are located within the so called ‘spatial scaffold’, composed of the structural proteins titin, actin and α -actinin. Hence, the correct formation of this macromolecular grid is absolutely crucial for normal functioning of the Z-disk as well as of the entire sarcomere.

In the forthcoming sections, a more detailed description of the role of titin, actin and α -actinin in assembly of Z-disk scaffold will be provided. The domain composition of these proteins, interactions and their regulation will be thoroughly reviewed.

1.6 Domain composition of α -actinin

The protein α -actinin was first discovered almost 50 years ago (Ebashi and Ebashi, 1964) by its precipitating action on actomyosin. It has been shown that α -actinin is an integral component of the Z-disk. When actinin is extracted from the myofibril, the Z-line loses its structure (Briskey & Fukazawa, 1970). Now the antibodies to α -actinin are routinely used as reliable Z-line marker in co-localization experiments *in vivo*.

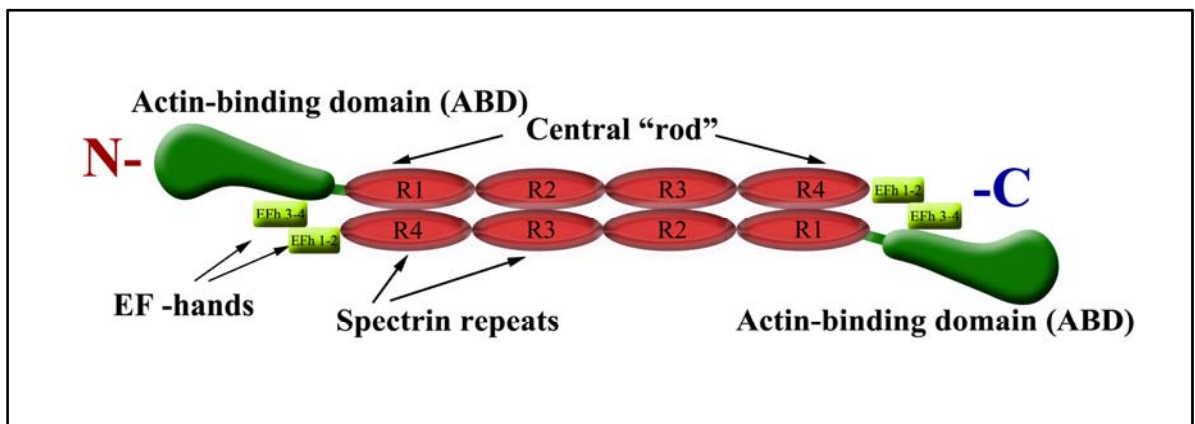


Figure 5. Schematic representation of α -actinin dimer domain structure.

α -actinin belongs to the spectrin superfamily of proteins. All proteins of this family possess a number of spectrin repeats and are able to interact with F-actin filaments by their actin-binding domain located at the N-terminus. Other members of this superfamily include such proteins as dystrophin, utrophin and spectrins (Broderick and Winder, 2005). In humans, four separate genes encode four separate isoforms of α -actinin. The α -actinin 2 and α -actinin 3 isoforms are found only in striated muscle cells, where they are localized at the Z-disks. These isoforms are Ca^{2+} -insensitive. It is worth mentioning that α -actinin 3 is often absent in muscle cells due to a null mutation (~16% of population worldwide are affected). However, this does not usually produce a pathological phenotype

suggesting that these two isoforms of α -actinin are interchangeable to a large extent. α -actinin 2 is a dominant isoform in the slow oxidative muscle fibers and in cardiac syncytium. α -actinin 3 can be found mainly in fast glycolytic muscles and is absent in heart tissue (MacArthur & North, 2004; Berman & North, 2010).

α -actinin 1 and α -actinin 4 are calcium-sensitive and are ubiquitously expressed in various types of cells. They play a role in the organization of the actin cytoskeleton (bundling), particularly within stress fibers and focal contacts.

Human muscle α -actinin 2 (Uniprot accession: P35609 ACTN2_HUMAN) is 894 amino acid residues long; its MW is \approx 100 kDa. It has the following structural domains: **a)** the actin-binding domain at the amino-terminus; **b)** the central rod of 4 spectrin repeats; **c)** the EF-hands domains at the carboxy-terminus (**Fig.5**). The actin-binding domain is separated from the rod by a highly flexible “neck” region. This protein forms a functional antiparallel homodimer. A detailed description of α -actinin molecular architecture is given in subsequent sections.

The actin-binding domain (ABD) is highly conserved within the actinin protein family. This is due to the evolutionary conservation of actin – the key interaction partner of α -actinin. A number of actin-binding domain structures were determined by high-resolution methods. They include ABDs from plectin, fimbrin, dystrophin, utrophin and human α -actinin 1, 3 and 4. In the majority of these structures a closed conformation of the ABD is observed due to the inter-domain interactions. The α -actinin ABD is composed of a pair of calponin-homology (CH) domains (CH 1 and CH2 domains). Every CH-domain has four main α -helices in its structure: A, C, E and G. Together they constitute a core of the calponin-homology domain (Djinovic Carugo *et al.*, 1997). In the closed conformation of actin-binding domain (unbound state) helices A and G of CH1 are located against helices F and G of the CH2. These interdomain interactions

are facilitated by a combination of hydrophobic and electrostatic effects. Three actin-binding sites have been identified within ABD: **a)** the amino-terminal helix of CH1; **b)** helix G of CH1; **c)** the linker between CH domains and partially amino-terminus of CH2. It is necessary to mention that high-affinity binding is enabled only by combination of CH1 and CH2 domains. Calponin-homology domain 1 is able to interact with actin filaments, however, with much lower affinity. The CH2 is unable to bind actin alone.

The central rod domain (or simply the rod) in all vertebrate α -actinins contains 4 spectrin repeats. The spectrin repeat is a domain composed of 3 antiparallel coil-coiled α -helices - so called “*bundle*”. The core of this domain is stabilized by hydrophobic and, to lesser extend, electrostatic interactions between conserved residues (see Djinovic-Carugo *et al.*, 2002 for the comprehensive outline).

The rod is responsible for dimerisation of actinin molecules. A number of rod domain structures were determined by X-ray protein crystallography (Djinovic-Carugo *et al.*, 1999; Ylänné *et al.*, 2001). These structures reveal a characteristic feature of the rod domain, namely the 90° twist along the axis of the dimer. The entire rod is roughly 240 Å in length and 40–50 Å in width. The high-affinity interactions of rod domains within α -actinin dimer are mediated by electrostatic forces. The central rod is inflexible and provides the rigidity which is necessary to carry out structural functions of α -actinin within the Z-disk scaffold.

EF-hands are 2 pairs of small helix-loop-helix motifs located at the C-terminus of α -actinin molecule. They are named after the calcium-binding moiety of paralbumin, formed by α -helices E and F. In the vast majority of proteins, EF-hands are regulated by Ca^{2+} ions, which normally trigger transition from a closed to an open conformation (so called “canonical” EF-hands). The

main function of these motifs is to mediate interactions with other proteins (hydrophobic forces) upon calcium intake. The classical representative of this family is the 17 kDa protein calmodulin (**calcium modulated protein**). EF-hands usually occur in pairs, thus the majority of proteins in the family contain two, four or six EF-hands. These motifs often demonstrate cooperative effects, minimizing the amount of Ca^{2+} required for structural transitions. A detailed overview of EF-hands diversity as well as of structure-function relations is given in following comprehensive works: Gifford *et al.*, 2007; Grabarek, 2006 and Yap, 1999.

EF-hands domains are involved in the Z-disk targeting of α -actinin through highly specific interactions with the unique titin motifs called Z-repeats. The EF-hands of muscle α -actinin have lost their calcium-binding capability, because the metal-coordinating residues have been mutated through the course of evolution. The proposed regulatory mechanism of titin-actinin interactions requires presence of the phospholipid phosphatidylinositol 4,5-biphosphate (PiP2). In absence of PiP2 α -actinin remains in an autoinhibited state, as EF-hands are bound to a short amino acid moiety within the “neck” closely resembling the Z-repeat of titin.

A number of low-resolution (20 Å) structures of full-length α -actinin were obtained by electron microscopy imaging (Tang *et al.*, 2001; Liu *et al.*, 2004; Hampton *et al.*, 2007). These studies allowed the measurement of the dimensions of actinin dimers and to observe the protein’s overall shape. However, the achieved resolution was not sufficient to provide new insights in the positioning of ABD and EF-hands at both ends of α -actinin. Interestingly, it was shown that the permitted angles between α -actinin and F-actin filaments are restricted to values of 0, 60, 90 and 180 degrees. Moreover, the length of α -actinin dimers upon binding to actin can vary quite significantly ($\pm 55\text{Å}$). This suggests that α -

actinin indeed can be involved in mechanosensing either by itself or through interactions with other proteins.

α -actinin binds both F-actin filaments and titin with N- and C-terminal domains respectively, creating a flexible and robust macromolecular scaffold. The central rod of actinin dimer plays the role of a docking platform for a plethora of other proteins (particularly those containing PDZ and LIM domains). Furthermore, α -actinin is capable of mechanosensing and may link the Z-disk to adjacent costamere assemblies. In summary, it is possible to stipulate that unique structural features of muscle α -actinin reflect the multitude of functions this protein carries out in the Z-disk.

1.7 Domain composition of titin

The muscle protein titin, or connectin, (Maruyama *et al.*, 1977; Maruyama, 1994; Maruyama, 1997) is the largest protein in the human proteome. It consists of 38138 residues and has a molecular weight of ~ 3,7 MDa (Uniprot number for human titin is Q8WZ42 TITIN_HUMAN). The human gene encoding titin contains 363 exons and consists of 294 kilobases (Bang *et al.*, 2001). Titin is the third most abundant muscular protein together with actin and myosin (Wang *et al.*, 1979).

Titin filaments are 1- μ m in length and span from the Z-disk to the M-band of the sarcomere (Lange *et al.*, 2006). Titin is composed of immunoglobulin-like and fibronectin-type-III domains. It also possesses a number of unique structural modules, like a force-regulated titin kinase domain, N2B domain, PEVK motifs, Z-repeats (Gautel *et al.*, 2006). Because of titin's numerous globular domains, the protein looks like a string of beads on electron micrographs. Due to the alternative splicing the structural features and molecular weight of titin may vary significantly in different muscle fibers. The splicing events mainly affect the I-band moiety of titin (Labeit *et al.*, 2006).

The modular structure of titin is connected to its function in the sarcomere: certain regions of titin are capable of reversible unfolding/refolding. The interdomain α -helical linkers are unfolded by the action of longitudinal force. The Ig-like domains can also be unfolded if the applied force is significant. The unfolding process is reversible (Hsin *et al.*, 2011). Such properties allow titin to adjust to the changing of sarcomere length without compromising its integrity and functionality.

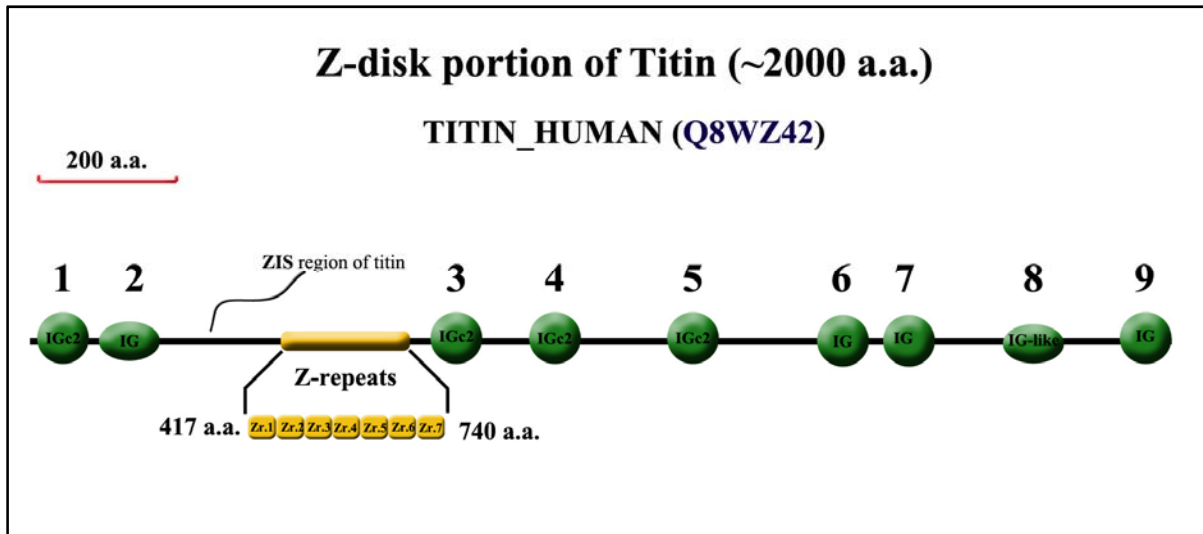


Figure 6. Domain composition of N-terminal (Z-disk) portion of titin. Domain numbering starts from the amino-terminus. IGe2 – immunoglobulin C-2 type domain; IG_like – immunoglobulin like domain; IG – immunoglobulin domain; ZIS – proline-rich unstructured region.

The N-terminus of connectin is completely buried within the Z-disk (**Fig.6**). As it mentioned previously, this portion of titin is inflexible, i.e. it is not capable of stretching and does not have any intrinsic elasticity in contrast to other parts of the macromolecule. Accordingly to present data, this fragment of titin performs mainly structural role within the Z-disk.

The N-terminal region of titin (**Fig.6**) is composed of immunoglobulin-type domains, a proline-rich ZIS region and a variable number of unique 45-residue motifs called Z-repeats. It can be roughly defined as a moiety starting from Ig-like domain 1, which is located in the middle of the Z-disk and ends at Ig-like domains 9-10 at the border of the Z-disk, where titin interacts with obscurin.

To date, a number of structural and biophysical studies of the Z-disk titin have been performed. These experimental studies were focused mainly on Ig-domains 1-2 and their interactions with telethonin. As a result, several high-resolution 3D structures were deposited in the Protein Data Bank. These structures represent the very N-terminus of titin (Marino *et al.*, 2006; PDB ID

2A38), titin-telethonin complexes (Zou *et al.*, 2006; Pinotsis *et al.*, 2006; PDB IDs 1YA5 and 2F8V) and the complex of titin Z-repeat 7 with EF-hand of α -actinin, solved by solution NMR (Atkinson *et al.*, 2001; PDB ID 1H8B). However, a large portion of the Z-disk titin has yet to be investigated using high-resolution, biophysical and *in vivo* techniques, so as to provide new insights into the Z-disk structure, assembly and functioning.

According to currently available data, the Z-disk titin interacts with a large number of other proteins. Majority of these interactions are mediated by telethonin. These contacts involve small ankyrin-1 (sANK1), minK (the potassium channel subunit), muscle LIM protein (MLP), E3 ubiquitin ligase MDM2 (mouse double minute-2) to name just a few. Among all these interactions, the crosslinking of titin by α -actinin is of utmost importance.

1.8 The interaction between titin and α -actinin and its regulation by PiP2

It is well understood that the processes of myogenesis in general, and of Z-disk assembly in particular, have to be both spatially and temporally coordinated. The giant filamentous proteins of the sarcomere take part in these processes by playing the role of molecular scaffolds and rulers.

In a pivotal study, Young *et al.* (1998) revealed the existence of two interaction sites between the Z-disk cross-linker α -actinin and the molecular ruler titin using a combined approach. The study included such methods as yeast two-hybrid screens, immunoelectron microscopy, co-precipitation assays and protein cross-linking. The first interaction involves two central spectrin repeats of the actinin rod (repeats 2 and 3) and titin moiety located between the Z-repeats and adjacent Ig-domains. The second interaction occurs between EF-hands domain

of α -actinin and flanking Z-repeats of titin (Peckham *et al.*, 1997; Ohtsuka *et al.*, 1997).

Early studies of Gautel *et al.* (1996) revealed the existence of unique sequence repeats, approximately 45 amino acid residues in length, within the N-terminal portion of titin (**Fig.7**). These motifs were called “Z-repeats”.

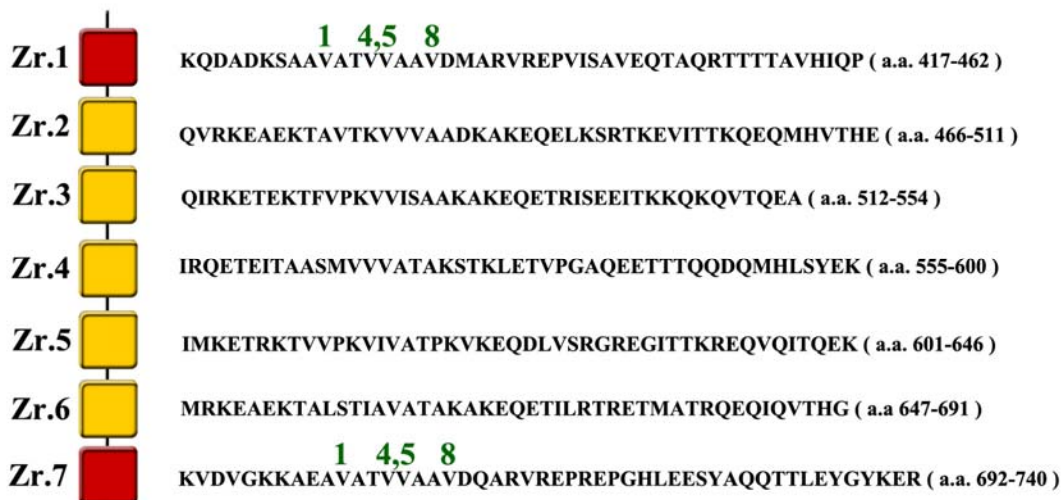


Figure 7. The sequences of titin Z-repeats. The numbers in green mark the EF-hands binding motif (4 valines) of repeats 1 and 7. The Uniprot entry Q8WZ42 (TITIN_HUMAN) was used for the residue numbering.

Notable heterogeneity of amplified fragments was observed during first attempts to isolate Z-repeat cDNA by PCR. It was the first evidence of alternative splicing occurring in the Z-disk portion of titin. Later experiments confirmed this finding and demonstrated that the number of Z-repeats varies from two to seven in different types of muscle fibers. The maximal number of repeats exists in cardiac tissue. Repeats 1 and 7 are the constitutive ones, and are always present in all muscle types. The other repeats are subject to alternative splicing.

Subsequent works by Ohtsuka *et al.* (1997), Young *et al.* (1998) and Ayoob *et al.* (2000) demonstrated the existence of interactions between titin Z-repeats

and the C-terminal domain of α -actinin. It was shown using *in vivo* techniques that different Z-repeats are invariably targeted to the Z-bands of myofibrils. The correlation of the number of titin repeats with the overall thickness of the Z-disk was also observed and, combined, a new hypothesis emerged. It was postulated that Z-repeats have a vital role in the organization of the entire Z-disk. It was proposed that the number of layers in the Z-disk is determined by the number of titin repeats, suggesting a “1 repeats=1 layer” rule. Such strict correlation, however, was disproven by later NMR and EM experiments (see Atkinson *et al.*, 2000; Luther & Squire, 2002).

The mechanisms of titin-actinin interactions and their putative role in the organization of Z-disk macromolecular scaffold present an intriguing scientific problem. The combination of several biophysical methods, as well as *in vivo* experiments, was used to get a glimpse of titin – α -actinin interactions and their regulation. NMR spectroscopy in conjunction with circular dichroism and limited proteolysis revealed that titin Z-repeats do not possess defined secondary or tertiary structure in solution (Atkinson *et al.*, 2000). The repeats demonstrate CD spectra typical for random coil peptides. However, a structural transition, which results in drastic increase of α -helical content, occurs upon binding α -actinin EF hand domains. The melting temperature of the complex is also significantly higher compared to that of the individual components (Joseph *et al.*, 2001).

The same techniques, applied to EF-hands domain, provided solid evidence of existence of α -helical elements. It was also shown that EF-hands 3–4 alone have a different fold than EF-hands 3–4 within larger constructs (EF-hands 1–2–3–4). This means that the amino-terminal half of the EF-hand domain strongly influences folding of the carboxy-terminal half, i.e. there is an additive folding effect (Joseph *et al.*, 2001). This finding is in contrast to other proteins which

contain EF-hands, for example calmodulin. The latter demonstrates complete independence of folding of its two calcium-binding domains.

It was shown that only α -actinin EF-hands 3–4 are “necessary and sufficient” to interact with titin Z-repeats (Joseph *et al.*, 2001). EF-hands 1–2 do not take part in this process. Subsequent titration experiments demonstrated 1:1 stoichiometry of the components in the complex. It was demonstrated that Z-repeats 1 and 7 have the highest binding affinity, $0,2\text{--}0,3\times 10^{-6}$ M and $0,1\text{--}0,25\times 10^{-6}$ M, respectively. As it was mentioned before, these repeats are present in all titin isoforms. Intermediate Z-repeats (subject to the alternative splicing) have insignificant affinity and, hence, are unlikely to form stable complexes with EF-hands 3–4. It was also shown that binding affinity does not change when the essential repeats 1 and 7 are tested both alone and in larger constructs, containing other repeats.

Further experiments with EF-hands 3-4 and Zr.7 provided additional details on the interaction mechanism. It was confirmed that Zr.7 adopts an α -helical conformation upon binding to EF-hands 3–4 of α -actinin. The orientation of the peptide between semi-open lobes of EF-hands is a result of combined action of hydrophobic and electrostatic forces. Four valine residues located in the middle of the Z-repeat are especially important for binding. In different species the numbering of amino acid residues in α -actinin homologues is different. However, the valine residues are generally conserved and are located at position 1-4,5-8 relative to each other. This fact gave the general name (i.e. *1-4,5-8 motif*) for such hydrophobic moieties.

Recent studies (Beck *et al.*, 2011) provided solid evidence that the same mechanism is involved in the interaction of α -actinin with muscle proteins palladin, myotilin and myopalladin. All of these proteins possess the above-mentioned binding motif composed of 4 hydrophobic residues, located at

positions 1-4,5-8. These residues are located within moieties with weakly defined secondary structure, and not in globular domains. The interaction occurs due to the burial of exposed hydrophobic side chains on the surface of both EF-hands 3–4 and the peptide ligand. The gain of secondary structure content as well as the rigidification of the protein backbone takes place during complex formation.

Taking into account available data, it is possible to conclude that binding via the 1-4,5-8 motif is a characteristic mechanism of α -actinin interactions with other Z-disk proteins. This binding plays a pivotal role in protein targeting and the Z-disk assembly.

As it was mentioned before, EF -hands of α -actinin 2 and α -actinin 3 are calcium insensitive. The amino acid residues which coordinate metal ions have mutated in the course of evolution of the muscle actinins. An alternative mechanism regulates binding of titin, palladin and other proteins to the EF hand domain.

α -actinin forms highly stable anti-parallel dimers through its central rod, made of spectrin repeats. At each end, these dimers have the ABD from one molecule of actinin and the EF-hands from the other molecule. A flexible linker (neck) exists between the ABD and the first spectrin repeat. This linker generates flexibility, which is necessary for binding of F-actin filaments. It was demonstrated by EM imaging that α -actinin can be positioned at different angles relatively to actin. However, the neck region plays another important role. It contains an array of hydrophobic residues which closely resembles the binding motif of titin Z-repeats. Hence, newly formed α -actinin dimers are unable to interact with titin or other proteins due to an autoinhibition effect. The presence of phosphoinositide PiP2 (**Fig.8**) disrupts the interaction between EF-hands 3–4

and the neck, so that the autoinhibition is lifted and α -actinin can interact with its binding partners.

The precise mechanism of PiP₂ interaction with α -actinin remains obscure to a large extent. It is suggested that the inositol head group of the molecule binds to the calponin-homology domain 2 of ABD, whereas the fatty-acid tail directly abolishes the binding of EF-hands 3–4 to the autoinhibitory moiety in the neck region of α -actinin.

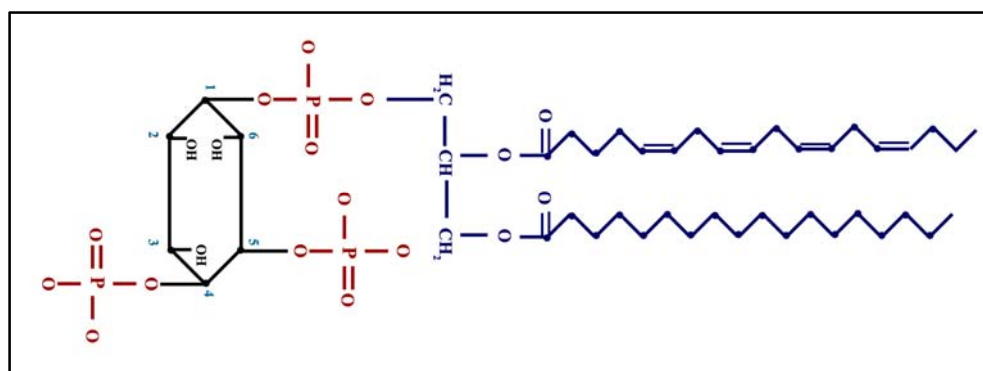


Figure 8. Chemical structure of phosphatidylinositol 4,5-bisphosphate

The enzyme phosphatidylinositol-4-phosphatase-5-OH-kinase is responsible for synthesis of PiP₂ (reviewed in Kwiatkowska, 2010). The enzyme appears in Z-disks of neonatal myocytes, proving the necessity of PiP₂ for the regulation of developmental processes at early stages, particularly for the formation of the Z-disk molecular scaffold (Young and Gautel, 2000). It is worth mentioning that phosphoinositides also regulate the functioning of α -actinin in non-muscle cells by affecting α -actinin binding to the actin cytoskeleton (Corgan *et al.*, 2004; Full *et al.*, 2007). Complementary regulatory mechanisms for interaction in the Z-disk scaffold involve proteolytic processing of α -actinin by calpain.

The goal of this brief introduction was to provide the reader with an outline of muscle biology, comprising such topics as tissue architecture, the basics of

contraction, proteome composition and, finally, the macromolecular scaffolds of the Z-disk. It was necessary to depict various aspects of the sarcomere structure and functions in order to demonstrate the importance of an ordered placement of its components and the organizing role of the Z-disk macromolecular grid. Although more than half a century of intensive research has greatly advanced our understanding of muscle function at a molecular level, significant gaps still exist in our knowledge regarding structural details of sarcomeric organization, in particular the structural and regulatory role of the Z-disk. It is clear that new advancements in muscle biology can be made only by involving experimental methods from different areas of biological science and implementing an interdisciplinary approach.

2 AIMS OF THE THESIS

The sarcomere – an elementary contractile unit of striated muscle fibers – clearly demonstrates amazing, almost crystalline-like arrangement of its components. Such a high degree of order is necessary to support numerous cycles of contraction-relaxation during muscle functioning. The correct arrangement of thin and thick filaments as well as of other muscular proteins is possible due to the existence of macromolecular grids at the Z-disk and the M-band of the sarcomere. The M-band, being a target of many researchers around the world, is actively investigated now. Conversely, the Z-disk – one of the most complicated macromolecular assemblies known – remains unexplored to a large extent.

The macromolecular grid is a key part of the Z-band. It provides an ordered space for all other protein to function in. Hence, the assembly of this grid and interaction of its components constitute an exciting topic in muscle biology. The present work aims at elucidating the fundamental aspects of titin – α -actinin interactions and their role in the formation of the Z-disk spatial scaffold.

The main goals of the present thesis are:

- ✓ Preparation of a library of titin and α -actinin protein constructs that will enable comprehensive studies of interactions between these structural proteins.
- ✓ Development of simple and reliable method(s) of reconstitution of muscle protein complexes using titin and α -actinin 2 as model proteins. The method(s) should allow production of the complexes in mg-scale and of high

purity, thus suitable for further structural studies with high-resolution techniques.

- ✓ Characterization of produced proteins and their complexes by biophysical methods. In particular, the Ca^{2+} -insensitive EF-hands of α -actinin 2 will be investigated to observe possible difference between domains 1-2 and 3-4.
- ✓ Generation of averaged molecular envelope models of titin/actinin complexes by SAXS to define their molecular dimensions. This information can be useful for judging if titin Z-repeats can perform the role of “macromolecular ruler”, defining Z-disk periodicity and width.

3 Materials and Methods

3.1 Chemicals

All chemical were ordered either from Sigma-Aldrich Co. or from Carl Roth GmbH. Ni-NTA Agarose (Cat. # 30210) was purchased from QIAGEN GmbH. The agarose for DNA electrophoresis was purchased from SERVA (“Agarose SERVA for DNA electrophoresis”, research grade; Cat. # 11404).

The concentrated 5^x dye from “Bio-Rad” was used for protein quantification accordingly to Bradford (“Bio-Rad Protein Assay Dye Reagent Concentrate”, Cat. # 500-0006).

The cDNA libraries of human skeletal and human heart muscle tissues were kindly provided by Dr. M.-L. Bang (Istituto Tecnologie Biomediche – Consiglio Nazionale delle Ricerche, Via Fratelli Cervi 93, 20090 Segrate, Milano.).

5 constructs of α -actinin 2 EF-hands 1-4 in Kan^R vectors were received from Prof. Dr. K. Djinovic-Carugo, University of Vienna, Vienna, Austria.

3.2 Kits

Purification of PCR products	Wizard® SV Gel and PCR Clean-Up System (“Promega”), Cat. # A9282
Plasmid purification from <i>E.coli</i> DH5 α	QIAprep Spin Miniprep kit (50) (“QIAGEN”), Cat. # 27104
DNA ligation (cohesive ends ligation)	Rapid DNA Ligation Kit (“Thermo Scientific”), Cat # K1422

3.3 Enzymes

Restrictions enzymes (type II restriction endonucleases)	“New England Biolabs” or “Fermentas” (now part of “Thermo Scientific”)
DNA polymerase for PCR	Phusion™ High-Fidelity DNA Polymerase (“Finnzymes”, now part of “Thermo Scientific”), Cat # F-534S
TEV protease / 3C-protease	Own preparation

3.4 Molecular markers and other reagents

“Roti®-Mark 10-150 kDa” marker (“Carl Roth”, Cat. # T850.1) was used for determination of protein molecular weight in SDS-PAGE. Size-exclusion chromatography standards were supplied by “Bio-Rad” (Cat. # 151-1901).

For estimation of DNA fragments sizes following markers were used: **a)** “GeneRuler 1kb DNA Ladder” from “Thermo Scientific” (Cat. # SM0312); **b)** “100 bp DNA Ladder” from “New England Biolabs” (Cat. # N3231S); **c)** “1 kb DNA Ladder” from “New England Biolabs” (Cat. # N3232S).

“Deoxynucleotide (dNTP) solution mix” (an equimolar solution of dATP, dCTP, dGTP, dTTP) was ordered from “New England Biolabs” (Cat. # N0447S).

3.5 Buffers and stock solutions

Milli-Q grade water was used for preparation of all buffers, media and solutions.

1 M Tris-HCl pH 7.5:

121.13 g of Tris (base) were dissolved in ~ 700 ml of Milli-Q water. pH was adjusted with HCl to 7.5. Water was added to the volume of 1 L. The buffer solution was filtered through 0.22 μm filter.

1 M Tris-HCl pH 9.0:

121.13 g of Tris(base) were dissolved in ~ 700 ml of Milli-Q water. pH was adjusted with HCl to 9.0. Water was added to the volume of 1 L. The buffer solution was filtered through 0.22 μm filter.

10^x phosphate buffered saline (PBS):

Na ₂ HPO ₄	14.4 g
NaH ₂ PO ₄	2.6 g
NaCl	79.8 g
KCl	2.0 g

The salts were dissolved in 800 ml of H₂O, pH was adjusted to 7.4 with HCl. Water was added up to 1 L. The saline was sterilized by autoclaving.

1 M dithiothreitol:

To prepare 1 M dithiothreitol (DTT) stock solution, 1.54 g of DTT powder were dissolved in Milli-Q water. Water was added to total volume of 10 ml, the solution was mixed thoroughly and filter through 0.22 μm filter. The solution was stored at – 20 degrees Celsius and used when required. Alternatively, DTT powder was added to the desired concentration during buffer preparation (for example, all SEC buffers).

1 M isopropyl- β -D-thiogalactoside (IPTG):

To prepare 1 M IPTG solution, 2.36 g of IPTG (“Carl Roth GmbH”) were dissolved in Milli-Q water. Water was added to total volume of 10 ml. The solution was filter-sterilized and stored at – 20 degrees Celsius, if not used immediately.

1 M sodium phosphate buffer, pH 7.0:

In order to prepare 1 L of Na-phosphate buffer, pH 7.0, 577 ml of 1M Na_2HPO_4 solution were mixed with 423 ml of 1 M NaH_2PO_4 solution. The final pH was checked with a “Mettler Toledo” pH-meter and adjusted, if necessary.

1 M sodium phosphate buffer, pH 7.4:

In order to prepare 1 L of Na-phosphate buffer, pH 7.4, 774 ml of 1M Na_2HPO_4 solution were mixed with 226 ml of 1 M NaH_2PO_4 solution. The final pH was checked with a “Mettler Toledo” pH-meter.

1 M sodium phosphate buffer, pH 8.0

In order to prepare 1 L of Na-phosphate buffer, pH 8.0, 932 ml of 1M Na_2HPO_4 solution were mixed with 68 ml of 1 M NaH_2PO_4 solution. The final pH was checked with a “Mettler Toledo” pH-meter.

2 M glucose stock solution:

To prepare 2 M stock solution of glucose, 18 g of D-glucose (MW=180.16 g/mol) were dissolved in Milli-Q water. Water was added then to final volume of 50 ml. The solution was filter-sterilized.

5 M NaCl stock solution:

This solution was prepared by dissolving 292.2 g of NaCl (MW=58.44 g/mol) in Milli-Q water to reach final volume of 1 L. The solution was filtered through 0.22 μm filter.

3 M KCl stock solution:

This solution was prepared by dissolving 223.65 g of KCl (MW=74.55 g/mol) in water to the total volume of 1 L.

1 M MgSO_4 :

This solution was prepared by dissolving 24.6 g of $\text{MgSO}_4 \times 7\text{H}_2\text{O}$ in Milli-Q water (final volume should be 100 ml). The solution was sterilized by autoclaving or by filtering.

1 M di-sodium phosphate buffer:

This solution was prepared by dissolving 268 g of $\text{Na}_2\text{HPO}_4 \times 7\text{H}_2\text{O}$ (MW=268.03 g/mol) in Milli-Q water to reach final volume of 1 L.

1 M sodium di-hydrogene phosphate buffer:

This solution was prepared by thorough mixing 137.99 g of $\text{NaH}_2\text{PO}_4 \times \text{H}_2\text{O}$ (MW=137.99 g/mol) with Milli-Q water to reach final volume of 1 L.

Staining solution for SDS-gels (“safe-stain”):

100 mg of Coomassie Brilliant Blue G-250 were dissolved in 1 L of Milli-Q water and stirred thoroughly to produce highly homogeneous solution. Hydrochloric acid (HCl) was added to final concentration of 35 mM.

Destaining solution for SDS-gels:

This solution was prepared by mixing 200 ml of ethanol (technical grade), 50 ml of glacial acetic acid and 25 ml of 100 % glycerol. The Milli-Q water was added to the total volume of 500 ml.

Sample loading buffer for SDS-PAGE:

In order to prepare 10 ml of 4^x sample loading buffer for SDS-PAGE 2 ml of 1M Tris-HCl (pH 6.8), 0.8 g of SDS, 4 ml of glycerol (100%), 0.4 ml of 14.7 M β -ME, 1 ml of 0.5 M EDTA and 8 mg of bromophenol blue were mixed in 14 ml “falcon” tube. Water was added to final volume of 10 ml. The mixture was vortexed thoroughly to produce homogeneous solution. The loading buffer was aliquoted in 1 ml portions and stored at – 20 degrees Celsius for several months.

3.6 Antibiotics

1000^x Kanamycin 50 mg/ml in Milli-Q water, filter-sterilized.

1000^x Chloramphenicol 34 mg/ml in 100 % ethanol (molecular biology grade), filter-sterilized.

1000^x Spectinomycin 50 mg/ml in Milli-Q water, filter-sterilized.

3.7 Bacterial growth media

LB (lysogeny broth):

This medium was used both for general bacteria cultivation and for protein expression. There are Miller and Lennox recipes of this medium. The following recipe is for 1 L of medium accordingly to Miller (Miller, 1972):

NaCl	10 g
Trypton	10 g
Yeast extract	5 g

Final pH was adjusted to ~7.0 with 5 M NaOH. Then Milli-Q water was added to final volume of 1 L. LB medium was sterilized by autoclaving.

TB (terrific broth):

This rich medium was used for protein overexpression, because it generally gave higher yield of bacterial biomass than LB and, hence, more protein was produced. The described recipe is for 1 L of medium:

24 g	yeast extract
12 g	casein, enzymatically digested
4 ml	glycerol (100%)
12.5 g	K ₂ HPO ₄
2.3 g	KH ₂ PO ₄

The final pH of the medium was adjusted to ~7.2 with 5 M NaOH. The TB medium was sterilized by autoclaving.

Autoinduction medium:

Autoinduction is an alternative approach for heterologous protein expression in *E.coli* which has some advantages over conventional system that utilizes T7lac promoter. The basic principles of the method are outlined in Studier, 2005. The key advantages of given system are following: **a)** there is no

Trace elements, 1000^x:

FeCl ₃ -6H ₂ O	1.35 g
CaCl ₂ -2H ₂ O	0.294 g
MnCl ₂ -4H ₂ O	0.197 g
ZnSO ₄ -7H ₂ O	0.287 g
CoCl ₂ -6H ₂ O	0.04 g
CuCl ₂ -2H ₂ O	0.034 g
NiCl ₂ -6H ₂ O	0.047 g
Na ₂ MoO ₄ -2H ₂ O	0.048 g
Na ₂ SeO ₃	0.034 g
H ₃ BO ₃	0.012 g

Milli-Q water was added up to 100 ml. The solution was sterilized by filtering.

Complete ZYP-5052 autoinduction medium for protein expression (1 L):

ZY medium	928 ml
P solution, 20 ^x	50 ml
Solution 5052, 50 ^x	20 ml
Trace elements, 1000 ^x	200 µl
1 M MgSO ₄	2 ml

SOB medium:

This medium was used for small-scale *E.coli* cultivation, particularly in preparation of competent cells. The following recipe is for 1 L of medium:

20 g tryptone (2 % w/v)

5 g yeast extract (0.5 % w/v)

2.4 g MgSO₄ (20 mM final)

0.584 g NaCl (10 mM final)

0.186 g KCl (2,5 mM final)

The final pH of the medium was adjusted to ~7.5 with NaOH. Milli-Q water was added then to the exact volume of 1 L. Medium was sterilized by autoclaving.

SOC medium:

This medium was used for the efficient transformation of competent cells. In order to prepare it, previously prepared and sterilized SOB medium was supplemented with 2 M glucose stock solution to 20 mM final glucose concentration.

3.8 Expression plasmids:

All proteins, used in this study, were cloned into plasmids that contain T7lac promoter and, hence, allow inducible protein overexpression in *E.coli* cells. All plasmids were taken from vector collection of EMBL Protein Expression and Purification Facility.

Vector	Characteristics
pET M-11	contains 6His-tag at N-terminus, TEV cleavage site, Kan ^R
pET M-14	contains 6His-tag at N-terminus, 3C-protease cleavage site, Kan ^R
pET GST-1a	contains 6His-GST-tag at N-terminus, TEV cleavage site, Kan ^R
pET Z2_1a	contains 6His-Z-tag at N-terminus, TEV cleavage site, Kan ^R
pET 28a	contains 6His-T7-tag, thrombin cleavage site, Kan ^R
pCDF-11	contains 6His-tag at N-terminus, TEV cleavage site, Spec ^R
pCDF-13	contains no affinity tags, Spec ^R
pCDF-Duet	contains 6His-tag at N-terminus and TEV cleavage site for multiple cloning site (MCS) I, no tags for MCS II, derived from pACYC-Duet (Novagene), Spec ^R

Table 1. Vectors that were used for protein expression/co-expression experiments and their specific features.

Plasmids, utilized in this study, allowed expression of recombinant proteins fused with either single 6His-tag or double affinity tags at N-terminus of a protein. Polyhistidine affinity tag allowed rapid purification of proteins of interest by immobilised metal ion affinity chromatography.

3.9 *E.coli* strains and their genotypes

The key *E.coli* strains used in present study and their genotypes are listed below:

DH5 α F⁻ endA1 glnV44 thi-1 recA1 relA1 gyrA96 deoR nupG Φ 80dlacZ Δ M15 Δ (lacZYA-argF)U169, hsdR17(r_K⁻ m_K⁺), λ -

BL21 DE3 F⁻ ompT gal dcm lon hsdS_B(r_B⁻ m_B⁻) λ (DE3 [lacI lacUV5-T7 gene 1 ind1 sam7 nin5])

BL21 DE3 RIL F ompT hsdS_B(r_B⁻ m_B⁻) dcm⁺ Tet^r gal endA Hte [argU ileY leuW Cam^r]

BL21 DE3 RP F⁻ ompT hsdS_B(r_B⁻ m_B⁻) dcm⁺ Tet^r gal endA Hte [argU proL Cam^r]

BL21 DE3 Rosetta2 pRARE II F⁻ ompT hsdS_B(r_B⁻ m_B⁻) gal dcm (DE3) pRARE2 (Cam^R)

Detailed information about commonly used *E.coli* strains and their genotypes was found in Casali, 2003 (*Methods in Molecular Biology*). All “rare codon” optimized expression strains possessed additional chloramphenicol resistance.

3.10 Electrophoresis and enzymatic manipulation of DNA

DNA fragments (PCR products, linearized plasmids etc) were separated by electrophoresis in agarose gels (0.8-1%) in 1^x TAE or TBE buffers. The electrophoresis was run at 80 V (constant voltage). DNA fragments were visualized under UV light; ethidium bromide was added to the agarose gels during preparation. The separated fragments were purified from agarose gels using Wizard® purification kit from “Promega”

Enzymes for DNA restriction were ordered either from “New England Biolabs” (“High Fidelity” type of improved enzymes) or “Fermentas” (“Fast Digest” type of improved enzymes). The restriction reactions were carried out accordingly to protocols, outlined by corresponding vendors.

DNA fragments, produced by PCR, were cloned into expression vectors by using ordinary molecular cloning protocols (concisely described in “*Molecular cloning: a laboratory manual*”, Cold Spring Harbor Laboratory Press, 3rd Ed.). In brief, both the vector of choice and DNA fragment were digested by selected pair of restriction enzymes. This resulted in a pair of compatible cohesive ends, which allowed correct positioning of the insert within vector. Both digested insert and linearised vector were separated by electrophoresis in agarose gel. DNA fragments were isolated from gel using Wizard® SV Gel and PCR Clean-Up System (“Promega”) accordingly to vendor’s protocol. Purified vector backbone and insert were mixed in 1:3 ratio and ligated using “Quick ligation kit” from “Fermentas”. The ligation mix was directly used to transform chemically competent *E.coli* DH 5 α cells.

So called “PCR cloning” (overlap extension PCR cloning) was utilized as an alternative method for quick cloning of small constructs. The original protocol described at Bryksin and Matsumura, 2010 was strictly followed for PCR cloning applied in this study.

3.11 DNA sequencing

Plasmid DNA sequencing was ordered as a service from company “Eurofins” (MWG-Operon). The “Value Read” sequencing (from “Single Read Services”) was ordinarily used. For conventional sequencing reads T7 and T7term primers, available from “Eurofins”, were utilized.

3.12 Coding DNA sequence of human titin Z-repeats

```
1 AAA CAA GAT GCT GAC AAA AGT GCA GCT GTT GCG ACT GTT GTT GCT GCC GTT GAT ATG GCC
61 AGA GTG AGA GAA CCA GTG ATC AGC GCT GTA GAG CAG ACT GCT CAG AGG ACA ACC ACG ACT
121 GCT GTG CAC ATC CAA CCT GCT CAA GAA CAG GTA AGA AAG GAA GCG GAG AAG ACT GCT GTA
181 ACT AAG GTA GTA GTG GCC GCC GAT AAA GCC AAG GAA CAA GAA TTA AAA TCA AGA ACC AAA
241 GAA GTA ATT ACC ACA AAG CAA GAG CAG ATG CAC GTA ACT CAT GAG CAG ATA AGA AAA GAA
301 ACT GAA AAA ACA TTT GTA CCA AAG GTA GTA ATT TCC GCA GCT AAA GCC AAA GAA CAA GAA
361 ACT AGA ATT TCT GAA GAA ATT ACT AAG AAA CAG AAA CAA GTA ACT CAA GAA GCA ATA AGA
421 CAG GAA ACT GAG ATA ACT GCT GCA TCC ATG GTG GTA GTT GCC ACT GCA AAG TCC ACA AAA
481 CTA GAA ACA GTC CCG GGA GCT CAA GAA GAA ACT ACC ACA CAA CAA GAT CAA ATG CAC CTA
541 AGT TAT GAA AAG ATA ATG AAG GAA ACT AGG AAA ACA GTT GTA CCT AAA GTC ATA GTT GCC
601 ACA CCC AAA GTC AAA GAA CAA GAT TTA GTA TCA AGA GGT AGA GAA GGC ATT ACT ACC AAA
661 AGA GAA CAA GTG CAA ATA ACT CAG GAG AAG ATG AGA AAG GAA GCC GAG AAA ACT GCC TTG
721 TCT ACA ATA GCA GTT GCT ACT GCT AAA GCC AAA GAA CAA GAA ACA ATA CTG AGA ACT AGA
781 GAA ACT ATG GCT ACT AGA CAA GAA CAA ATC CAA GTT ACC CAT GGA AAG GTG GAC GTT GGA
841 AAA AAG GCT GAA GCT GTA GCA ACA GTT GTT GCT GCA GTA GAC CAG GCC CGA GTC AGA GAG
901 CCC AGA GAG CCT GGG CAT CTT GAA GAA TCC TAT GCT CAG CAG ACC ACT TTG GAG TAC GGA
961 TAT AAG GAA CGC
```

3.13 Translation of cDNA sequence of human titin Z-repeats

```
KQDADKSAAVATVVAAVDMARVREPVISAVEQTAQRTTTTAVHIQPAQEQRKEAEKTAV
TKVVVAADKAKEQELKSRTKEVITTKQEQMHVTHEQIRKETEKTFVPKVVISAACAKEQE
TRISEEITKKQKQVTQEAIRQETEITAASMVVATAKSTKLETVPGAQEETTTQDDQMHLL
SYEKIMKETRKTVVPKIVATPKVKEQDLVSRGREGITTKREQVQITQEKMRKEAEKTAL
STIAVATAKAKEQETILRTRETMATRQEIQVTHGKVDVGKKA EAVATVVAAVDQARVRE
PREPGHLEESYAQQTTLEYGYKER
```

This protein sequence represents the complete array of titin Z-repeats from 1 to 7. Corresponding amino acid residues in full-length titin sequence (Uniprot entry Q8WZ42) are 417-740.

3.14 The list of primers

Table. 2. The primers that were used for cloning of titin and α -actinin protein constructs.

Primer	Sequence	Comment
Zr1-Zr7forward	5 ' GAATCTTTATTTTCAGGGCGCCATGAAACA AGATGCTGACAAAAGTGCAG-3 '	PCR-cloning of Zr.1- 7 into pET-M 11 vector
Zr1-Zr7reverse	5 ' CAAGACACGCCTTGTGACTGTCTCAGCGTT CCTTATATCCGTACTCCAAAG-3 '	PCR-cloning of Zr.1- 7 into pET-M11 vector
Zr. 1forward	5 ' GAATCTTTATTTTCAGGGCGCCATGAAACA AGATGCTGACAAAAGTGCAGC-3 '	PCR-cloning of Zr.1 into pET-M 11 vector
Zr. 1reverse	5 ' CGGAGCTCGAATTCGGATCCGGTACTCAAG GTTGGATGTGCACAGCAGTCGTG-3 '	PCR-cloning of Zr.1 into pET-M 11 vector
Zr. 2forward	5 ' GAATCTTTATTTTCAGGGCGCCATGCAGGT AAGAAAGGAAGCGGAGAAGAC-3 '	PCR-cloning of Zr.2 into pET-M 11 vector
Zr. 2reverse	5 ' CGGAGCTCGAATTCGGATCCGGTACTCACT CATGAGTTACGTGCATCTGCTC-3 '	PCR-cloning of Zr.2 into pET-M 11 vector
Zr. 3forward	5 ' GAATCTTTATTTTCAGGGCGCCATGCAGAT AAGAAAAGAACTGAAAAAC-3 '	PCR-cloning of Zr.3 into pET-M 11 vector
Zr. 3reverse	5 ' CGGAGCTCGAATTCGGATCCGGTACTCATG CTTCTTGAGTTACTTGTCTG-3 '	PCR-cloning of Zr.3 into pET-M 11 vector
Zr. 4forward	5 ' GAATCTTTATTTTCAGGGCGCCATGATAAG ACAGGAACTGAGATAACTG-3 '	PCR-cloning of Zr.4 into pET-M 11 vector
Zr. 4reverse	5 ' CGGAGCTCGAATTCGGATCCGGTACTCACT TTTCATAACTTAGGTGCATTTG-3 '	PCR-cloning of Zr.4 into pET-M 11 vector
Zr. 5forward	5 ' GAATCTTTATTTTCAGGGCGCCATGATAAT GAAGGAACTAGGAAAACAG-3 '	PCR-cloning of Zr.5 into pET-M 11 vector
Zr. 5reverse	5 ' CGGAGCTCGAATTCGGATCCGGTACTCACT TCTCCTGAGTTATTTGCACTTG-3 '	PCR-cloning of Zr.5

		into pET-M 11 vector
Zr. 6forward	5 ' GAATCTTTATTTTCAGGGCGCCATGATGAG AAAGGAAGCCGAGAAAAGT-3 '	PCR-cloning of Zr.6 into pET-M 11 vector
Zr. 6reverse	5 ' CGGAGCTCGAATTCGGATCCGGTACTCATC CATGGGTAACCTTGGATTTGTTC-3 '	PCR-cloning of Zr.6 into pET-M 11 vector
Zr. 7forward	5 ' GAATCTTTATTTTCAGGGCGCCATGAAGGT GGACGTTGGAAAAAGGCTGAA-3 '	PCR-cloning of Zr.7 into pET-M 11 vector
Zr. 7reverse	5 ' CGGAGCTCGAATTCGGATCCGGTACTCAGC GTTCCCTTATATCCGTAATC-3 '	PCR-cloning of Zr.7 into pET-M 11 vector
Zr. 1-7 (pET Z2_1a) forward	5 ' GAATCTTTATTTTCAGGGCGCCATGAAACA AGATGCTGACAAAAGTGCAGC-3 '	PCR-cloning of Zr.1- 7 into pET Z2_1a vector
Zr. 1-7 (pET Z2_1a) reverse	5 ' CTCGAATTCGGATCCGGTACCTCACCACCA CCAGCGTTCCTTATATCCGTAATC-3 '	PCR-cloning of Zr.1- 7 into pET Z2_1a vector
Zr.1 (GST) forw	5 ' CCTCCAAAAGGATCTGGCAGTGGTTCTGAG AATCTTTATTTTCAGGGCAAACAAGATGCTGA CAAAGTGCAGC-3 '	cloning of Zr.1 into pET GST-1a
Zr.1 (GST) rev	5 ' CGGAGCTCGAATTCGGATCCGGTACTCACC ACCACCAAGGTTGGATGTGCACAGCAGTCGTG -3 '	cloning of Zr.1 into pET GST-1a
Zr.3 (GST) forw	5 ' CCTCCAAAAGGATCTGGCAGTGGTTCTGAG AATCTTTATTTTCAGGGCCAGGTAAGAAAGGA AGCGGAG-3 '	cloning of Zr.3 into pET GST-1a
Zr.3 (GST) rev	5 ' CGGAGCTCGAATTCGGATCCGGTACTCACC ACCACCATGCTTCTTGAGTACTTGTCTG- 3 '	cloning of Zr.3 into pET GST-1a
Zr.7 (GST) forw	5 ' CCTCCAAAAGGATCTGGCAGTGGTTCTGAG AATCTTTATTTTCAGGGCAAAGGTGGACGTTGG AAAAAG-3 '	cloning of Zr.7 into pET GST-1a
Zr.7 (GST) rev	5 ' CGGAGCTCGAATTCGGATCCGGTACTCACC	cloning of Zr.7 into

	ACCACCAGCGTTCCTTATATCCGTA	pET GST-1a
EF1-4 (pCDF-11) forward	5' GTTTAACTTTAAGAAGGAGATATAATGGAA GTTCTGTTCCAGGGGCCCGCC	re-cloning EF-hands 1-4 into pCDF-11 vector
EF1-4 (pCDF-11) reverse	5' AGTTAGAGACCAAGACACGCCTAGTTACAG ATCGCTCTCCCCGTAGAGTG-3'	re-cloning EF-hands 1-4 into pCDF-11 vector
EF1-4 (pCDF-13) forward	5' CTTTAATAAGGAGATATACCATGGAGCAGA TGAATGAGTTCAGAGCCTCC-3'	re-cloning EF-hands 1-4 into pCDF-13 vector
EF1-4 (pCDF-13) reverse	5' CGGAGCTCGAATTCGGATCCGGTACCATAG TTACAGATCGCTCTCCCCGTAGAGTG-3'	re-cloning EF-hands 1-4 into pCDF-13 vector
EF3-4 (pCDF-13) forward	5' CTTTAATAAGGAGATATACCATGGCCATGA CCGACACTGCCGAGCAGGTC-3'	re-cloning EF-hands 3-4 into pCDF-13 vector
EF3-4 (pCDF-13) reverse	5' CGGAGCTCGAATTCGGATCCGGTACCATAG TTACAGATCGCTCTCCCCGTAGAGTGC-3'	re-cloning EF-hands 3-4 into pCDF-13 vector
α -actinin Δ forward	5' CACATGGCGGCCGCGAGAGGCTGATGGAAG AATATGAGAGGC-3'	primers for α -actinin with deleted ABD (pET-28a)
α -actinin Δ reverse	5' CATGTGCTCGAGTGATCACAGATCGCTCTC CCCGTAGAGTGCG-3'	primers for α -actinin with deleted ABD (pET-28a)
$\frac{1}{2}$ α -actinin Δ forward (the 1 st half)	5' AGCCAGGATCCGAATTCTGAGAGGCTGATG GAAGAATATGAGAGGC-3'	
$\frac{1}{2}$ α -actinin Δ reverse (the 1 st half)	5' CACATGGTTCGACCTATCTCTCTAGGGCTTC TCTCCTCTTCTG-3'	
$\frac{1}{2}$ α -actinin Δ forward (the 2 nd)	5' CACATGCATATGCAGCTTCACCTGGAGTTT GCCAAGAGG-3'	

half)		
½ α -actinin Δ reverse (the 2 nd half)	5 ' CACATGCTCGAGCTATCACAGATCGCTCTC CCCGTAGAGTGCG - 3 '	

3.15 Preparation of the chemically competent *E.coli* cells

The chemically competent cells (both for cloning and protein expression) were prepared accordingly to the protocols, described in Inoue, 1990 and Tu, 2005.

3.16 Transformation of the chemically competent *E.coli* cells

The transformation of chemically competent cells was performed by so called “heat-shock” method. In brief, 10 µl of ligation mix was added to 50 µl of competent cells. The cell suspension was gently mixed and incubated on ice for 15 min. The eppendorf tube with cell suspension was placed for 60 second in water bath (+ 42 degrees Celsius) for heat shock. At next step cells were incubated on ice for 5 min. The cell suspension was supplemented with SOC medium and incubated for 1 hour in shaking incubator (+ 37 degrees Celsius) in order to revitalize cells. After incubation cells were plated at LB-agar plates containing appropriate antibiotics.

Comprehensive guidelines and troubleshooting for this method were found in Seidman *et al.*, 1997, Hanahan, 1983 and Hanahan, 1985.

3.17 Protein overexpression in *E.coli*

The *E.coli* strain BL21 DE3 Rosetta2 pRARE II was chosen as a main expression strain after several rounds of testing and optimization. LB or TB media were used for large-scale bacteria cultivation. A typical protocol for protein overexpression includes following steps:

- 1) The chemically competent *E.coli* cells were transformed with expression plasmid, carrying the protein construct of choice. The transformation was performed accordingly to the described above “heat-shock” method. After transformation cells were grown in SOC medium for 1 hour and plated on the LB-agar plates, supplemented with the appropriate antibiotics. The plates were incubated overnight at the incubator (+37 degrees Celsius). The cells should be plated with care in order to result in separate colonies after incubation.
- 2) A single colony was transferred with sterile inoculation loop into 250 ml baffled flask with LB or TB medium, containing antibiotics. The amount of medium in the flask allowed sufficient aeration. This pre-culture was incubated overnight in the shaking incubator (+ 37 degrees Celsius, 200 rpm).
- 3) The overnight pre-culture of high optical density was used as a starter for large 1 L cultures next morning. It was diluted with fresh cultivation medium with antibiotics to produce final ratio of 1:100 (i.e. 10 ml per 1 L of fresh LB). The expression cultures were typically grown in 3 L baffled conical flasks with cotton plugs in order to ensure proper aeration (+ 37 degrees Celsius, 190 rpm).
- 4) When *E.coli* cultures reached the $OD_{600nm} \approx 0.8$, the protein expression was induced with 1 M IPTG solution. It was added to the cultures to 0.7 mM final concentration.
- 5) The temperature was decreased to 21 degrees Celsius for the overnight cultivation.
- 6) The cells were harvested by centrifugation (JLA 8.1000 rotor, “Beckman” centrifuge, 25 min at 4500 rpm) next morning.

3.18 Size-exclusion chromatography/analytical size-exclusion chromatography

Preparative purification of proteins and protein complexes was performed using either “Superdex 75” or “Superdex 200” 16/60 columns (“GE Healthcare”). Analytical SEC was performed with pre-packed “Tricorn” 10/30 columns (either “Superdex 75” or “Superdex 200” matrix) from “GE Healthcare”. All SEC buffers were degassed under low pressure and filtered through 0.22 µm filter.

3.19 Protein identification

Protein identification was performed either by MALDI-TOF or by “peptide fingerprinting” (MALDI mass-spectrometry of enzymatically digested protein). These services were provided both by “Sample Preparation and Characterization” facility (EMBL-Hamburg) and Proteomics core facility (EMBL-Heidelberg).

3.20 Protein electrophoresis

3.20.1 Protein electrophoresis equipment:

Following equipment was routinely used for protein electrophoresis:

- 1) Mini-PROTEAN® Tetra Cell (“Bio-Rad”) for Tris-Tricine minigels and native PAGE.
- 2) XCell SureLock® Mini-Cell (“Life Technologies™”) for 4-20% gradient gels.

3.20.2 SDS-PAGE (gradient gel, 4%-20%):

The standard equipment for gradient gel preparation was used. The gels were made to be used with “Invitrogene” gel-running system. The gels were casted in batches of 10 gels.

Gel buffer, 3^x:

Tris (base)	3 M
HCl	1 M
SDS	0.3 % w/v
Final pH	8.45

“Low percentage gel” recipe:

- 13 ml of gel buffer (3^x)
- 6.5 ml of acrylamide/bis-acrylamide mixture
- 30.5 ml of Milli-Q water

“High percentage gel” recipe:

- 13 ml of of gel buffer (3^x)
- 25 ml of acrylamide/bis-acrylamide mixture
- 8 ml of Milli-Q water
- 4 ml glycerol (100%)

500 µl of TEMED and 51 µl of APS were added to the gel solutions for the polymerization.

3.20.3 SDS-PAGE (Tris-Tricine):

Tricine-SDS-PAGE is widely used method when it is necessary to separate small proteins (MW less than 30 kDa) and peptides. This method is reliable and produces results of good quality. Tricine-SDS-PAGE can also be used for proteins up to 100 kDa. Given method is described in great details in Schägger, 2006. The timeline and the troubleshooting guide are also provided in the paper mentioned above. Here only the basic solution recipes will be outlined.

Gel buffer, 3^x:

Tris (base)	3 M
HCl	1 M
SDS	0.3 %
Final pH	~8.45

Anode buffer, 10^x:

Tris (base)	1 M
HCl	0.225 M
Final pH	~8.9

Cathode buffer, 10^x:

Tris (base)	1 M
Tricine	1 M
SDS	1 %
Final pH	~8.25

3.20.4 Native-PAGE (for acidic and neutral proteins with pI less than 7.0):

This method can be used as a supplementary for estimating oligomeric state of a protein or formation of a protein-protein complex. In present study, native-PAGE was employed to characterise α -actinin Δ and its complex with titin. The suitable percentage of the gel and running conditions were detected experimentally. Only freshly made gels were used. The gel runs were performed at + 4 degrees Celsius, ideally on ice bath.

The recipes provided here are for 5 mini-gels (10%).

Separating gel:

1.5M Tris-HCl, pH 8.9	7 ml
30% Acrylamide /0.8% bis Acrylamide	9.3 ml
Milli-Q water	12.3 ml
TEMED	23 μ l
10% APS	100 μ l

Stacking gel:

0.5 M Tris-HCl, pH 6.8	2.5 ml
30% Acrylamide /0.8% bis Acrylamide	1 ml
Milli-Q water	6.4 ml
TEMED	10 μ l
10% APS	100 μ l

Gel running buffer, 1^x:

Trizma	1.21 g
Glycine	5.32 g
Milli-Q water	200 ml

Note: pH of the running buffer has to be adjusted to 8.9.

3.20.5 Protocol for staining gels with “safe-stain”:

SDS-PAGE gels were normally stained with “safe-stain” solution which contains Coomassie Brilliant Blue G-250. This protocol is quick and reliable; the “safe-stain” solution does not contain hazardous components. Gels were rinsed 3 times with MilliQ water (~50 ml per gel). For a rinse a cuvette with a gel and water was heated for 30 seconds in a microwave oven and placed on a shaker for 5 min. This step was necessary to remove an SDS from the gel because it affects staining. The gel was covered with safe-stain” (~30 ml per gel), heated for 30 seconds in a microwave oven for staining and placed on a shaker for 15 min.

Samples for mass-spectrometry analysis were stained without heating. The staining without heating usually took 2-3 hours. In case of small quantity of analyzed protein, the silver staining was used instead of the “safe-stain” protocol mentioned above.

3.20.6 Protocol for silver staining of the gels:

Stock solutions required: 1) 50 % v/v acetone in Milli-Q water; 2) 50 % w/v trichloroacetic acid in Milli-Q water; 3) 37 % v/v formaldehyde; 4) 10 % w/v Na₂SO₃ in Milli-Q water; 4) 20 % w/v AgNO₃ in Milli-Q water (protect from sunlight).

The routinely utilised protocol contained following steps:

- 1) The gel was fixed for 5 min in “fixing solution” (30 ml of acetone stock solution, 750 µl of trichloroacetic acid stock solution, 12.5 µl of formaldehyde stock solution).
- 2) The gel was rinsed with Milli-Q water 3 times, 50 ml of water each time.
- 3) The gel was washed thoroughly in 30 ml of water for 5 min.
- 4) The gel was pre-treated with 30 ml of acetone stock solution.
- 5) The gel was rinsed with Milli-Q water 3 times, 50 ml of water each time.
- 6) The gel was impregnated in following solution: 30 ml of Milli-Q water, 300 µl of formaldehyde stock solution, 400 µl of AgNO₃ stock solution.
- 7) The gel was rinsed with Milli-Q water 5 times, 50 ml of water each time.
- 8) The gel was developed in “developing solution” (30 ml of Milli-Q water, 600 mg of Na₂Ca₃, 12 µl of formaldehyde stock solution, 12.5 µl of Na₂SO₃ stock solution).
- 9) When the clear bands had appeared, the further development was stopped with “stopper solution” (30 ml of Milli-Q water, 300 µl of glacial acetic acid).

This protocol was quick and reliable. It gave the quality of staining comparable with that of commercial kits. It was possible to detect as little as 1-5 ng of protein on SDS-gel using this highly sensitive method.

3.21 Concentration of the purified proteins

Purified proteins and protein complexes were concentrated for SEC, spectroscopic and SAXS measurements by using centrifugal concentrators of different volumes and molecular weight cut-offs. TheSpin-X® UF concentrators were ordered from Corning®.

Following types of concentrators were used:

20 ml	6 ml
Corning® #431487 (5 kDa cut-off)	Corning® # 431482 (5 kDa cut-off)
Corning® # 431488 (10 kDa cut-off)	Corning® # 431483 (10 kDa cut-off)
Corning® # 431489 (30 kDa cut-off)	Corning® # 431484 (30 kDa cut-off)

Regenerated cellulose Amicon® Ultra Centrifugal filters Ultracell® -3k (“Merck KGaA”) were used for concentration of separate titin Z-repeats (MW≈5 kDa).

3.22 Storage of the purified proteins

Purified proteins were concentrated using Corning® concentrators, aliquoted into 1.5 ml eppendorf tubes or 0.5 ml thin-wall PCR tubes and flash-frozen in liquid nitrogen. In case of necessity, sterile glycerol was added to protein samples as a cryoprotectant (5% (v/v) final concentration) before freezing.

3.23 Protein dialysis

Spectra/Por® Dialysis membranes were used for the dialysis of protein samples against the buffer of choice. Molecular weight cut-offs of 3500 Da, 6000-8000 Da and 12 000-14 000 Da were routinely used. The dialysis was usually performed overnight.

3.24 Measurements of protein concentration

Protein concentration was routinely measured by “Nanodrop-1000” (“Thermo Scientific”). For these measurements, the molecular weight and extinction coefficient ϵ of a protein were used. The “Bradford Assay” was applied for an approximate estimation of protein concentration (Bradford, 1976; Compton & Jones, 1985).

3.25 Routine calculation of protein parameters

Essential protein parameters, such as molecular mass, extinction coefficient, isoelectric point etc., were calculated by using ProtParam software at ExPASy server (Gasteiger *et al.*, 2005). Raw amino acid sequences of proteins were used as an input. The sequences were retrieved from Uniprot database (Jain *et al.*, 2009).

3.26 Static Light Scattering

The guidelines for experimental design of SLS measurements were taken from Folta-Stogniew, 2006.

In brief, purified proteins or protein complexes were run on analytical “Tricorn” size-exclusion column with “miniDAWN” SLS device (“Wyatt Technology Corporation”) connected to the chromatograph (AEKTA Purifier). The “miniDAWN” SLS machine measured scattering from 3 different angles. Molecular mass of the proteins was determined by applying “Astra” software (v.5.3.4.11) to the recorded scattering data. UV absorption was recorded by AEKTA Purifier software “Unicorn” v5.1.

3.27 Circular Dichroism measurements

The following buffer was used for the circular dichroism measurements:

30 mM Na-phosphate, pH 8.0

2 mM β -ME

The samples were exhaustively dialyzed against given buffer overnight.

All CD spectra measurements were performed at the “Chirascan™” CD Spectrometer (“Applied Photophysics”, UK) available at the “Sample Preparation and Characterization Facility” (EMBL-Hamburg). Following software was used in experiments: **a)** CDNN v2.1 (CD spectra deconvolution) by Dr. Gerald Böhm; **b)** “Pro-Data Viewer” by “Applied Photophysics” v4.2.13 (supplied with the CD instrument); **c)** “Chirascan” by “Applied Photophysics” (supplied with the instrument). For data analysis the K2D3 server (<http://www.ogic.ca/projects/k2d3//index.html>) was used (Louis-Jeune *et al.*, 2012). Quartz cuvettes (“Hellma”) with path-length of 1 mm were used for

measurements. The spectra were recorded at +10 degrees Celsius (as well as all SAXS measurements). The far-UV spectra from 190 nm to 260 nm were recorded. The concentrations of proteins or their complexes were in range of 5-10 μ M (adjustment of the concentration was necessary in order to provide the spectra of the best possible quality). Protein concentrations for experiments were measured by “Nanodrop-1000” (“Thermo Scientific”), using molecular mass and absorption coefficient. Each CD spectrum was recorded 10 times.

The general experimental guidelines were taken from Greenfield, 2006. Additional information on the application of circular dichroism spectroscopy to protein interactions studies was found in Kelly and Price, 2006.

3.28 Analytical ultracentrifugation

Analytical ultracentrifugation of α -actinin Δ and of α -actinin Δ plus Zr. 1-2-3 complex was performed with the kind assistance of Dr. Vladimir Rybin (Protein Expression and Purification Core Facility, EMBL-Heidelberg). Following buffer was used for AUC experiments: 50 mM Na-phosphate, pH 8.0, 150 mM NaCl, 2 mM TCEP. The protein concentrations ranging from 0,5 mg/ml to 2 mg/ml were used for the sedimentation velocity measurements.

The sedimentation velocity plots were obtained by monitoring protein absorbance at OD_{280nm} during centrifugation (+ 4 degrees Celsius; 48 000 rpm). Following equipment was used for AUC experiments: centrifuge Beckman Optima XL-A; rotor AN-60 with double-sector aluminum centerpieces. The data were analyzed by “Sedfit” software (Schuck, 2000) with assistance of Dr. Vladimir Rybin.

3.29 Protein crystallization experiments

The reconstituted protein complexes of titin and α -actinin (EF-hands 1-4 plus Zr.1, EF-hands 1-4 plus Zr.7, EF-hands 3-4 plus Zr.1, EF-hands 3-4 plus Zr.7, EF-hands 1-4 plus Zr.1-2-3, EF-hands 1-4 plus Zr.5-6-7) were submitted for crystallization trials at the high-throughput crystallization facility at EMBL-Hamburg. The following NeXtal QIAGEN crystallization screens were used for the trials: Classics Suite, Classics II Suite, PEGs Suite, PEGs II Suite. Approximately 400 conditions were tested for each of the complexes. Unfortunately, neither automated nor manual screening resulted in crystallization hints for titin – α -actinin complexes.

3.30 Small angle X-ray scattering (SAXS)

All SAXS measurements were performed at P12 beam-line (EMBL c/o DESY), storage ring – PETRA-III. The samples were measured at 10 °C in a concentration range 0.5÷3 mg/ml for α -actinin Δ and 5÷20 mg/ml for separate EF-hands domains. The data were recorded using a 2M PILATUS detector (DECTRIS, Baden, Switzerland) at a sample – detector distance 3.1 m and a wavelength of $\lambda=0.124$ nm, covering the range of momentum transfer $0.07 < s < 4.50 \text{ nm}^{-1}$ ($s=4\pi \sin\theta / \lambda$ where 2θ is the scattering angle). No measurable radiation damage was detected by comparison of 20 successive frames with 50 ms exposures. The data were averaged after normalization to the intensity of the transmitted beam and the scattering of the buffer was subtracted

A number of programs were used for SAXS data analysis:

data acquisition – BECQUEREL (Franke *et.al.*, 2012);

data processing – PRIMUS (Konarev *et al.*, 2003), GNOM (Svergun, 1992);

ab initio analysis – DAMMIN (Svergun, 1999), DAMMIF (Franke & Svergun, 2009), DAMAVER (Volkov & Svergun, 2003), MONSA (Svergun, 1999);
computation of model intensities – CRY SOL (Svergun *et al.*, 1995);
rigid body modeling – SASREF (Petoukhov and Svergun, 2005)

These programs were developed in the research group of Dr. Dmitri Svergun (EMBL-Hamburg). They are currently included into integrated package ATSAS 2.5.1 for SAXS data analysis (Petoukhov *et.al.*, 2012).

4 Results and discussion

4.1 Gene amplification and protein constructs

The DNA fragments encoding titin Z-repeats were amplified by PCR, using human cDNA libraries (skeletal muscle and heart). Isoforms corresponding to four and six repeats were obtained from the skeletal muscle cDNA library. The isoform corresponding to 7 repeats was derived from the heart cDNA library.

These PCR products were cloned into both pETM-11 and pET-Z2a (Kan^R) vectors. Colonies which contained positive clones were selected using colony PCR. They were cultivated overnight in LB medium for plasmid preparation. The plasmids were isolated using a mini-prep DNA extraction kit accordingly to the manufacturer's protocol. The presence of correct inserts was confirmed by DNA sequencing. Using the "7 repeat isoform", a number of other Z-repeat constructs was created. The separate repeats were cloned into the pET M-11 vector. The "three repeat constructs" were cloned into the pET Z2_1a vector. These three constructs have repeats 1-2-3, 3-4-5 and 5-6-7, respectively. Three GST-tagged constructs (Zr.1; Zr.1-2-3 and Zr.1-6) were created additionally, as well as a "non-coding" Z-repeat moiety (Zrs.2-6).

The constructs containing the EF-hands domains of human α -actinin 2 were initially received from the University of Vienna (Prof. K. Djinovic Carugo). These constructs were re-cloned into pCDF-11 and pCDF-13 vectors (Spec^R) for the purpose of co-expression. The presence of the correct inserts was confirmed by DNA sequencing.

The truncated variant of human α -actinin 2 (α -actinin Δ) was created using the same skeletal muscle cDNA library. This construct lacks ABD and the

autoinhibitory neck. It starts from the residue 281 and carries the poly-histidine tag at the N-terminus. α -actinin Δ was cloned into the pET-28a vector (Kan^R).

Two constructs of human myopalladin (Uniprot accession number Q86TC9 MYPN_HUMAN), namely myopalladin 1 (amino acid residues 800-920) and myopalladin 2 (C-terminal domain, residues 945-1320) were also amplified by PCR from human striated muscle cDNA library. They were cloned into pCDF-11 (Spec^R) and pCDF-Duet (Spec^R) vectors.

4.2 Protein over-expression

A number of different *E.coli* strains were selected for initial expression trials: BL21 DE3, BL21 pLysS, DE3BL21 DE3 RIL, BL21 DE3 RP, Rosetta, Rosetta pLysS, BL21 DE3 Rosetta2 pRARE II. The strain BL21 DE3 Rosetta2 pRARE II (contains a Cam^R plasmid encoding an array of human tRNAs to account for codon bias) showed the best performance. All further protein expression was performed using this strain. LB was employed as the growth medium for initial expression experiments. Later it was changed to TB. This medium generally gives high amount of biomass and, hence, a higher yield of protein.

All proteins were expressed according to the standard protocol, outlined in the “Methods” section. It gave satisfactory and reproducible results for all the proteins, except for the large titin 6-repeats and 7-repeats constructs. These proteins were insoluble to a large extent. The soluble fraction obtained by IMAC contained significant amounts of contaminants. It was impossible to remove the contaminants by either subsequent size-exclusion or anion-exchange chromatography.

4.3 Co-transformation/co-expression experiments

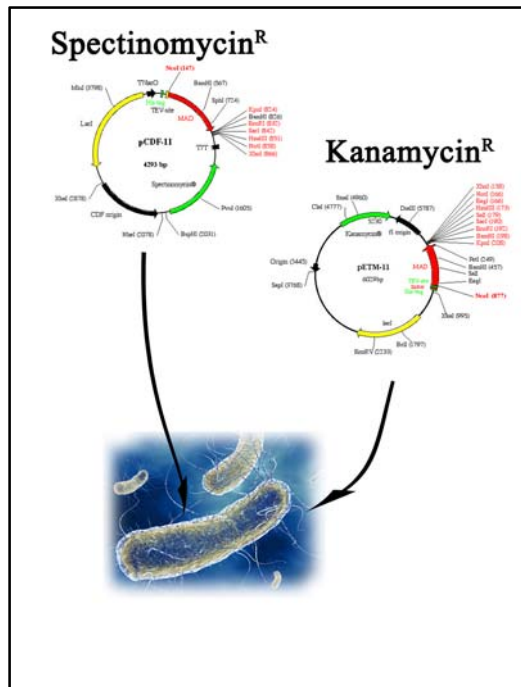


Figure 9. The schematic depiction of co-transformation experiment when two plasmid vectors with different antibiotic resistance are introduced into the same *E. coli* cell.

In order to obtain large quantities of protein-protein complexes in the most economical way, the co-expression approach was implemented. This procedure required careful planning at the stage of molecular cloning.

The interacting protein partners were cloned into expression vectors with different antibiotic resistance. This allowed propagation of both plasmids within the same host cells under selective pressure (**Fig.9**). It is necessary to mention that this approach may be of particular usefulness when the desired complexes cannot be reconstituted by simple mixing of two purified components.

All titin Z-repeats (both separate peptides and larger constructs) were cloned into vectors with kanamycin resistance. All α -actinin EF-hands domain were re-cloned into pCDF vectors bearing the spectinomycin resistance. For

“large” complexes of α -actinin Δ and titin Z-repeats 1-2-3, the antibiotic markers were opposite, i.e. truncated α -actinin was cloned into vector pET-28a (Kan^R) and Zr.1-2-3 were cloned into vector pCDF-11 (Spec^R). These antibiotics were used as selective markers for the inducible protein over-expression in *E.coli* cells.

4.4 Recombinant protein purification

The general IMAC purification protocol included a number of consequent steps:

- 1) The 1 L *E.coli* cultures in LB or TB medium were cultivated overnight at + 21 degrees Celsius. These cultures were harvested by centrifugation (pre-cooled JLA 8.1000 rotor, “Beckman” centrifuge, 25 min at 4500 rpm; + 4 degrees Celsius) next morning. All further procedures were carried out either in cold room (+ 10 degrees Celsius) or on ice bath.
- 2) The pellets were thoroughly resuspended in ice-cold IMAC (lysis) buffer. ~ 30-35 ml of the buffer were used per 1 L pellet, depending on the amount of wet biomass. The resuspension mixture was additionally homogenised by vortexing in 50 ml falcon tube.
- 3) The cells were lysed by sonication of the resuspension mixture (i.e. bacterial pellet in IMAC buffer) in order to obtain “crude bacterial extract”.
- 4) The crude extract was centrifuged in order to separate cell debris from supernatant which contained soluble recombinant proteins (pre-cooled SS-34 rotor, “Sorvall® RC 26 Plus” centrifuge, 19 000 rpm, + 4 degrees Celsius, 60 min).

- 5) The supernatant (“clarified extract”) was additionally filtered through sterile 0.22 μm syringe filter.
- 6) The filtered clarified extract was applied onto the gravity flow column, packed with Ni-NTA resin (QIAGEN). The gravity flow was used for all steps of affinity purification.
- 7) All clarified extract was passed through the resin (~45 ml of extract from 1 L of wet bacterial biomass). The latter was washed with 10 column volumes of ice-cold IMAC (lysis) buffer.
- 8) After initial wash step, the resin was washed with 5 column volumes of IMAC buffer with 20 mM imidazole in it (final concentration).
- 9) The recombinant protein (proteins) was eluted with IMAC buffer with 200 mM imidazole in it (the volume of the elution buffer was varied depending on expected yield of recombinant protein).
- 10) The protein in elution buffer was transferred into the dialysis tube for the exhaustive overnight dialysis. The protease (either TEV or 3C) was added for the tag-cleavage at this step.
- 11) The consequent purification steps included either size-exclusion chromatography (SEC) or SEC in conjunction with ion-exchange (“Mono Q” matrix) chromatography.

The overall purification procedure took from 2 to 4 days, depending on the number of chromatography steps employed. The buffers formulations for purification of separate titin and α -actinin constructs as well as their complexes are listed below. It is necessary to mention that an IMAC buffer was generally used as a resuspension/lysis, 1st and 2nd wash buffers, as well as elution buffer during purifications. The difference between these buffers was in the imidazole concentration. Imidazole was added to the solution to a final concentration of 20 mM for the 2nd wash buffer. Imidazole was added to the initial IMAC buffer to a

final concentration of 250 mM in order to prepare the elution buffer. The outlined general affinity chromatography protocol was used for all proteins and complexes, only the IMAC buffers were specifically formulated for every case. β -mercaptoethanol was used as a reducing agent for initial protein purification on Ni-NTA resin. It was substituted either with DTT or with TCEP for size-exclusion chromatography and ion-exchange chromatography.

The size-exclusion chromatography was performed using preparative columns packed with either “Superdex 75” or “Superdex 200” matrix (dextran and cross-linked agarose). The type of matrix was chosen depending on the molecular mass of a recombinant protein or complex.

The ion-exchange chromatography was performed using Mono Q HR 16/10 HR column (anion exchange) from “GE Healthcare Life Sciences”. This matrix has high binding capacity (20-50 mg of protein per ml of matrix, accordingly to manufacturer’s specifications). The non-specific protein binding to the MonoBeads (polystyrene/divinyl benzene beads) is negligible. A gradient from 25 mM to 700 mM was typically applied for ion-exchange. The buffer volume, in which the gradient was performed, was no less than 50 ml.

The following buffers were found to be optimal for purification of all α -actinin EF-hands domains:

IMAC buffer:

50 mM Na-phosphate, pH 8.0
300 mM NaCl
5 mM imidazole, pH 8.0
5 mM β ME
5 % v/v glycerol

SEC buffer:

50 mM Tris-Cl, pH 7.0
300 mM KCl
5 mM DTT
2 mM EDTA, pH 8.0

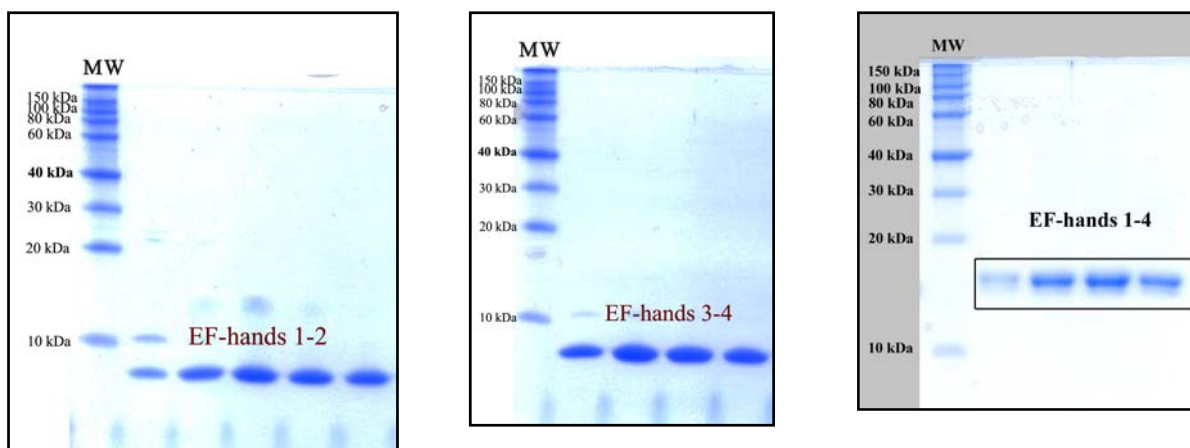


Figure 10. Purification of EF-hands of α -actinin 2. Left to right: 1) EF-hands 1-2 after size-exclusion chromatography; 2) EF-hands 3-4 after size-exclusion chromatography; 3) EF-hands 1-4 after size-exclusion chromatography.

Protein inhibitors and DNase were added to the IMAC buffer directly before use, according to the manufacturer's manuals.

After the immobilised metal affinity chromatography EF-hands were dialysed overnight against SEC buffer. TEV protease was added in order to remove the affinity His-tag during the dialysis step. Protein samples were concentrated in order to reduce the injection volume for size-exclusion chromatography.

This two-step protocol resulted in pure, stable and homogenous EF-hands domain proteins (**Fig.10**).

The titin Z-repeats are peptides of approximately 5 kDa weights. They require special attention during purification procedures due to their size and hydrophobic properties.

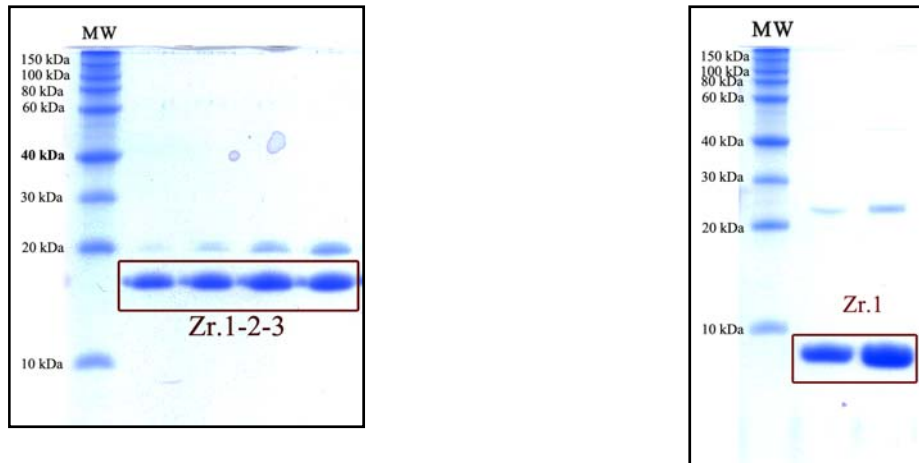


Figure 11. The final purity of titin Z-repeats was assessed by SDS-PAGE.

The following buffers were used in order to obtain pure Zr. peptides
(**Fig.11**):

IMAC buffer:

50 mM Na-phosphate, pH 8.0
250 mM NaCl
5 mM imidazole, pH 8.0
5 mM β ME
5 % v/v glycerol

SEC buffer:

50 mM Na-phosphate, pH 8.0
300 mM KCl
5 mM DTT
2 mM EDTA, pH 8.0
50 mM L-arginine

Buffers for ion-exchange („Mono-Q“ resin):

Buffer A:

25 mM Tris-Cl, pH 8.0
25 mM NaCl
5 mM DTT

Buffer B:

25 mM Tris-Cl, pH 8.0
700 mM NaCl
5 mM DTT

Special care has had to be taken during dialysis/concentration of titin Z-repeats. The dialysis membrane with smallest possible cut-off (1-2 kDa) was used. The concentrators with 3.5 kDa cut-off were used for separate Zr's. The repeats were prone to aggregation, so “over-concentration” not was permissible.

The separate titin Zrs used in the present study contained only a hexahistidine tag at the N-terminus for IMAC purification. The tag was cleaved during the dialysis. The alternative approach, according to which Z-peptides had been expressed as a GST-fusion, showed less satisfactory results in terms of protein yield.

The following buffers were found suitable for the purification of the complexes of EF-hands 3-4 plus Zr.1; EF-hands 3-4 plus Zr.7; EF-hands 1-4 plus Zr.1; EF-hands 1-4 plus Zr.7.

IMAC buffer:

50 mM Tris-Cl, pH 8.0
250 mM NaCl
5 mM imidazole, pH 8.0
5 mM β ME
5 % v/v glycerol

SEC buffer:

50 mM Tris-Cl, pH 8.0
200 mM KCl
5 mM DTT
2 mM EDTA, pH 8.0

Buffers for ion-exchange („Mono-Q“ resin):

Buffer A:

25 mM Tris-Cl, pH 8.0
25 mM NaCl
5 mM DTT

Buffer B:

25 mM Tris-Cl, pH 8.0
700 mM NaCl
5 mM DTT

The affinity chromatography purification was performed as described previously. The protein complexes were dialysed overnight and concentrated before SEC. The affinity tags were cleaved at this stage (**Fig.12**). After SEC the complexes were exhaustively dialysed against Buffer A for consequent anion-exchange chromatography. The purity of the IEX elution fractions was assessed by denaturing Tris-Tricine gel electrophoresis.

This three-step purification protocol allowed obtaining stable, homogeneous complexes of EF-hands domains with titin Z-repeats. The peak fractions in ion-

exchange chromatography contained proteins at concentration of 12-14 mg/mg (Fig.13).

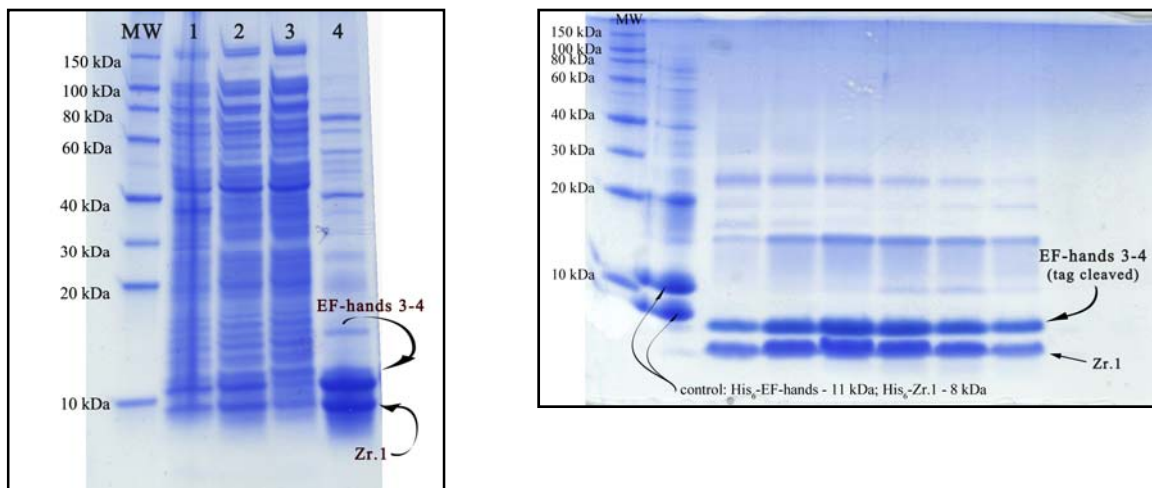


Figure 12. Reconstitution of EF-hands 3-4/ Zr.1 complex by co-expression. Left: IMAC purification of EF-34 plus Zr.1; right: complex after tag cleavage and size-exclusion chromatography.

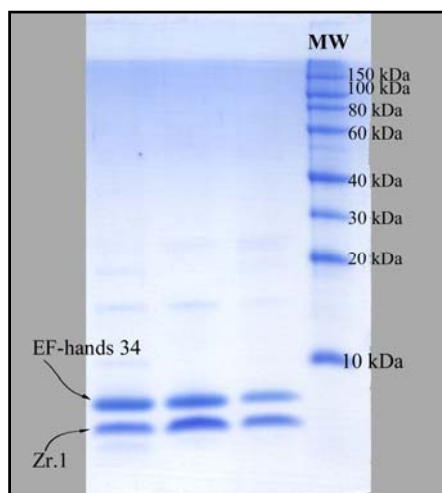


Figure 13. The EF-hands 3-4/ Zr.1 complex after ion-exchange chromatography.

Similar buffers were used for purification of the complexes of EF-hands domains 1-4 and titin repeats 1-2-3 and of EF-hands domains 1-4 and titin repeats 5-6-7.

IMAC buffer:

50 mM Na-phosphate, pH 8.0
250 mM NaCl
5 mM imidazole, pH 8.0
5 mM β ME
5 % v/v glycerol

SEC buffer:

50 mM Tris-Cl, pH 8.0
200 mM KCl
5 mM DTT
2 mM EDTA, pH 8.0
50 mM L-arginine

Proteins purified with these buffers were used for small angle X-ray scattering experiments. It is necessary to mention that an additional purification step might be required in case of EF-hands domains 1-4 and titin repeats 5-6-7 complex. The 7th constitutive repeat is often subject to proteolytic degradation. This has also been previously observed (Young *et al.*, 1998).

After initial purification trials, the buffer compositions for α -actinin Δ were optimized using the Thermofluor assay. It was shown that optimum stability of this protein could be observed in sodium phosphate buffer, pH 8.0 with low or no NaCl. Taking into account these findings the following buffers were used:

IMAC buffer:

50 mM Tris-Cl, pH 8.0
150 mM NaCl
5 mM imidazole, pH 8.0
5 mM β ME
5 % v/v glycerol

SEC buffer:

75 mM Na-phosphate, pH 8.0
100 mM NaCl
5 mM DTT
2 mM EDTA, pH 8.0
50 mM L-arginine

Protein inhibitors and DNase were added separately to the IMAC buffer, according to the manufacturer's manuals.

These buffer recipes were also successfully used for purification of the complex of α -actinin Δ and titin Zr.1-2-3. The latter was studied both by electron

microscopy and analytical ultracentrifugation. The same buffers and two-step purification protocol (IMAC/SEC) were applied to purification of α -actinin Δ / myopalladin complexes, expressed from bi-cistronic vectors.

All purification protocols were carefully optimized after initial trials. The analytical size-exclusion chromatography and Thermofluor assays were often employed in buffer optimization procedures in order to achieve high purity and stability of proteins. The purity and identity of recombinant proteins were confirmed by SDS-PAGE and mass spectrometry.

4.5 Size-exclusion chromatography and static light scattering experiments

The purified single-domain complexes of titin Z-repeats and α -actinin EF-hands were analysed by the analytical size-exclusion chromatography coupled to an on-line static light scattering instrument. The following complexes were characterized by these experiments: EF-hands 1-4 plus Zr.1, EF-hands 1-4 plus Zr.7, EF-hands 3-4 plus Zr.1, EF-hands 3-4 plus Zr.7. EF-hands 1-4 and EF-hands 3-4 were used as reference. Protein elution was monitored by UV absorption at three wavelengths (215 nm, 254 nm, 280 nm).

The chromatograms with symmetrical absorption peaks in column's separation range were obtained during analytical size-exclusion chromatography experiments. Only one peak was obtained per single run. These results can be interpreted as evidence of pure and homogeneous complexes.

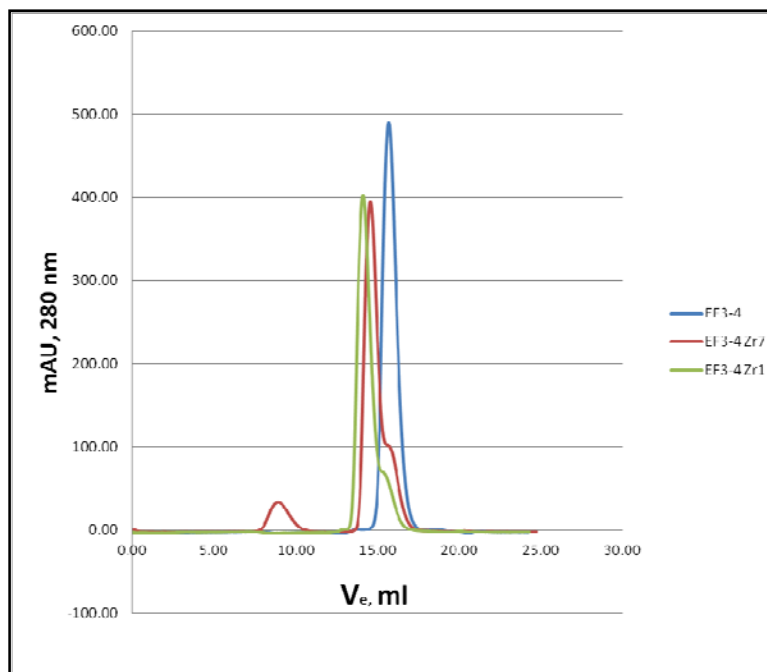


Figure 14. EF-hands 3-4 plus Zr.1 and EF-hands 3-4 plus Zr.7 complexes were characterized by analytical chromatography. **Red peak:** EF-hands 3-4 plus Zr.7, MW ~14 kDa; **Green peak:** EF-hands 3-4 plus Zr.1, MW ~14 kDa; **Blue peak:** EF-hands 3-4 alone, MW ~7 kDa (molecular weights were estimated by SLS in these experiments).

A visible shift of elution volume V_e was observed when chromatograms of separate EF-hands domains were compared with chromatograms of the complexes (**Fig.14**). The homogeneity of the EF-hands was additionally confirmed by dynamic light scattering (DLS) which showed less than 10 % of heterogeneous species in protein solution. It was demonstrated by DLS that the EF-hands domains were homogenous and monomeric in standard size-exclusion buffers (high ionic strength, reducing conditions).

The stability of the titin/ α -actinin complexes was additionally tested under different NaCl concentrations (from 50 to 300 mM) by analytical size-exclusion chromatography. It was shown that the EF-hands/Z-repeats complexes are stable up to 300 mM NaCl, with no visible changes in the elution profile or shifts of elution volume V_e .

The molecular masses calculated from static light scattering data (**Fig.15**, **Fig.16**) strongly support the 1:1 stoichiometry of the components in the complexes (i.e. the measured molecular masses of the complexes were equal to the mass of the corresponding EF-hands domain plus the mass of a single Z-repeat). The obtained results also suggest that only EF-hands 3-4 are necessary for the interaction with titin Z-repeats 1 and 7. The EF-hands 1-2 do not take part in this interaction. These findings are strongly supported by experimental data previously obtained by Atkinson *et al.* (2000) and Joseph *et al.* (2001).

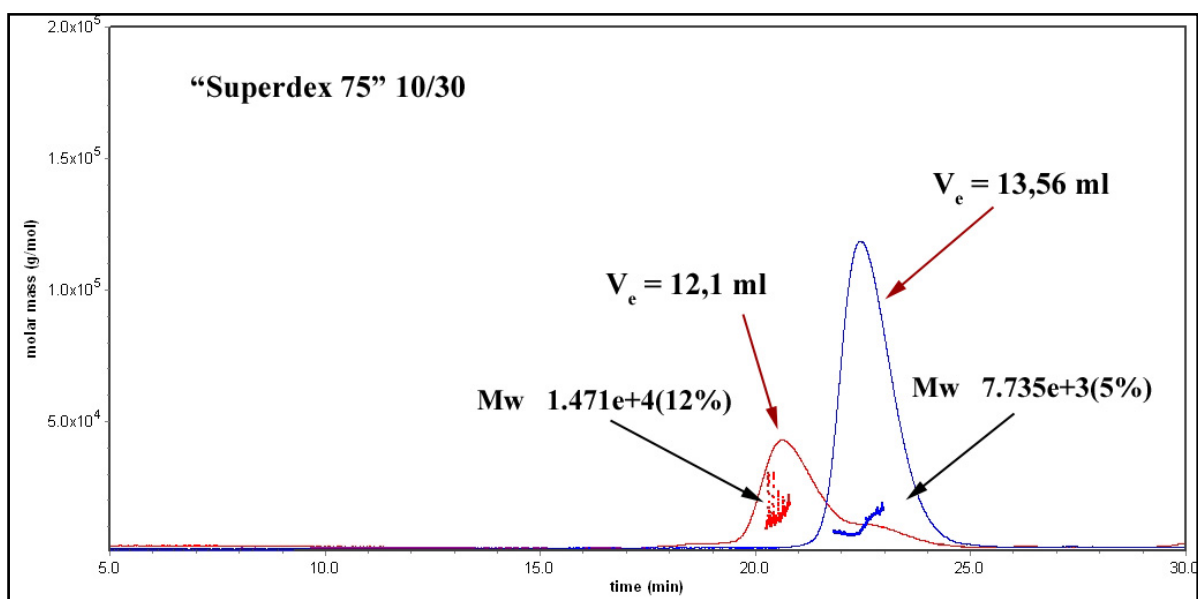


Figure 15. Characterisation of EF-hands 3-4/Zr.1 complex by analytical chromatography and static light scattering. **Red peak:** EF-hands 3-4 plus Zr.1. **Blue peak:** EF-hands 3-4 alone.

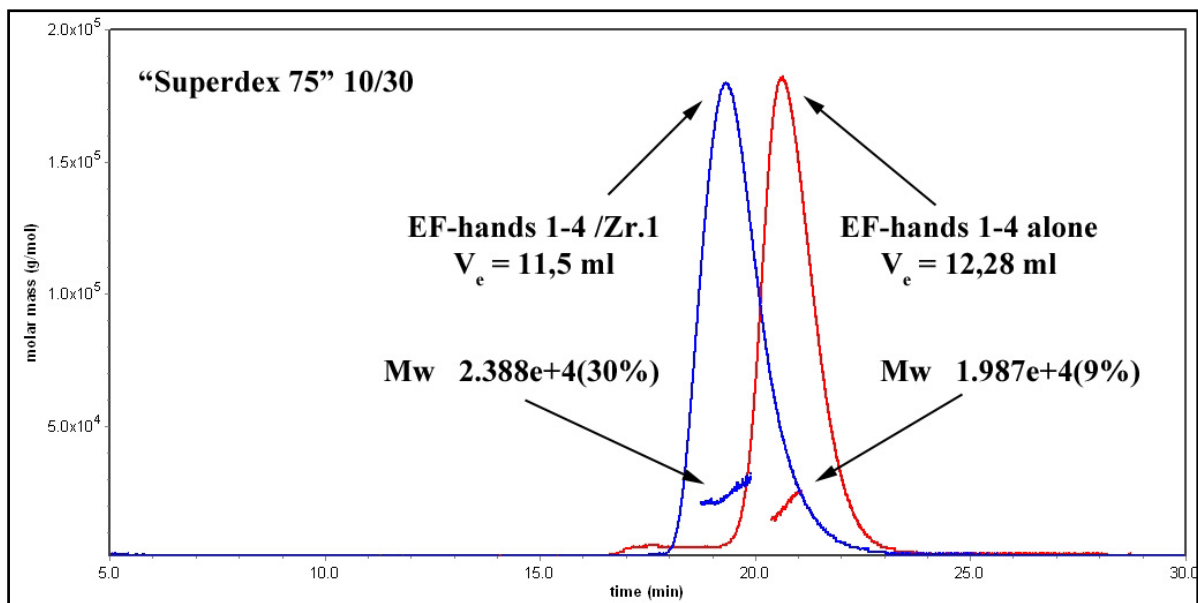


Figure 16. Characterisation of EF-hands 1-4 in complex with Zr.1 by analytical chromatography and static light scattering. **Red peak:** EF-hands 1-4 alone. **Blue peak:** EF-hands 1-4 plus Zr.1.

4.6 Far-UV circular dichroism spectroscopy of titin Z-repeats and α -actinin EF-hands

Circular dichroism (CD) spectroscopy is a powerful method for probing protein structural features and their changes. Protein CD spectroscopy can be divided into 2 classes: **a)** far-UV (190-250 nm) and **b)** near-UV (250-300 nm). The first can provide valuable information about the percentage of different secondary structure elements of a given protein in a particular condition. Near-UV spectroscopy can provide insight into micro-environment and orientation of aromatic side chains. This type of spectroscopy can also be used to monitor domain movements within a protein macromolecule.

In the present study, far-UV circular dichroism spectroscopy (190-260 nm) was employed to obtain information about the secondary structure content of titin repeats and α -actinin EF-hands domains. The spectra of these proteins were measured both separately (EF-hands 1-4, EF-hands 1-2 and EF-hands 3-4, as well as titin Z-repeats 1, 7 and Zr.1-2-3) and in complexes (EF-hands 3-4 plus Zr.1; EF-hands 3-4 plus Zr. 7).

It was demonstrated that EF-hands domains of human α -actinin have a large percentage of helical elements in the secondary structure. For instance, EF-hands 1-2 have ~ 47% of α -helices and ~ 11% of β -sheets; EF-hands 3-4 have ~ 33 % of helices and ~ 14 % of β -sheets (**Fig.18**).

The spectra were analyzed using the K2D3 server (Louis-Jeune *et al.*, 2012; <http://www.ogic.ca/projects/k2d3//index.html>). The experimentally measured structure content of EF-hands 3-4 is indeed different from bioinformatical predictions made by the NPS@ server (Combet *et al.*, 2000): 33 % of α -helices as confirmed by measurements versus 51 % expected from prediction).

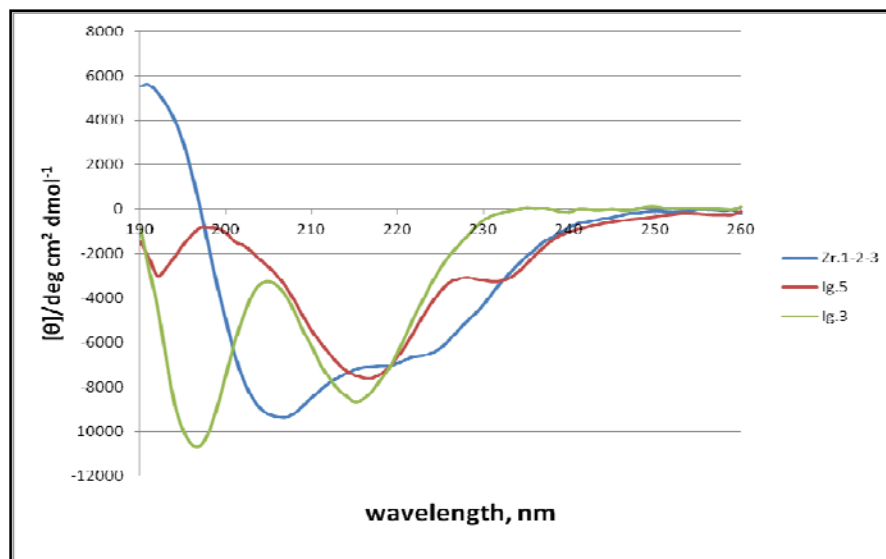


Figure 17. The far-UV circular dichroism spectra of titin Z-repeats 1-2-3 (blue curve), compared to spectra of titin Z-disk Ig-domains 3 and 5 (green and red curves, correspondingly).

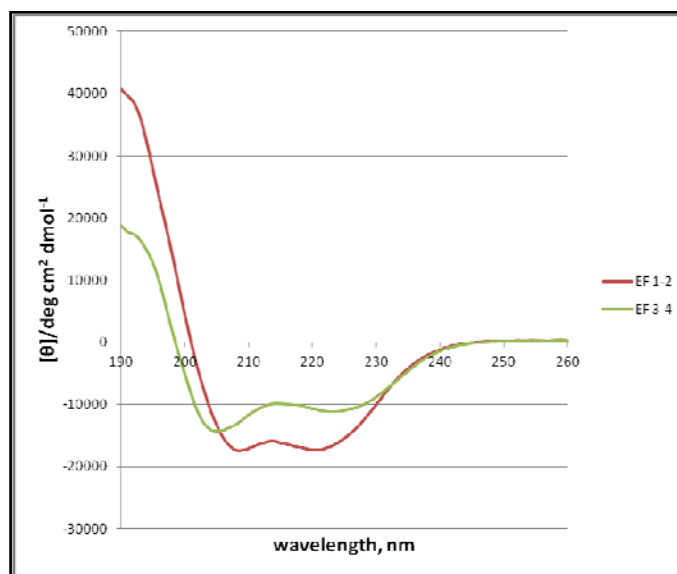


Figure 18. The far-UV circular dichroism spectra of α -actinin EF-hands 1-2 (red curve) and EF-hands 3-4 (green curve).

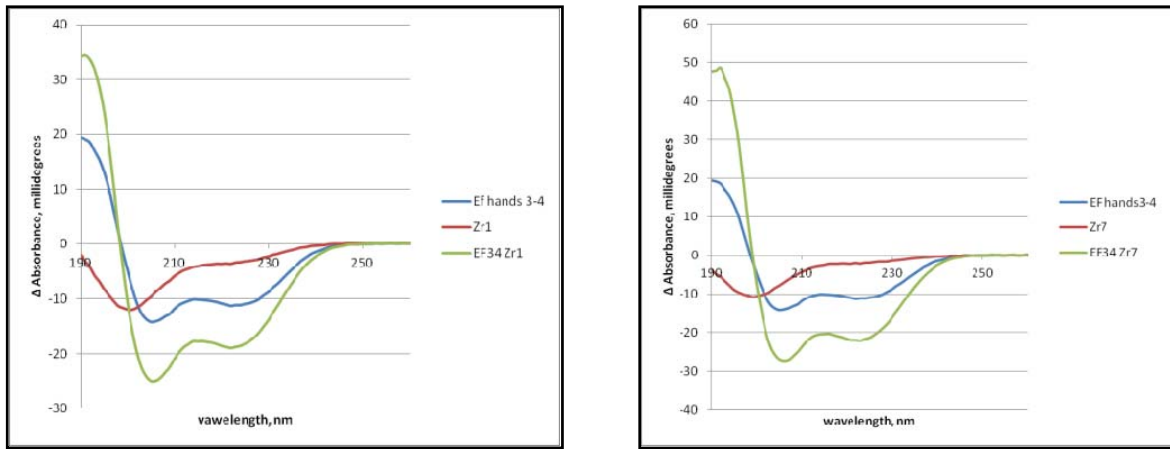


Figure 19. The far-UV circular dichroism spectra of α -actinin EF-hands 3-4 in complex with titin Zr.1 (left) and titin Zr.7 (right). Complexes were reconstructed by titration; 1:1 stoichiometry was obeyed. The spectra of the complexes (green curves) are shown in comparison with spectra of separate EF-hands 3-4 (blue curves) and Zr (red curves).

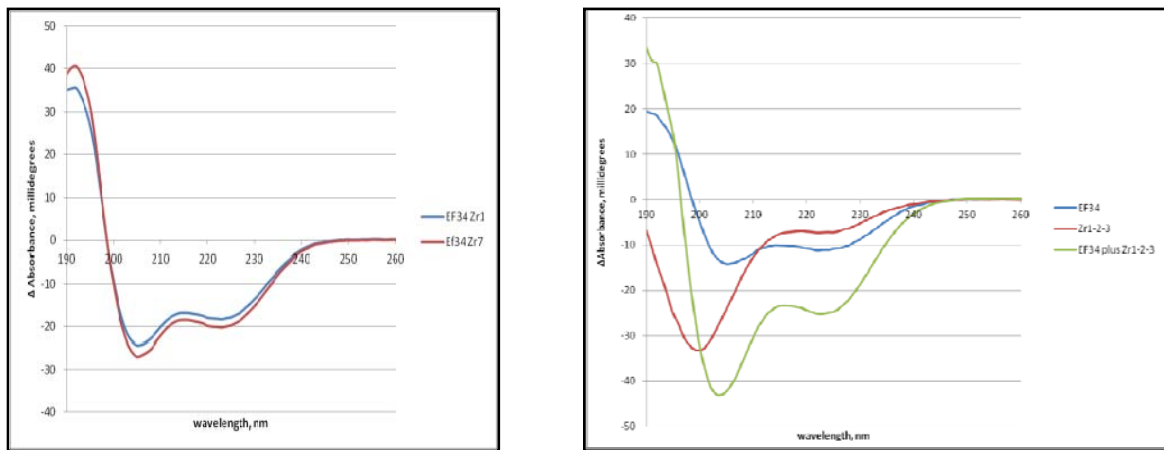


Figure 20. Left: CD spectra of complexes EF-hands 3-4 plus Zr 1 (blue curve); EF-hands 3-4 plus Zr. 7 (red curve), reconstituted by co-expression. Right: CD spectra of the complex EF 3-4 plus Zr.1-2-3 (green curve) in comparison with spectra of EF-hands 3-4 (blue curve) and Zr.1-2-3 (red curve).

The α -helical content of EF-hands 3-4 complexes was $\sim 63\%$ in case of binding with Zr.7 and $\sim 53\%$ in case of binding with Zr.1 (**Fig.19**). The gain of signal and overall increase of secondary structure content cannot be explained solely by additive effect.

This is rather an evidence of structural rearrangements and overall compaction of the EF-hands structure upon complex formation.

The measured spectra of titin repeats (Zr. 1 and 7) are typical for partially unstructured peptides, where no or very little elements of the secondary structure are present.

The circular dichroism spectrum of Z-repeats 1-2-3 (144 amino acid residues) was compared to the spectra of Ig-like domains 3 and 5 (approximately 100 amino acid residues each), also located within the Z-disk (**Fig.17**). The immunoglobulin domains are relatively small in size and composed mainly of β -sheets. The CD spectra of such domains contain characteristic minima at 204 nm or at 217 nm. This particular pattern was observed during spectroscopic measurements of Ig.3 and Ig.5 of titin. In contrast to measured immunoglobulin domains, the spectrum of Zr. 1-2-3 contained only one minimum at 208 nm. This is a clear indication that the Z-repeat region differs from typical Ig-domains which constitute the bulk of titin molecule. This region may totally lack any defined domain structure and serve only as interaction platform for other muscle proteins within the Z-disk.

The CD spectra of the complexes obtained from co-expression were compared with spectra of the complexes obtained by mixing of the separate components. These appeared to be almost identical, taking into account possible pipetting errors. These results strongly support the idea that co-transformation/co-expression is a reliable method for reconstruction of protein-protein complexes. The protocol allows obtaining the complexes of choice in

significant quantities and of high purity. The protein-protein complexes, reconstituted by /co-expression possess correct physiological stoichiometry of the components in the assembly.

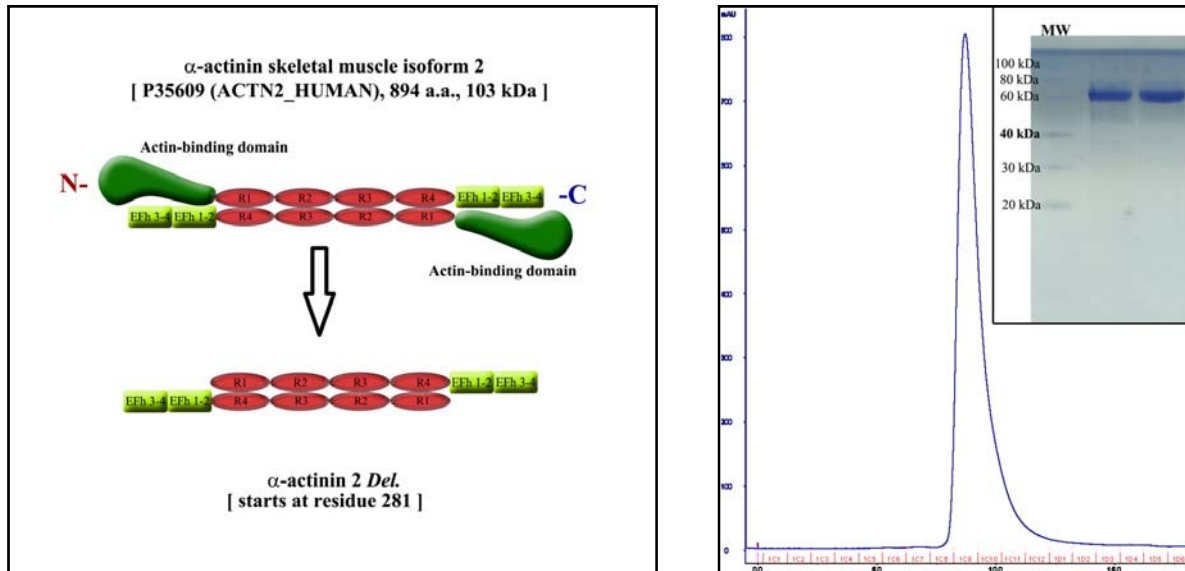


Figure 21. Left: the explanatory schema of α -actinin Δ construct design; right: α -actinin Δ elution profile and purity of the protein as estimated by SDS-PAGE.

4.7 The complex of α -actinin Δ and Zr.1-2-3

In order to confirm the findings obtained from the single domain complexes of titin and α -actinin, it was necessary to reconstruct somehow larger assemblies that resemble more closely the actual *in vivo* structures. A truncated version of human α -actinin 2 was created for these studies.

It is known that the full-length actinin dimer is autoinhibited. The “neck” region, located between ABD and the first spectrin repeat, is similar to the hydrophobic interaction motif of titin Zrs. The homodimer acquires an open conformation and the ability to interact only in presence of the phospholipid

PiP2. This molecule disrupts interactions between the “neck” and EF-hands domain 3-4.

Thus, it was decided to design a truncated construct of α -actinin (α -actinin Δ) which does not contain neither ABD nor the autoinhibitory neck region (**Fig.21**). This construct starts at amino acid residue 281 and contains 4 spectrin repeats and EF-hands 1-2-3-4. This protein is able to both form a rod-shaped antiparallel dimer and interact with its partners via EF-hands domains.

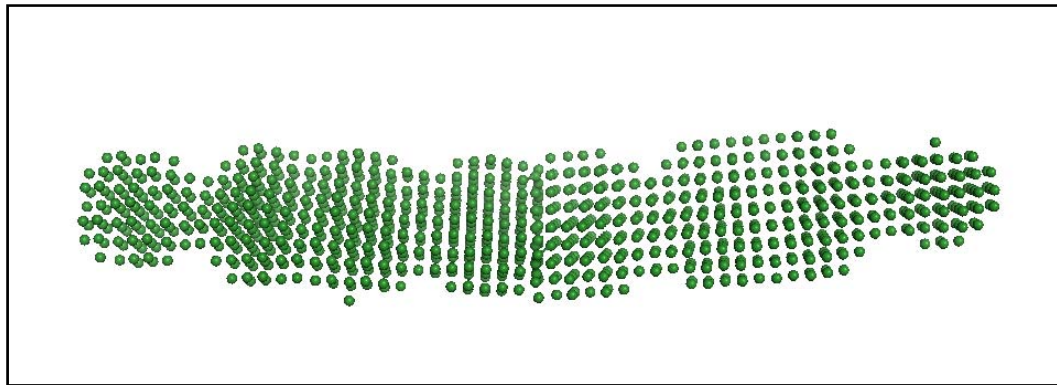


Figure 22. The low-resolution molecular envelope of α -actinin Δ (the homodimer, spheres representation). The “globules” at the both ends of the dimer are EF-hands domains.

At the initial stage of the experiment, the purification protocol was thoroughly optimized by applying the Thermofluor assay. The ability of α -actinin Δ to form homodimers was confirmed by analytical size-exclusion chromatography and static light scattering. This protein was also characterized by small angle X-ray scattering (**Fig.22**). The following values of molecular dimensions were obtained: $R_g = 7.8$ nm, $D_{max} = 30$ nm, $V_{porod} = 302$ nm³, $MM_{exp} = 130$ kDa. These data are in good agreement with dimension which can be derived from a high-resolution structure of the α -actinin rod (Djinovic-Carugo *et al.*, 1999; Yläanne *et al.*, 2001). After comprehensive characterization, α -actinin Δ

was used for co-expression experiments with titin 3-repeats construct (contains Zr. 1-2-3).

The co-transformation/co-expression protocol was successfully implemented and the large titin/actinin complex was reconstituted and purified (**Fig.23**). The presence of both titin and α -actinin Δ in complex was confirmed by SDS-PAGE and mass spectrometry. Analytical ultracentrifugation experiments with α -actinin Δ (control) and α -actinin Δ plus Zr.1-2-3 were carried out at the core facilities at EMBL-Heidelberg in order to characterize these proteins further. The obtained results confirmed 1:1 stoichiometry of the components in the reconstituted complex (i.e. 1 molecule of Zr. per 1 molecule of α -actinin Δ). This fact further supports the statement that only EF-hands 3-4 take part in Z-repeat recognition. No other domains of α -actinin are involved in this interaction. There is no apparent cooperativity effect in the case of large titin Z-repeat constructs. The latter means that only the 1-4,5-8 motif is necessary for binding. The neighboring Z-repeats do not influence significantly the binding affinity or change the stoichiometry of proteins in titin/actinin complex.

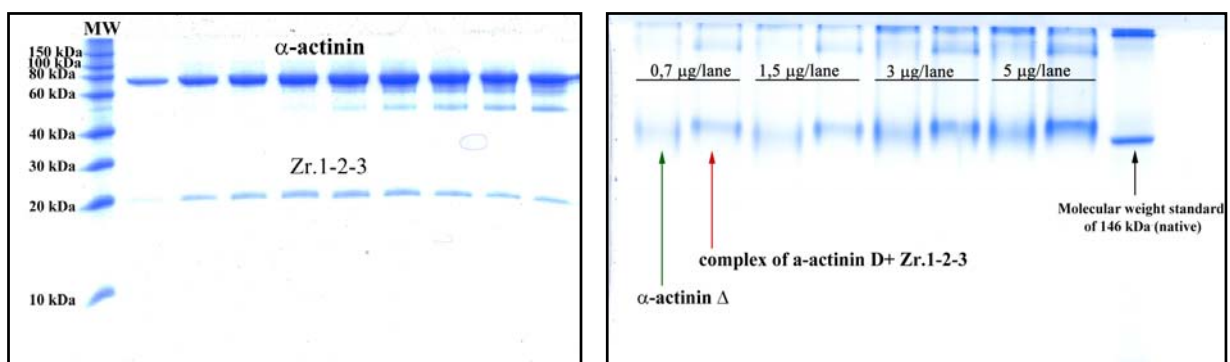


Figure 23. Left: the assessment of α -actinin Δ plus Zr.1-2-3 purity by SDS-PAGE. Right: – native gel of α -actinin Δ alone and in complex with titin repeats.

This large titin/ α -actinin complex is also suitable for EM imaging experiments. However, the re-design of titin Zr protein constructs may be required in this case.

4.8 Characterization of titin/ α -actinin complexes by small angle X-ray scattering

Small angle X-ray scattering (SAXS) is a low-resolution technique, which is often used for characterization of biological macromolecules and their assemblies. It requires only minimal amounts of pure homogenous protein in solution. Such parameters as overall shape of the molecule (“envelope”), radius of gyration, molecular mass and maximum distance within the particle can be easily determined by small angle X-ray scattering. It is possible to monitor changes in protein shape (i.e. domain movements in the range of dozens of nanometers) which are dependent on pH or the ionic strength of the solution. Small X-ray scattering is often used to cross-validate structures obtained by protein crystallography. SAXS measurements are performed in solution in the conditions, which are close to the physiological ones. Hence, common crystallographic artifacts as concentration-induced oligomerisation or non-physiological domain swap are absent in scattering experiments. It is possible to judge if the X-ray structure does not contain significant distortions, caused by crystallization conditions that affect either domain placement or oligomeric state of a protein.

Initially EF-hands 1-4, EF-hands 1-2 and EF-hands 3-4 were used in order to determine an average particle diameter and compute a set molecular envelope solutions for these domains (**Fig.24**, **Fig.25**). Difference of D_{\max} , as well as in overall shape was shown for EF-hands 1-2 and EF-hands 3-4. The latter has a

more elongated shape, which is also seen in the larger construct (EF-hands 1-4). This is in good agreement with the significant difference in the secondary structure content that was detected in the preceding CD experiments.

A number of complexes of EF-hands with titin Z-repeats were used to measure D_{\max} and compare values with the average distance between layers within the Z-disk (see **Table 3**). It was also necessary to measure the molecular mass of the complexes and cross-validate results of the static light scattering experiments.

It was shown that the binding of single Zr to EF-hands 3-4 does not cause a significant change of the particle size, i.e. the D_{\max} of the complex is the same as D_{\max} of EF-hands. The experimental molecular mass of the complex is in good agreement with anticipated 1:1 stoichiometry of the components. The results of the larger complexes scattering further support this assumption. The maximal distance values are the following: 18 nm and 15 nm for complexes of EF-hands 1-4 with Zr.1-2-3 and Zr.5-6-7 respectively; 20 nm for the complex of EF-hands 1-4 with Zr.1-2-3 -7 (the short isoform from skeletal muscles; it contains **two** binding sites). It is clear that only the complex of four repeats with EF-hands is comparable in size to the distance between the Z-disk layers (~ 19 nm).

It is known that the number of titin repeats is commensurate with the number of Z-disk layers. However, the obtained small x-ray scattering data on reconstituted complexes allow to conclude that single Z-repeats cannot determine by themselves the thickness of the Z-disk.

Sample	Conc, mg/ml	R _g , nm	D _{max} , nm	MM _{exp} , kDa	V _{porod} , nm ³
EF-hands 1-4	10 ÷ 20	2.60±0.03	9.0±0.5	18±4	41±4
EF-hands 1-2	5.5÷11	1.34±0.03	4.2±0.3	7±3	17±3
EF-hands 3-4	4.0÷8.0	1.70±0.03	6.0±0.5	8±3	18±3
EF-hands 3-4 plus Zr.1	5÷12	1.73±0.03	6.0±0.5	12±3	25±3
EF-hands 3-4 plus Zr.7	5÷12	1.75±0.03	6.0±0.5	12±3	20±3
EF-hands 1-4 plus Zr.1-2-3	5÷20	5.20±0.03	18.0±1.0	55±5	103±6
EF-hands 1-4 plus Zr.5-6-7	6÷23	4.01±0.03	14.5±0.5	48±4	83±5
EF-hands 1-4 plus Zr.1-2-3- 7	2.5÷4.5	5.45±0.03	20.0±0.5	55±5	115±5

Table 3. Overall parameters of α -actinin EF-hands and their complexes with titin Z-repeats were determined by SAXS. R_g – radius of gyration; D_{max} – maximal size of the particle; MM_{exp} – experimental molecular mass; V_{Porod} – excluded hydrated volume of the particle.

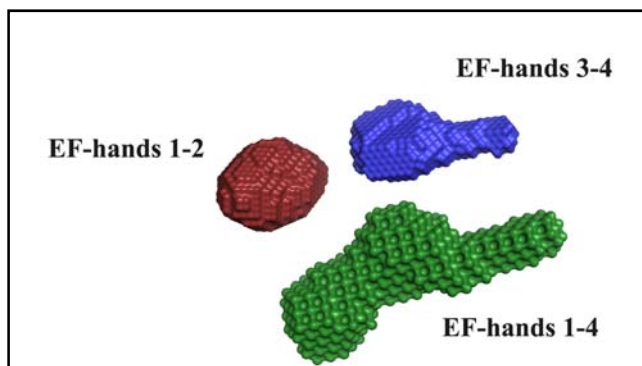


Figure 24. The low-resolution molecular envelopes (surface representation) of EF-hands 1-4 (green), EF-hands 1-2 (red) and EF-hands 3-4 (blue).

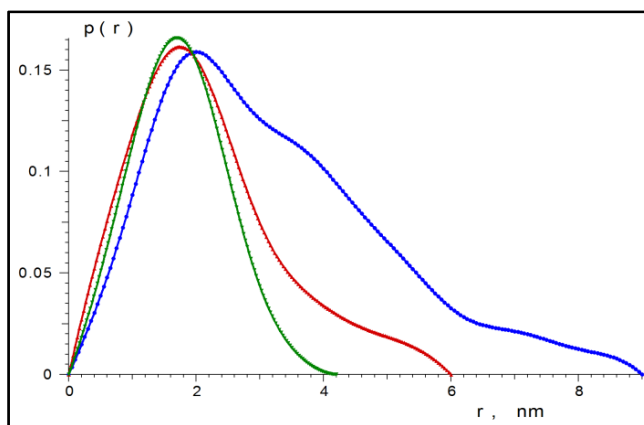


Figure 25. The distance distribution functions of EF-hands 1-4 (blue), EF-hands 1-2 (green) and EF-hands 3-4 (red).

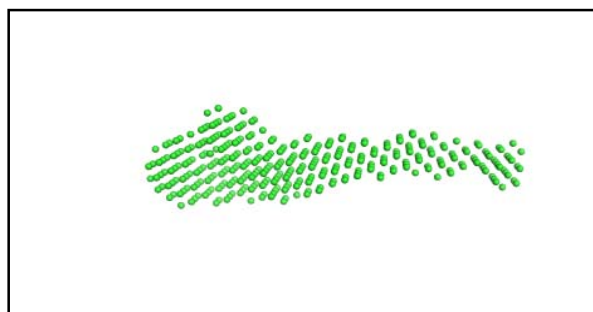
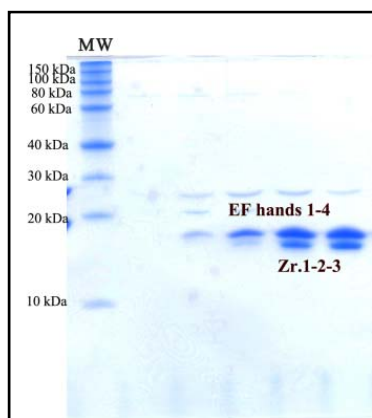


Figure 26. Left: the complex of EF-hands 1-4 and Zr.1-2-3 (the proteins are of similar molecular mass); the overall shape of the complex, obtained by SAXS (spheres representation).

4.9 Reconstruction of complexes of α -actinin and myopalladin

Experiments with muscle protein myopalladin, performed at the later stages of the project had two aims:

a) to test the applicability of the co-transformation/co-expression approach towards reconstitution of α -actinin complexes with other muscle proteins;

b) to reconstruct complexes that are based on the same type of interactions as titin/ α -actinin assemblies.

Now it is widely recognized that human α -actinin not only crosslinks F-actin filaments from adjacent sarcomeres, but also provides a docking platform for a number of Z-disk proteins (Sjöblom *et al.*, 2008; Luther, 2009). A significant amount of experimental evidence was generated during the past decade using state-of-the-art techniques. Three elegant papers dedicated to proteins palladin and myopalladin are particularly important in the context of the present study: Bang *et al.*, 2001; Ronty *et al.*, 2004; Beck *et al.*, 2011.

It was shown that the novel 145 kDa muscle protein myopalladin (**Fig.27**) is localized in the Z-disk and able to interact with both nebulin and α -actinin 2 (Bang *et al.*, 2001).

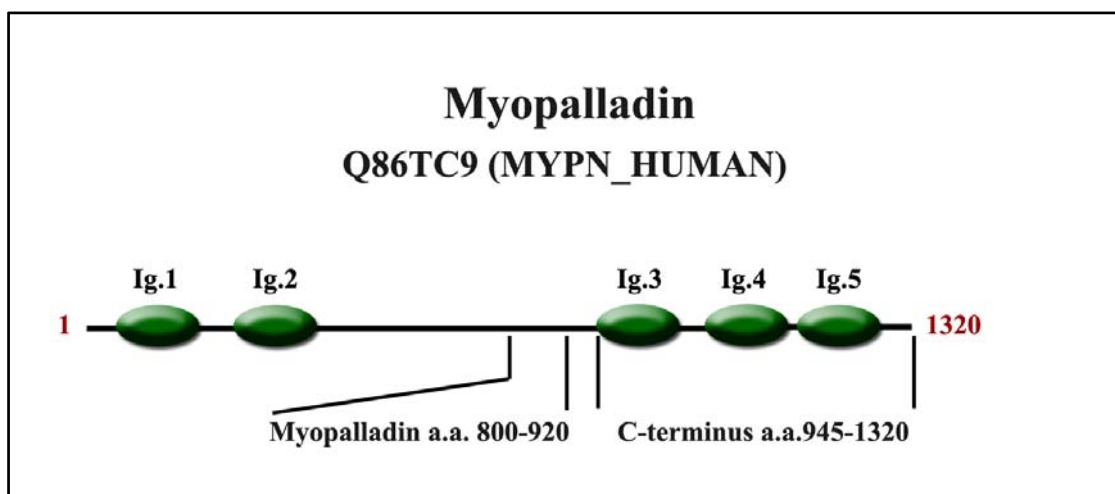


Figure 27. The domain schema of human myopalladin and location of the fragments which were selected for co-expression experiments using bi-cistronic vector.

The binding sites were found to be highly similar to the amino acid sequences previously found in palladin (Parast and Otey, 2000). Moreover, it was shown that both palladin and myopalladin bind to EF-hands domains at the very C-terminus of α -actinin. It is necessary to mention that the described interactions were shown by pull-down assays, yeast two-hybrid analysis and similar methods.

Recent work by Beck *et al.* (2011) demonstrated that the interaction of palladin with EF-hands is mediated by the same type of hydrophobic interactions that are involved in binding of Z-repeats to α -actinin. This work proposed that a similar mechanism may also be responsible for putative complex formation between myopalladin and α -actinin. This information was used in planning of the myopalladin experiments.

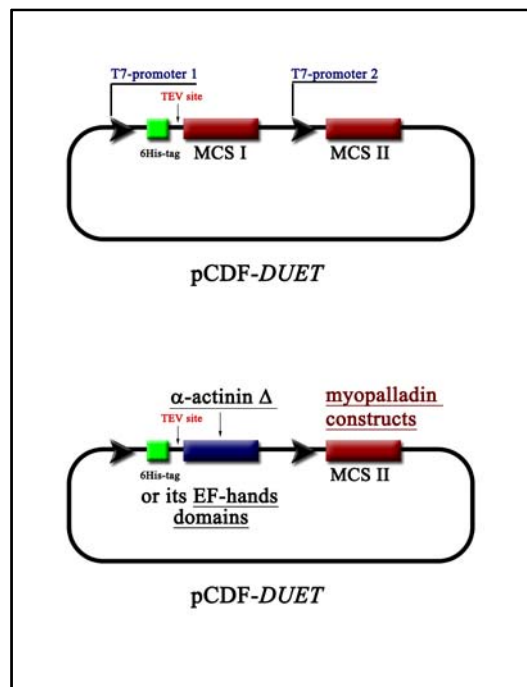


Figure 29. The principal schema of bi-cistronic vector, utilized in this study (top) and cloning strategy for α -actinin/myopalladin co-expression (bottom).

A slightly different approach for protein complex reconstitution was implemented in this case. A bi-cistronic vector (pCDF-Duet), similar to Novagene Duet™ plasmids, was created for co-expression. This vector contains two multiple cloning sites and has spectinomycin resistance. Proteins which were cloned into MCS I, would be expressed with polyhistidine tag, whereas proteins which were cloned into MCS II would be expressed without any tag (**Fig.29**). This approach allows detecting complex formation already at the stage of metal affinity chromatography. If a stable complex is formed, both components will be co-purified and detected by SDS-PAGE. If no interaction occurs, only the protein with His-tag will be present on the SDS-gel. Moreover, such an approach enables easier transformation and protein expression because only one plasmid vector is used and one antibiotic is required as the selection marker.

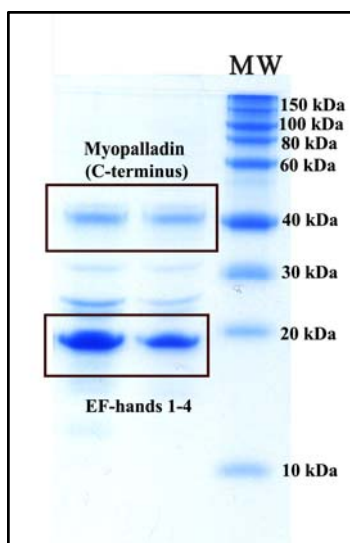


Figure 30. SDS-PAGE of the complex of EF-hands 1-4 and C-terminal moiety of myopalladin (amino acid residues 945 – 1320) after size-exclusion chromatography.

Two different plasmids were created in order to test myopalladin interaction with EF-hands domain. The first bi-cistronic vector contains his-tagged EF-hands 1-4 of α -actinin 2 (cloned into MCS I) and un-tagged C-terminal fragment of myopalladin (amino acid residues 945 – 1320). The second vector contains α -actinin Δ at the MCS I and a smaller myopalladin fragment (amino acid residues 800 – 920) at the MCS II. The *E.coli* expression strain BL21 DE3 Rosetta2 pRARE II and TB growth medium were employed as in previous experiments. These plasmids allow reconstituting two α -actinin/ myopalladin complexes of different molecular weight.

A two-step protein purification protocol (IMAC/size-exclusion chromatography) was applied for the complexes. The obtained results were positive in both cases. The presence of myopalladin and actinin protein constructs was confirmed both by SDS-PAGE (**Fig.30**) and by mass-spectrometry (“peptide fingerprinting”). These complexes, however, appear to be less stable than Zr’s/EF-hands assemblies. No further biophysical characterization experiments were performed on these complexes.

5 CONCLUSIONS AND FUTURE PERSPECTIVES

Present treatise is dedicated to experimental studies of the complexes of muscle proteins titin and α -actinin. These proteins together with F-actin fibers constitute the macromolecular scaffold of the Z-disk. This robust grid creates a structured space in which other proteins can perform their functions in coordinated and ordered manner. The investigation of the Z-band structural lattice and its components is of particular importance taking into account the growing interest of scientific community to the molecular biology of muscles in health and disease.

This research project was based on experimental works of Atkinson *et al.*, 2001 and Joseph *et al.*, 2001. The project was aimed at confirming the existing data and further expanding them. Correspondingly to this idea both the aims of the thesis and overall research plan were defined.

The majority of the aims were successfully achieved in course of experimental work. The toolkit of titin and α -actinin protein constructs was created. It was proven that the co-transformation/co-expression strategy was applicable for the reconstitution of Z-repeats and EF-hands protein complexes. The following complexes were reconstructed: EF-hands 1-4 plus Zr.1; EF-hands 1-4 plus Zr.7; EF-hands 3-4 plus Zr.1; EF-hands 3-4 plus Zr.7; EF-hands 1-4 plus Zr.1-2-3; EF-hands 1-4 plus Zr.5-6-7; EF-hands 1-4 plus Zr.1-2-3-7; α -actinin Δ plus Zr.1-2-3.

The purification protocols were established and optimized both for the separate components and for complexes of different size. These protocols

allowed obtaining mentioned complexes in large quantities (mg-scale) and of high purity, thus suitable for studies by high-resolution techniques of structural biology.

The 1:1 stoichiometry of the components in titin/ α -actinin complexes was confirmed by using such biophysical methods as analytical size-exclusion chromatography, static light scattering and analytical ultracentrifugation. The estimation was based on proteins molecular weights which had been determined by mentioned methods. The body of obtained and already existing experimental data also suggests that the interaction sites are located only within titin repeats 1 and 7 and not within other Zrs. The only α -actinin domain which is able to interact with titin via 1-4,5-8 set of Zr.1 and Zr.7 hydrophobic residues is the EF-hands 3-4 domain.

The co-expression/co-purification experiments demonstrated further that Zr. 2, 3, 4, 5, 6 did not interact with EF-hands 3-4 of α -actinin. It is known that given repeats are often subject to alternative splicing and may be absent in some titin isoforms. It is possible that these non-interacting Z-repeats play merely a role of spacers by changing the distance between interacting Zr.1 and Zr.7. The exact physiological role of the “spacer repeats” is yet to be elucidated.

The titin Zrs are distinct from typical Ig-like and Fn.III-like domains which constitute the large part of titin macromolecule. The repeats alone do not possess well-defined secondary structure in solution. The overall compactisation of proteins and significant increase of the secondary structure content occur only upon binding of Zrs to the EF-hands 3-4 domain. The supporting evidences of this were obtained in course of circular dichroism spectroscopy experiments. The CD measurements also confirmed that the complexes of Z-repeats and EF-hands domains reconstituted by co-expression were identical to those reconstructed by mixing of the components.

It was shown that the presence of non-interacting repeats (Zrs. 2, 3, 4, 5, 6) did not lead to the change of mentioned 1:1 stoichiometry of the components in reconstituted complexes. This was shown by studying the complexes of EF-hands 1-4 plus Zr.1-2-3-7, EF-hands 1-4 plus Zr.1-2-3, EF-hands 1-4 plus Zr.5-6-7 and α -actinin Δ plus Zr.1-2-3.

The purified proteins and their complexes were used for further small angle X-ray scattering experiments. The low-resolution molecular envelopes and overall molecular parameters (radius of gyration, experimental molecular mass, maximal distance within particle) were calculated. It was shown that that the maximal distance within complexes of Z-repeats/EF-hands was smaller than the average distance between the layers in the Z-disk (19 nm). Only the complex of EF-hands 1-4 with four titin repeats that possesses two binding sites had length of 20 nm which is comparable with the distance between the Z-band layers. These findings support the idea of Dr. P.Luther (Luther & Squire, 2002) that sole Z-repeats cannot act as a determinant of number of the layers and, hence, of the Z-disk thickness. It is apparent that neither separate Zrs nor their pairs are large enough to define the distance between the Z- band layers. It is likely that studied titin/ α -actinin interaction has solely structural role. By means of binding to EF-hands domains 3-4 titin filaments from adjacent sarcomeres are robustly anchored within the Z-disk macromolecular grid. The anchored titin in its turn provides an interaction platform for a number of auxiliary Z-disk proteins.

The co-expression approach was used for the reconstitution of the complexes of myopalladin and α -actinin at the concluding stages of the project. The bi-cistronic vectors were employed for these experiments. The existence of the interactions between α -actinin and myopalladin was shown previously by qualitative methods such as pull-downs and western-blot (Bang *et al.*, 2001) which, indeed, are often known to produce false positive results. In present study

it was shown directly that these complexes can be reconstituted by co-expression and purified by immobilized metal ion affinity chromatography and SEC. These results further emphasize the value of co-expression as a method of choice for rapid and reliable reconstruction of protein-protein complexes. Moreover, this technique was very useful not only for the reconstruction of the complexes but also for rapid probing of putative protein-protein interactions by co-expressing/co-purifying the components with and without affinity tags.

Taking into account available data (Bang *et al.*, 2000; Beck *et al.*, 2011) it is also apparent that not only titin but many other proteins may interact with α -actinin via its EF-hands 3-4 domain. These interactions are most likely to be mediated by the similar mechanism: the combined action of hydrophobic and, to lesser extent, electrostatic forces. Depending on the hydrophobic residues which are involved in binding, the strength of the interaction may vary significantly. It is permissible to hypothesise that these interactions can be regulated by the phosphatidylinositol 4,5-bisphosphate.

In order to develop given project further it would be desirable to obtain a number of high-resolution structures of titin – α -actinin complexes of different size. This is necessary for further advancement of knowledge of given interactions and their regulation. The extensive crystallization trials which had been performed at EMBL-Hamburg Highthroughput crystallization facility did not result in positive hints. Taking into account this fact it is clear that further structural studies should be done by nuclear magnetic resonance (NMR) methods. The molecular weights of single-domain complexes are in the weight range when NMR can be successfully applied. The developed expression and purification protocols allow obtaining the desired complexes in sufficient quantity and of high purity. This is achievable even when the protein expression is performed in minimal M9 medium for the purpose of isotope labeling.

The electron microscopy imaging can also be employed for further investigation of titin/ α -actinin or myopalladin/ α -actinin interactions. The reconstituted α -actinin Δ /Zr.1-2-3 complex possesses the molecular weight that allows it to be successfully studied by EM. However, for this type of experiments the peptide constructs of titin and, possibly, of myopalladin have to be expressed and purified as fusions containing large globular protein tag. The maltose binding protein (MBP) can be particularly useful in these experiments. The applicability of protein cross-linking for mentioned complexes has to be additionally tested. In case of success, this approach will allow obtaining more stable and robust protein complexes. This in turn will significantly increase the possibility of generating high-quality data by electron microscopy imaging.

It is necessary to mention that such methods as isothermal titration calorimetry, mass-spectrometry, fluorescence microscopy and immunolabelling should be employed for future studies of titin – α -actinin interactions. Only by following the interdisciplinary approach and implementing techniques from different fields of molecular biology, it is possible to generate the necessary body of data and get new insights into functioning of one of the most complex molecular assemblies – the Z-disk.

REFERENCES:

- Arimura, C., Suzuki, T., Yanagisawa, M., Imamura, M., Hamada, Y., Masaki, T. (1988) Primary structure of chicken skeletal muscle and fibroblast alpha-actinins deduced from cDNA sequences. *Eur. J. Biochem.* **177(3)**, 649-55
- Atkinson, R.A., Joseph, C., Dal Piaz, F., Birolo, L., Stier, G., Pucci, P., Pastore, A. (2000) Binding of alpha-actinin to titin: implications for Z-disk assembly. *Biochemistry* **39(18)**, 5255-64
- Atkinson, R.A., Joseph, C., Kelly, G., Muskett, F.W., Frenkiel, T.A., Pastor, A. (2000) Assignment of the ^1H , ^{13}C and ^{15}N resonances of the C-terminal EF-hands of α -actinin in a 14 kDa complex with Z-repeat 7 of titin. *J. Biomol. NMR* **16(3)**, 277-8
- Atkinson, R., Joseph, C., Kelly, G., Muskett, F., Frenkiel, T., Nietlispach, D., Pastore, A. (2001) Ca^{2+} -independent binding of an EF-hand domain to a novel motif in the α -actinin–titin complex. *Nature Structural Biology* **8(10)**, 853-857
- Ayoob, J.C., Turnacioglu, K.K., Mittal, B., Sanger, J.M., Sanger, J.W. (2000) Targeting of cardiac muscle titin fragments to the Z-bands and dense bodies of living muscle and non-muscle cells. *Cell. Motil. Cytoskeleton* **45(1)**, 67-82
- Baines, A.J. (2003). Comprehensive analysis of all triple helical repeats in betaspectrins reveals patterns of selective evolutionary conservation. *Cell Mol. Biol. Lett.* **8(1)**, 195-214
- Bang, M.-L., Centner, T., Fornoff, F., Geach, A.J., Gotthardt, M., McNabb, M., Witt, C.C., Labeit, D., Gregorio, C.C., Granzier, H., Labeit, S. (2001) The complete gene sequence of titin, expression of an unusual approximately 700-

- kDa titin isoform, and its interaction with obscurin identify a novel Z-line to I-band linking system. *Circ. Res.* **89(11)**, 1065-72
- Bang, M-L., Mudry, R.E., McElhinny, A.S., Trombitás, K., Geach, A.J., Yamasaki, R., Sorimachi, H., Granzier, H., Gregorio, C.C., Labeit, S. (2001) Myopalladin, a novel 145-kilodalton sarcomeric protein with multiple roles in Z-disc and I-band protein assemblies. *J. Cell. Biol.* **153(2)**, 413-27
- Barral, J.M. and Epstein, H.F. (1999) Protein machines and self assembly in muscle organization. *BioEssays* **21(10)**, 813-23
- Barstead, R.J., Kleiman, L., Waterston, R.H. (1991) Cloning, sequencing, and mapping of an alpha-actinin gene from the nematode *Caenorhabditis elegans*. *Cell. Motil. Cytoskeleton* **20(1)**, 69-78
- Beck, M.R., Otey, C.A., Campbell, S.L. (2011) Structural characterization of the interactions between palladin and α -actinin. *J. Mol. Biol.* **413(3)**, 712-25
- Beggs, A.H., Byers, T.J., Knoll, J.H., Boyce, F.M., Bruns, G.A., Kunkel, L.M. (1992) Cloning and characterization of two human skeletal muscle alpha-actinin genes located on chromosomes 1 and 11. *J. Biol. Chem.* **267(13)**, 9281-9288
- Berman, Y., North, K.N. (2010) A gene for speed: the emerging role of alpha-actinin-3 in muscle metabolism. *Physiology (Bethesda)* **25(4)**, 250-9
- Blanchard, A., Ohanian, V., Critchley, D. (1989) The structure and function of alpha-actinin. *J. Muscle Res. Cell Motil.* **10(4)**, 280-289
- Borisov, A.B., Sutter, S.B., Kontogianni-Konstantopoulos, A., Bloch, R.J., Westfall, M.V., Russell, M.W. (2006) Essential role of obscurin in cardiac myofibrillogenesis and hypertrophic response: evidence from small interfering RNA-mediated gene silencing. *Histochem. Cell Biol.* **125**, 227-238

- Bradford, M.M. (1976) A rapid and sensitive method for the quantitation of microgram quantities of protein utilizing the principle of protein-dye binding. *Anal. Biochem.* **72**, 248–254
- Brancaccio, M., Fratta, L., Notte, A., Hirsch, E., Poulet, R., Guazzone, S., De Acetis, M., Vecchione, C., Marino, G., Altruda, F., Silengo, L., Tarone, G., Lembo, G. (2003) Melusin, a muscle-specific integrin beta1-interacting protein, is required to prevent cardiac failure in response to chronic pressure overload. *Nat. Med.* **9(1)**, 68-75
- Briskey, E.J., Fukazawa, T. (1970) Low-temperature extraction of alpha-actinin-like protein from the I-Z-I brush of striated muscle. *Biochim. Biophys. Acta* **205(3)**, 317-327
- Broderick, M.J., Winder, S.J. (2005) Spectrin, alpha-actinin, and dystrophin. *Adv. Protein. Chem.* **70**, 203-246
- Bryksin A.V., Matsumura I. (2010) Overlap extension PCR cloning: a simple and reliable way to create recombinant plasmids. *BioTechniques* **48(6)**, 463–465
- Burridge, K., Feramisco, J.R. (1981) Non-muscle alpha actinins are calcium sensitive actin-binding proteins. *Nature* **294(5841)**, 565-567
- Casali, N. (2003) *Escherichia coli* host strains. In *Methods in Molecular Biology*, Vol. 235: *E. coli* Plasmid Vectors (Casali, N., Preston, A., Ed.), pp 27-48, Humana Press Inc., Totowa, NJ
- Chan, Y., Tong, H.Q., Beggs, A.H. and Kunkel L.M. (1998) Human skeletal muscle-specific alpha-actinin-2 and -3 isoforms form homodimers and heterodimers *in vitro* and *in vivo*. *Biochem. Biophys. Res. Commun.* **248(1)**, 134-139

- Clark, K.A., McElhinny, A.S., Beckerle, M.C., Gregorio, C.C. (2002) Striated muscle cytoarchitecture: an intricate web of form and function. *Annu. Rev. Cell Dev. Biol.* **18**, 637-706
- Combet, C., Blanchet, C., Geourjon, C., Deléage, G. (2000) NPS@: network protein sequence analysis. *Trends Biochem. Sci.* **25(3)**, 147-150
- Compton, S.J., Jones, C.G. (1985) Mechanism of dye response and interference in the Bradford protein assay. *Anal. Biochem.* **151**, 369–374
- Corgan, A.M., Singleton, C., Santoso, C.B., Greenwood, J.A. (2004) Phosphoinositides differentially regulate alpha-actinin flexibility and function. *Biochem. J.* **378(Pt 3)**, 1067-72
- Crabtree, G.R., Olson, E.N. (2002) NFAT signaling: choreographing the social lives of cells. *Cell* **109(Suppl)**, S67–S79
- Davison, M.D., Critchley, D.R. (1988) alpha-Actinins and the DMD protein contain spectrin-like repeats. *Cell* **52(2)**, 159-160
- De Acetis, M., Notte, A., Accornero, F., Selvetella, G., Brancaccio, M., Vecchione, C., Sbroggiò, M., Collino, F., Pacchioni, B., Lanfranchi, G., Aretini, A., Ferretti, R., Maffei, A., Altruda, F., Silengo, L., Tarone, G., Lembo, G. (2005) Cardiac overexpression of melusin protects from dilated cardiomyopathy due to long-standing pressure overload. *Circ. Res.* **96(10)**, 1087-94
- Dixon, J.D., Forstner, M.J., Garcia, D.M. (2003) The alpha-actinin gene family: a revised classification. *J. Mol. Evol.* **56(1)**, 1-10
- Djinovic Carugo, K., Bañuelos, S., Saraste, M. (1997) Crystal structure of a calponin homology domain. *Nat. Struct. Biol.* **4(3)**, 175-9
- Djinovic-Carugo, K., Gautel, M., Ylänne, J., Young, P. (2002) The spectrin repeat: a structural platform for cytoskeletal protein assemblies. *FEBS Lett.* **513(1)**, 119-23

- Djinovic-Carugo, K., Young, P., Gautel, M., Saraste, M. (1999) Structure of the α -actinin rod: molecular basis for cross-linking of actin filaments. *Cell* **98(4)**, 537–546
- Ebashi, S., Ebashi, F. (1964) A new protein factor promoting contraction of actomyosin. *Nature* **203**, 645-6
- Ebashi, S., Ebashi, F. (1965) Alpha-actinin, a new structural protein from striated muscle. I. Preparation and action on actomyosin-ATP interaction. *J. Biochem.* **58(1)**, 7-12
- Flood, G., Kahana, E., Gilmore, A.P., Rowe, A.J., Gratzer, W.B., Critchley, D.R. (1995) Association of structural repeats in the alpha-actinin rod domain. Alignment of inter-subunit interactions. *J. Mol. Biol.* **252(2)**, 227-234
- Folta-Stogniew, E. (2006) Oligomeric states of proteins determined by size-exclusion chromatography coupled with light scattering, absorbance, and refractive index detectors. In *Methods in Molecular Biology*, Vol. 328: New and Emerging Proteomic Techniques (Nedelkov, D., Nelson, R. W., Eds.), pp 97-112, Humana Press Inc., Totowa, NJ
- Fraleigh, T.S., Tran, T.C., Corgan, A.M., Nash, C.A., Hao, J., Critchley, D.R., Greenwood, J.A. (2003) Phosphoinositide binding inhibits alpha-actinin bundling activity. *J. Biol. Chem.* **278(26)**, 24039-24045
- Frank, D., Frey, N. (2011) Cardiac Z-disc signaling network. *J. Biol. Chem.* **286(12)**, 9897-904
- Frank, D., Kuhn, C., Katus, H.A. and Frey, N. (2006) The sarcomeric Z-disc: a nodal point in signaling and disease. *J. Mol. Med.* **84(6)**, 446-468
- Franke, D., Kikhney, A.G. and Svergun, D.I. (2012) Automated Acquisition and Analysis of Small Angle X-ray Scattering Data. *Nuclear Instruments and Methods in Physics Research Section A* **689**, 52-59

- Franke, D. and Svergun, D.I. (2009) DAMMIF, a program for rapid ab-initio shape determination in small-angle scattering. *J. Appl. Cryst.*, **42**, 342-346
- Franzot, G., Sjoblom, B., Gautel, M., Djinovic Carugo, K. (2005) The crystal structure of the actin binding domain from α -actinin in its closed conformation: structural insight into phospholipid regulation of α -actinin. *J. Mol. Biol.* **348(1)**, 151–165
- Frey, N., Richardson, J.A., Olson, E.N. (2000) Calsarcins, a novel family of sarcomeric calcineurin-binding proteins. *Proc. Natl. Acad. Sci. USA* **97**, 14632–14637
- Fukami, K., Endo, T., Imamura, M. and Takenawa, T. (1994) Alpha-actinin and vinculin are PIP2-binding proteins involved in signaling by tyrosine kinase. *J. Biol. Chem.* **269(2)**, 1518-1522
- Fukami, K., Furuhashi, K., Inagaki, M., Endo, T., Hatano, S., Takenawa, T. (1992) Requirement of phosphatidylinositol 4,5-bisphosphate for alpha-actinin function. *Nature* **359(6391)**, 150-152
- Fukami, K., Sawada, N., Endo, T., Takenawa, T. (1996) Identification of a phosphatidylinositol 4,5-bisphosphate-binding site in chicken skeletal muscle alphaactinin. *J. Biol. Chem.* **271(5)**, 2646-2650
- Full, S.J., Deinzer, M.L., Ho, P.S. and Greenwood, J.A. (2007) Phosphoinositide binding regulates alpha-actinin CH2 domain structure: analysis by hydrogen/deuterium exchange mass spectrometry. *Protein Sci.* **16**, 2597–2604
- Fyrberg, E., Kelly, M., Ball, E., Fyrberg, C., Reedy, M.C. (1990) Molecular genetics of *Drosophila* alpha-actinin: mutant alleles disrupt Z disc integrity and muscle insertions. *J. Cell Biol.* **110(6)**, 1999-2011
- Galkin, V.E., Orlova, A., Salmazo, A., Djinovic-Carugo, K., Egelman, E.H., (2010) Opening of tandem calponin homology domains regulates their affinity for F-actin. *Nat. Struct. Mol. Biol.* **17(5)**, 614-616

- Gasteiger, E., Hoogland, C., Gattiker, A., Duvaud, S., Wilkins, M.R., Appel, R.D., Bairoch, A. (2005) Protein Identification and Analysis Tools on the ExPASy Server. In *The Proteomics Protocols Handbook* (Walker, J.M., Ed.), pp 571-607, Humana Press Inc., Totowa, NJ
- Gautel, M. (1996) The super-repeats of titin/connectin and their interactions: glimpses at sarcomeric assembly. *Adv. Biophys.* **33**, 27-37
- Gautel, M. (2011) The sarcomeric cytoskeleton: who picks up the strain? *Curr. Opin. Cell Biol.* **23(1)**, 39-46
- Gautel, M., Goulding, D., Bullard, B., Weber, K., Furst, D.O. (1996) The central Z-disc region of titin is assembled from a novel repeat in variable copy numbers. *J. Cell Sci.* **109**, 2747–2754
- Geeves, M.A., Holmes, K.C. (2005) The molecular mechanism of muscle contraction. *Adv. Protein Chem.* **71**, 161-93
- Gifford, J.L., Walsh, M.P., Vogel, H.J. (2007) Structures and metal-ion-binding properties of the Ca²⁺-binding helix-loop-helix EF-hand motifs. *Biochem. J.* **405(2)**, 199-221
- Gimona, M., Djinovic-Carugo, K., Kranewitter, W.J., Winder, S.J., (2002) Functional plasticity of CH domains. *FEBS Lett.* **513(1)**, 98-106
- Goldstein, M.A., Michael, L.H., Schroeter, J.P., Sass, R.L. (1986) The Z-band lattice in skeletal muscle before, during and after tetanic contraction. *J. Muscle Res. Cell Motil.* **7(6)**, 527-536
- Goldstein, M.A., Michael, L.H., Schroeter, J.P., Sass, R.L. (1989) Two structural states of Z-bands in cardiac muscle. *Am. J. Physiol.* **256(2 Pt 2)**, H552-559
- Goldstein, A.M., Michael, H.L., Schroeter, P.J., Sass, L.R. (1988) Structural states in the Z Band of skeletal muscle correlate with states of active and passive tension. *J. Gen. Physiol.* **92(1)**, 113-119

- Goldstein, M.A., Schroeter, J.P., Sass, R.L. (1982) The Z-band lattice in a slow skeletal muscle. *J. Muscle Res. Cell Motil.* **3(3)**, 333-348
- Goldstein, M.A., Schroeter, J.P., Sass, R.L. (1990) Two structural states of the vertebrate Z band. *Electron Microsc. Rev.* **3(2)**, 227-248
- Goldstein, M.A., Schroeter, J.P., Michael, L.H. (1991) Role of the Z-band in the mechanical properties of the heart. *FASEB J.* **5(8)**, 2167-2174
- Grabarek, Z. (2006) Structural basis for diversity of the EF-hand calcium-binding proteins. *J. Mol. Biol.* **359(3)**, 509-525
- Granzier, H.L., Labeit, S. (2004) The giant protein titin: a major player in myocardial mechanics, signaling, and disease. *Circ. Res.* **94**, 284–295
- Granzier, H.L., Labeit, S. (2005) Titin and its associated proteins: the third myofilament system of the sarcomere. *Adv. Protein Chem.* **71**, 89-119
- Granzier, H., Labeit, S. (2007) Structure-function relations of the giant elastic protein titin in striated and smooth muscle cells. *Muscle Nerve* **36(6)**, 740-755
- Granzier, H., Kellermayer, M., Helmes, M., Trombitas, K. (1997) Titin elasticity and mechanism of passive force development in rat cardiac myocytes probed by thin-filament extraction. *Biophys. J.* **73**, 2043–2053
- Greenfield, N.J. (2006) Using circular dichroism spectra to estimate protein secondary structure. *Nat. Protoc.* **1(6)**, 2876-90
- Gregorio, C.C., Trombitas, K., Centner, T., Kolmerer, B., Stier, G., Kunke, K., Suzuki, K., Obermayr, F., Herrmann, B., Granzier, H., Sorimachi, H. and Labeit, S. (1998) The NH₂ terminus of titin spans the Z-disc: its interaction with a novel 19-kD ligand (T-cap) is required for sarcomeric integrity. *J. Cell Biol.* **143(4)**, 1013-1027
- Guy, P.M., Kenny, D.A., Gill, G.N. (1999) The PDZ domain of the LIM protein enigma binds to beta-tropomyosin. *Molecular Biology of the Cell* **10(6)**, 1973–1984

- Hackman, J.P., Vihola, A.K., Udd, A.B. (2003) The role of titin in muscular disorders. *Ann. Med.* **35**, 434-41
- Hampton, C.M., Taylor, D.W., Taylor, K.A., (2007) Novel structures for alpha-actinin:F-actin interactions and their implications for actin-membrane attachment and tension sensing in the cytoskeleton. *J. Mol. Biol.* **368(1)**, 92-104
- Hanahan, D. (1983) Studies on transformation of *Escherichia coli* with plasmids *J. Mol. Biol.* **166**, 557-77.
- Hanahan, D. (1985) Techniques for transformation of *E.coli*. In *DNA Cloning, a Practical Approach* (Glover, D.M. Ed.), vol. 1, pp. 109-135, IRL Press, Ltd. London, UK
- Hoshijima, M. (2006) Mechanical stress-strain sensors embedded in cardiac cytoskeleton: Z disk, titin, and associated structures. *Am. J. Physiol. Heart Circ. Physiol.* **290(4)**, H1313-1325
- Hsin, J., Strümpfer, J., Lee, E.H., Schulten, K. (2011) Molecular origin of the hierarchical elasticity of titin: simulation, experiment, and theory. *Annu. Rev. Biophys.* **40**, 187-203
- Huxley, H.E. (1961) The contractile structure of cardiac and skeletal muscle. *Circulation* **24**, 328-35
- Huxley, A.F., Niedergerke, R. (1954) Structural changes in muscle during contraction; interference microscopy of living muscle fibres. *Nature* **173(4412)**, 971-973
- Huxley, H., Hanson, J. (1954) Changes in the cross-striations of muscle during contraction and stretch and their structural interpretation. *Nature* **173(4412)**, 973-976
- Inoue H, Nojima H, Okayama H. (1990) High efficiency transformation of *Escherichia coli* with plasmids. *Gene* **96(1)**, 23-8

- Jain, E., Bairoch, A., Duvaud, S., Phan, I., Redaschi, N., Suzek, B.E., Martin, M.J., McGarvey, P., Gasteiger, E. (2009) Infrastructure for the life sciences: design and implementation of the UniProt website. *BMC Bioinformatics* **10**, 136
- Joseph, C., Stier, G., O'Brien, R., Politou, A.S., Atkinson, R.A., Bianco, A., Ladbury, J.E., Martin, S.R., Pastore, A. (2001) A structural characterization of the interactions between titin Z-repeats and the alpha-actinin C-terminal domain. *Biochemistry* **40(16)**, 4957-65
- Kaplan, J.M., Kim, S.H., North, K.N., Rennke, H., Correia, L.A., Tong, H.Q., Mathis, B.J., Rodriguez-Perez, J.C., Allen, P.G., Beggs, A.H., Pollak, M.R. (2000) Mutations in ACTN4, encoding alpha-actinin-4, cause familial focal segmental glomerulosclerosis. *Nat. Genet.* **24(3)**, 251-256
- Kelly, S. M., Price, N. C. (2006) Circular Dichroism to Study Protein Interactions. In *Current Protocols in Protein Science* 20.10.1-20.10.18, John Wiley & Sons, Inc.
- Knupp, C., Luther, P.K., Squire, J.M., (2002) Titin organisation and the 3D architecture of the vertebrate-striated muscle I-band. *J. Mol. Biol.* **322(4)**, 731-739
- Knöll, R., Buyandelger, B., Lab M. (2011) The sarcomeric Z-disc and Z-discopathies. *J. Biomed. Biotechnol.* Article ID:569628, 12 pages, doi:10.1155/2011/569628
- Knöll, R., Hoshijima, M., Hoffman, H.M., Person, V., Lorenzen-Schmidt, I., Bang, M-L., Hayashi, T., Shiga, N., Yasukawa, H., Schaper, W., McKenna, W., Yokoyama, M., Schork, N.J., Omens, J.H., McCulloch, A.D., Kimura, A., Gregorio, C.C., Poller, W., Schaper, J., Schultheiss, H.P., Chien, K.R. (2002) The cardiac mechanical stretch sensor machinery involves a Z disc complex

- that is defective in a subset of human dilated cardiomyopathy. *Cell* **111(7)**, 943-55
- Konarev, P.V., Volkov, V.V. and Sokolova, A.V. (2003) PRIMUS: a Windows PC-based system for small-angle scattering data analysis. *J. Appl. Cryst.*, **36**, 1277-1282
- Kontrogianni-Konstantopoulos, A., Ackermann, M., Bowman, A., Yap, S., Bloch, R.J. (2009) Muscle giants: molecular scaffolds in sarcomerogenesis. *Physiol. Rev.* **89(4)**, 1217-1267
- Kontrogianni-Konstantopoulos, A., Bloch, R.J. (2005) Obscurin: a multitasking muscle giant. *J. Muscle Res. Cell Motil.* **26(6-8)**, 419-26
- Kostin, S., Hein, S., Arnon, E., Scholz, D., Schaper, J. (2000) The cytoskeleton and related proteins in the human failing heart. *Heart Fail. Rev.* **5(3)**, 271-80
- Krüger, M., Linke, W.A. (2011) The giant protein titin: a regulatory node that integrates myocyte signaling pathways. *J. Biol. Chem.* **286(12)**, 9905-12
- Kruger, M., Wright, J., Wang, K. (1991) Nebulin as a length regulator of thin filaments of vertebrate skeletal muscles: correlation of thin filament length, nebulin size, and epitope profile. *J. Cell Biol.* **115**, 97–107
- Kuroda, S., Tokunaga, C., Kiyohara Y., Higuchi, O., Konishi, H., Mizuno, K., Gill, G.N., Kikkawa, U. (1996) Protein-protein interaction of zinc finger LIM domains with protein kinase C. *Journal of Biological Chemistry*, **271(49)**, 31029–31032
- Kwiatkowska, K. (2010) One lipid, multiple functions: how various pools of PI(4,5)P(2) are created in the plasma membrane. *Cell Mol. Life Sci.* **67(23)**, 3927-46
- Labeit, S., Lahmers, S., Burkart, C., Fong, C., McNabb, M., Witt, S., Witt, C., Labeit, D., Granzier, H. (2006) Expression of distinct classes of titin isoforms

- in striated and smooth muscles by alternative splicing, and their conserved interaction with filamins. *J. Mol. Biol.* **362(4)**, 664-81
- Lan, S., Wang, H., Jiang, H., Mao, H., Liu, X., Zhang, X., Hu, Y., Xiang, L., Yuan, Z. (2003) Direct interaction between alpha-actinin and hepatitis C virus NS5B. *FEBS Lett.* **554(3)**, 289-294
- Lange, S., Ehler, E., Gautel, M. (2006) From A to Z and back? Multicompartment proteins in the sarcomere. *Trends Cell Biol.* **16(1)**, 11-18
- Lazarides, E., Hubbard, B.D. (1976) Immunological characterization of the subunit of the 100 A filaments from muscle cells. *Proc. Natl. Acad. Sci. USA* **73**, 4344–4348
- Lek, M., North, K.N. (2010) Are biological sensors modulated by their structural scaffolds? The role of the structural muscle proteins alpha-actinin-2 and alpha-actinin-3 as modulators of biological sensors. *FEBS Lett.* **584(14)**, 2974-80
- Lewit-Bentley, A., Rety, S. (2000) EF-hand calcium-binding proteins. *Curr. Opin. Struct. Biol.* **10(6)**, 637-643
- Linke, W.A. (2008) Sense and stretchability: the role of titin and titin-associated proteins in myocardial stress-sensing and mechanical dysfunction. *Cardiovasc. Res.* **77(4)**, 637-48
- Liu, J., Taylor, D.W. and Taylor, K.A. (2004) A 3-D reconstruction of smooth muscle alpha-actinin by CryoEm reveals two different conformations at the actin-binding region. *J. Mol. Biol.* **338**, 115–125
- Louis-Jeune, C., Andrade-Navarro, M.A., Perez-Iratxeta, C. (2012). Prediction of protein secondary structure from circular dichroism using theoretically derived spectra. *Proteins* **80**, 374–381
- Luther, P.K. (2009) The vertebrate muscle Z-disc: sarcomere anchor for structure and signaling. *J. Muscle Res. Cell Motil.* **30(5-6)**, 171–185

- Luther, P.K., Barry, J.S., Squire, J.M. (2002) The three-dimensional structure of a vertebrate wide (slow muscle) Z-band: lessons on Z-band assembly. *J. Mol. Biol.* **315(1)**, 9-20
- Luther, P.K., Padrón, R., Ritter, S., Craig, R., Squire, J.M. (2003) Heterogeneity of Z-band structure within a single muscle sarcomere: implications for sarcomere assembly. *J. Mol. Biol.* **332(1)**, 161-169
- Luther, P.K., Squire, J.M. (2002) Muscle Z-band ultrastructure: titin Z-repeats and Z-band periodicities do not match. *J. Mol. Biol.* **319(5)**, 1157-64
- Lymn, R.W. and Taylor, E.W. (1971). Mechanism of adenosine triphosphate hydrolysis by actomyosin. *Biochemistry* **10**, 4617–4624
- MacArthur, D.G., North, K.N. (2004) A gene for speed? The evolution and function of alpha-actinin-3. *BioEssays* **26(7)**, 786-795
- Marino, M., Zou, P., Svergun, D., Garcia, P., Edlich, C., Simon, B., Wilmanns, M., Muhle-Goll, C., Mayans, O. (2006) The Ig doublet Z1Z2: a model system for the hybrid analysis of conformational dynamics in Ig tandems from titin. *Structure* **14(9)**, 1437-47
- Maruyama, K. (1994) Connectin, an elastic protein of striated muscle. *Biophys. Chem.* **50(1-2)**, 73-85
- Maruyama, K. (1997) Connectin/titin, giant elastic protein of muscle. *FASEB J.* **11(5)**, 341-345
- Maruyama, K., Kimura, S., Ohashi, K., Kuwano, Y. (1981) Connectin, an elastic protein of muscle. Identification of "titin" with connectin. *J. Biochem.* **89(3)**, 701-9
- Maruyama, K., Matsubara, S., Natori, R., Nonomura, Y., Kimura, S. (1977) Connectin, an elastic protein of muscle. Characterization and function. *J. Biochem.* **82(2)**, 317-37

- Masaki, T., Endo, M., Ebashi, S. (1967) Localization of 6S component of a alpha-actinin at Z-band. *J. Biochem.* **62(5)**, 630-632
- Matsumoto, Y., Hayashi, T., Inagaki, N., Takahashi, M., Hiroi, S., Nakamura, T., Arimura, T., Nakamura, K., Ashizawa, N., Yasunami, M., Ohe, T., Yano, K., Kimura, A. (2005) Functional analysis of titin/connectin N2-B mutations found in cardiomyopathy. *J. Muscle Res. Cell Motil.* **26(6-8)**, 367-74
- Miller, J.H. (1972). *Experiments in molecular genetics*. Cold Spring Harbor Laboratory, Cold Spring Harbor, New York
- Mills, M., Yang, N., Weinberger, R., Vander Woude, D.L., Beggs, A.H., Eastal, S., and North, K. (2001) Differential expression of the actin-binding proteins, alpha-actinin-2 and -3, in different species: implications for the evolution of functional redundancy. *Hum. Mol. Genet.* **10(13)**, 1335-1346
- Mues, A., van der Ven, P.F., Young, P., Furst, D.O., Gautel, M. (1998) Two immunoglobulin-like domains of the Z-disc portion of titin interact in a conformation-dependent way with telethonin. *FEBS Lett.* **428**, 111–114
- Nakayama, S., Kretsinger, R.H. (1994) Evolution of the EF-hand family of proteins. *Annu. Rev. Biophys. Biomol. Struct.* **23**, 473-507
- Newton, A.C. (1995) Protein kinase C: structure, function, and regulation. *J. Biol. Chem.* **270**, 28495–28498
- Newton, P.M., Messing, R.O. (2010) The substrates and binding partners of protein kinase Cepsilon. *Biochem. J.* **427(2)**, 189-96
- Noegel, A., Witke, W., Schleicher, M. (1987) Calcium-sensitive non-muscle alpha-actinin contains EF-hand structures and highly conserved regions. *FEBS Lett.* **221(2)**, 391-396
- Ohtsuka, H., Yajima, H., Maruyama, K., Kimura, S. (1997) The N-terminal Z repeat 5 of connectin/titin binds to the C-terminal region of alpha-actinin. *Biochem. Biophys. Res. Commun.* **235(1)**, 1-3

- Ohtsuka, H., Yajima, H., Maruyama, K., Kimura, S. (1997) Binding of the N-terminal 63 kDa portion of connectin/titin to alpha-actinin as revealed by the yeast two-hybrid system. *FEBS Lett.* **401(1)**, 65-67
- Otey, C.A., Carpen, O. (2004) Alpha-actinin revisited: a fresh look at an old player. *Cell Motil. Cytoskeleton.* **58(2)**, 104-111
- Otey, C.A., Rachlin, A., Moza, M., Arneman, D., Carpen, O. (2005) The palladin/myotilin/myopalladin family of actin-associated scaffolds. *Int. Rev. Cytol.* **246**, 31-58.
- Otto, J.J. (1994) Actin-bundling proteins. *Curr. Opin. Cell Biol.* **6(1)**, 105-109
- Parast, M.M., Otey, C.A. (2000) Characterization of palladin, a novel protein localized to stress fibers and cell adhesions. *J. Cell Biol.* **150**, 643–656
- Peckham, M., Young, P., Gautel, M. (1997) Constitutive and variable regions of Z-disk titin/connectin in myofibril formation: a dominant-negative screen. *Cell Struct. Funct.* **22(1)**, 95-101
- Petoukhov, M.V. and Svergun, D.I. (2005) Global rigid body modeling of macromolecular complexes against small-angle scattering. *Biophys. J.* **89(2)**, 1237-1250
- Petoukhov, M.V., Franke, D., Shkumatov, A.V., Tria, G., Kikhney, A.G., Gajda, M., Gorba, C., Mertens, H.D.T., Konarev, P.V. and Svergun, D.I. (2012) New developments in the ATSAS program package for small-angle scattering data analysis. *J. Appl. Cryst.* **45**, 342-350
- Pinotsis, N., Petoukhov, M.V., Lange, S., Svergun, D., Zou, P., Gautel, M., Wilmanns, M. (2006) Evidence for a dimeric assembly of two titin/telethonin complexes induced by the telethonin C-terminus. *J. Struct. Biol.* **155(2)**, 239-50

- Rief, M., Pascual, J., Saraste, M., Gaub, H.E. (1999) Single molecule force spectroscopy of spectrin repeats: low unfolding forces in helix bundles. *J. Mol. Biol.* **286(2)**, 553-561
- Ross, R.S., Borg, T.K. (2001) Integrins and the myocardium. *Circ. Res.* **88**, 1112–1119
- Ross, R.S. (2004) Molecular and mechanical synergy: cross-talk between integrins and growth factor receptors. *Cardiovasc. Res.* **63**, 381–390
- Rönty, M., Taivainen, A., Moza, M., Otey, C.A., Carpén, O. (2004) Molecular analysis of the interaction between palladin and alpha-actinin. *FEBS Lett.* **566(1-3)**, 30-4
- Russell, B., Curtis, M.W., Koshman, Y.E., Samarel, A.M. (2010) Mechanical stress-induced sarcomere assembly for cardiac muscle growth in length and width. *J. Mol. Cell Cardiol.* **48(5)**, 817-23
- Samarel, A.M. (2005) Costameres, focal adhesions, and cardiomyocyte mechanotransduction. *Am. J. Physiol. Heart Circ. Physiol.* **289(6)**, H2291-301
- Sambrook, J., David W.R. (2001) *Molecular cloning: a laboratory manual*, Cold Spring Harbor Laboratory Press, Cold Spring Harbor, New York
- Sanger, J.W., Chowrashi, P., Shaner, N.C., Spalhoff, S., Wang, J., Freeman, N.L., Sanger, J.M. (2002) Myofibrillogenesis in skeletal muscle cells. *Clin. Orthop. Relat. Res.* **403 Suppl**, S153-62
- Sanger, J.W., Sanger, J.M. (2001) Fishing out proteins that bind to titin. *J. Cell Biol.* **154(1)**, 21-24
- Schafer, D.A., Hug, C., Cooper, J.A. (1995) Inhibition of CapZ during myofibrillogenesis alters assembly of actin filaments. *J. Cell Biol.* **128**, 61–70
- Schafer, D.A., Jennings, P.B., Cooper, J.A. (1996) Dynamics of capping protein and actin assembly in vitro: uncapping barbed ends by polyphosphoinositides. *J. Cell Biol.* **135**, 169–179

- Schägger, H. (2006) Tricine-SDS-PAGE. *Nat. Protoc.* **1(1)**, 16-22
- Schuck, P. (2000) Size-distribution analysis of macromolecules by sedimentation velocity ultracentrifugation and lamm equation modeling. *Biophys. J.* **78**, 1606-1619
- Seidman, C.E., Struhl, K., Sheen, J., Jessen, T. (1997) In *Current Protocols in Molecular Biology* (Ausubel, F.M. et al. Eds.) John Wiley and Sons, NY
- Selcen, D., Engel, A.G. (2004) Mutations in myotilin cause myofibrillar myopathy. *Neurology* **62**, 1363–1371
- Semenyuk, A.V. and Svergun, D.I. (1991) GNOM-a program package for small-angle scattering data processing. *J. Appl. Cryst.* **24**, 537-540
- Sjöblom, B., Salmazo, A., Djinočić-Carugo, K. (2008) Alpha-actinin structure and regulation. *Cell Mol. Life Sci.* **65(17)**, 2688-701
- Sjöblom, B., Ylanne, J., Djinočić-Carugo, K. (2008). Novel structural insights into F-actin-binding and novel functions of calponin homology domains. *Curr. Opin. Struct. Biol.* **18(6)**, 702-708
- Small, J.V., Gimona, M. (1998) The cytoskeleton of the vertebrate smooth muscle cell. *Acta Physiol. Scand.* **164(4)**, 341-348
- Small, J.V., Sobieszek, A. (1977) Studies on the function and composition of the 10-NM(100-A) filaments of vertebrate smooth muscle. *J. Cell Sci.* **23**, 243–268
- Sorimachi, H., Freiburg, A., Kolmerer, B., Ishiura, S., Stier, G., Gregorio, C.C., Labeit, D., Linke, W.A., Suzuki, K., Labeit, S. (1997) Tissue-specific expression and alpha-actinin binding properties of the Z-disc titin: implications for the nature of vertebrate Z-discs. *J. Mol. Biol.* **270(5)**, 688-695
- Squire, J.M. (1997). Architecture and function in the muscle sarcomere. *Curr. Opin. Struct. Biol.* **7(2)**, 247-257

- Squire, J.M., Al-Khayat, H.A., Knupp, C., Luther, P.K. (2005). Molecular architecture in muscle contractile assemblies. *Adv. Protein Chem.* **71**, 17-87
- Spalteholz, W. (1898-1903) *Handatlas der Anatomie Des Menschen*, Verlag von S. Hirzel, Leipzig.
- Stout, A.L., Wang, J., Sanger, J.M., Sanger, J.W. (2008). Tracking changes in Z-band organization during myofibrillogenesis with FRET imaging. *Cell Motil. Cytoskeleton* **65(5)**, 353-367
- Stromer, M.H. (1998) The cytoskeleton in skeletal, cardiac and smooth muscle cells. *Histol. Histopathol.* **13(1)**, 283-91
- Studier, F.W. (2005) Protein production by auto-induction in high-density shaking cultures. *Prot. Exp. Pur.* **41**, 207-234
- Studier, F.W., Moffatt, B.A. (1986) Use of bacteriophage T7 RNA polymerase to direct selective high-level expression of cloned genes, *J. Mol. Biol.* **189**, 113–130
- Studier, F.W., Rosenberg, A.H., Dunn, J.J., Dubendorff J.W. (1990) Use of T7 RNA polymerase to direct expression of cloned genes, *Methods Enzymol.* **185**, 60–89
- Suzuki, A., Goll, D.E., Singh, I., Allen, R.E., Robson, R.M., Stromer, M.H. (1976) Some properties of purified skeletal muscle alpha-actinin. *J. Biol. Chem.* **251(21)**, 6860-6870
- Svergun, D.I. (1992) Determination of the regularization parameter in indirect-transform methods using perceptual criteria. *J. Appl. Crystallogr.* **25**, 495-503
- Svergun, D.I. (1999) Restoring low resolution structure of biological macromolecules from solution scattering using simulated annealing. *Biophys. J.* **76(6)**, 2879-2886

- Svergun, D.I., Barberato, C., Koch, M.H.J. (1995) CRY SOL - a program to evaluate X-ray solution scattering of biological macromolecules from atomic coordinates. *J. Appl. Cryst.* **28**, 768-773
- Svergun, D.I. and Nierhaus, K.H. (2000). A map of protein-rRNA distribution in the 70 S *Escherichia coli* ribosome. *J. Biol. Chem.* **275**, 14432-14439
- Svergun, D.I., Petoukhov, M.V. and Koch, M.H. (2001) Determination of domain structure of proteins from X-ray solution scattering. *Biophys. J.*, **80**, 2946-2953
- Takahashi, K., Hattori, A. (1989) Alpha-actinin is a component of the Z-filament, a structural backbone of skeletal muscle Z-disks. *J Biochem (Tokyo)* **105**, 529–536
- Tang, J., Taylor, D.W. and Taylor, K.A. (2001) The three dimensional structure of alpha-actinin obtained by cryoelectron microscopy suggests a model for Ca²⁺-dependent actin binding. *J. Mol. Biol.* **310**, 845–858
- Thompson, T.G., Chan, Y.M., Hack, A.A., Brosius, M., Rajala, M., Lidov, H.G., McNally, E.M., Watkins, S., Kunkel, L.M. (2000) Filamin 2 (FLN2): a muscle-specific sarcoglycan interacting protein. *J. Cell. Biol.* **148**, 115–126
- Trave, G., Pastore, A., Hyvonen, M., Saraste, M. (1995). The C-terminal domain of alpha-spectrin is structurally related to calmodulin. *Eur. J. Biochem.* **227(1-2)**, 35-42
- Trinick, J. (1996) Titin as a scaffold and spring. *Cytoskeleton. Curr. Biol.* **6(3)**, 258-260
- Tu, Z.; He, G.; Li, K.; Chen, M.; Chang, J.; Chen, L.; Yao, Q.; Liu, D.; Ye, H.; Shi, J.; Wu, X.. (2005) An improved system for competent cell preparation and high efficiency plasmid transformation using different *Escherichia coli* strains. *Electronic Journal of Biotechnology* **8(1)**, 114-120

- van der Ven, P.F., Wiesner, S., Salmikangas, P., Auerbach, D., Himmel, M., Kempa, S., Hayess, K., Pacholsky, D., Taivainen, A., Schroder, R., Carpen, O., Furst, D.O. (2000) Indications for a novel muscular dystrophy pathway. gamma-filamin, the muscle-specific filamin isoform, interacts with myotilin. *J. Cell Biol.* **151**, 235–248
- Viel, A. (1999). Alpha-actinin and spectrin structures: an unfolding family story. *FEBS Lett.* **460(3)**, 391-394
- Virel, A., Backman, L. (2004). Molecular evolution and structure of alpha-actinin. *Mol. Biol. Evol.* **21(6)**, 1024-1031
- Volkov, V.V. and Svergun, D.I. (2003). Uniqueness of *ab initio* shape determination in small angle scattering. *J. Appl. Crystallogr.* **36**, 860-864
- Wang, K., McClure, J., Tu, A. (1979) Titin: major myofibrillar components of striated muscle. *Proc. Natl. Acad. Sci. USA* **76(8)**, 3698-702
- Wang, J., Shaner, N., Mittal, B., Zhou, Q., Chen, J., Sanger, J.M., Sanger, J.W. (2005) Dynamics of Z-band based proteins in developing skeletal muscle cells. *Cell Motil. Cytoskeleton.* **61(1)**, 34-48
- Wang, K., Ramirez-Mitchell, R. (1983) A network of transverse and longitudinal intermediate filaments is associated with sarcomeres of adult vertebrate skeletal muscle. *J. Cell Biol.* **96(2)**, 562-70
- Witt, C.C., Burkart, C., Labeit, D., McNabb, M., Wu, Y., Granzier, H., Labeit, S. (2006) Nebulin regulates thin filament length, contractility, and Z-disk structure *in vivo*. *EMBO J.* **25(16)**, 3843-55
- Yang, N., Garton, F., North, K. (2009) alpha-actinin-3 and performance. *Med. Sport Sci.* **54**, 88-101.
- Yap, K.L., Ames, J.B., Swindells, M.B., Ikura, M. (1999) Diversity of conformational states and changes within the EF-hand protein superfamily. *Proteins* **37(3)**, 499-507

- Yläanne, J., Scheffzek, K., Young, P., Saraste, M. (2001) Crystal structure of the alpha-actinin rod reveals an extensive torsional twist. *Structure* **9(7)**, 597-604
- Young, P., Gautel, M. (2000) The interaction of titin and α -actinin is controlled by a phospholipid-regulated intramolecular pseudoligand mechanism. *EMBO J.* **19(23)**, 6331-6340
- Young, P., Ferguson, C., Banuelos, S., Gautel, M. (1998) Molecular structure of the sarcomeric Z-disc: two types of titin interactions lead to an asymmetrical sorting of α -actinin. *EMBO J.* **17(6)**, 1614–1624
- Zhou, Q., Chu, P.H., Huang, C., Cheng, C.F., Martone, M.E., Knoll, G., Shelton, G.D., Evans, S., Chen, J. (2001) Ablation of Cypher, a PDZ-LIM domain Z-line protein, causes a severe form of congenital myopathy,” *Journal of Cell Biology* **155(3)**, 605–612
- Zou P., Pinotsis N., Lange S., Song Y-H., Popov A., Mavridis I., Mayans O.M., Gautel M., Wilmanns M. (2006) Palindromic assembly of the giant muscle protein titin in the sarcomeric Z-disk. *Nature* **439(7073)**, 229-33

Note: literature references in the bibliography are formatted accordingly to the instructions to authors by the *Biochemical Journal*.

CURRICULUM VITAE

NAME	Viktor
SURNAME	Deineko
DATE OF BIRTH	September 17, 1985
CITIZENSHIP	Ukraine
LANGUAGES	English, Ukrainian, Russian
EDUCATION	
2010 – 2013	PhD studies. International PhD program of the European Molecular Biology Laboratory (EMBL-Hamburg/University of Vienna). Thesis project title: “Structural investigation of titin – α -actinin interactions in the Z-disk context”.
2006-2008	Master of Science degree in biochemistry. National Taras Shevchenko University of Kyiv, Faculty of Biology, Department of Biochemistry. Master Thesis project title: “Structural studies of transcription factor MiTF in complex with DNA”. Degree (<i>cum laude</i>) granted June, 27, 2008.
2002-2006	Bachelor degree in biochemistry and molecular biology. National Taras Shevchenko University of Kyiv, Faculty of Biology, Department of Biochemistry. Bachelor Thesis project title: “Bacterial adaptation to the presence of heavy metals in environment: case study of <i>P.aeruginosa</i> ”. Degree (<i>cum laude</i>) granted June, 30, 2004.

RESEARCH EXPERIENCE

- 06/2010–present European Molecular Biology Laboratory (Hamburg Unit).
Member of the Marie Curie initial training network
“MUZIC”.
- 09/2008–01/2010 Researcher at ETH-Zurich, Zurich, Switzerland.
- 03/2007– 04/2007 Research trainee at European Molecular Biology
and Laboratory (Hamburg Unit).
- 07/2006– 12/2006
- 09/2005–05/2006 Research internship at the Institute of Biocolloidal
Chemistry, NAS, Kyiv, Ukraine.
- 01/2005–07/2005 Research internship at the Institute of Cell Biology and
Genetic Engineering, NAS, Kyiv, Ukraine.
- 01/2004-01/2005 Research internship at the Institute of Molecular Biology &
Genetics, NAS, Kyiv, Ukraine.

PUBLICATIONS

1. Pogenberg, V., Ogmundsdottir, M.H.,
Bergsteinsdottir, K., Schepsky, A., Phung, B., **Deineko, V.**,
Milewski, M., Steingrimsson, E., Wilmanns, M. (2012)
Restricted leucine zipper dimerization and specificity of
DNA recognition of the melanocyte master regulator MITF.
Genes Dev. **26(23)**, 2647-58.

CONFERENCES

1. V. Deineko, L. Fiaschi, E. De Almeida Ribeiro, J.
Trinick, K. Djinovic-Carugo, M. Wilmanns. “Structural
investigation of titin—a-actinin interactions” The 41st
European Muscle Conference, 1–5 Sept 2012, Rhodes,
Greece.

WORKSHOPS

EMBL-Hamburg lectures on protein crystallography (EMBL-Hamburg, Germany).

MUZIC workshop dedicated to Microarray technologies and genotype profiling (University of Padova, Padova, Italy)

MUZIC workshop on “Protein Interaction Analysis” (King’s College London, London, UK)

MUZIC workshop on Electron Microscopy imaging (University of Leeds, Leeds, UK)

EMBL-EBI PreDoc course with focus on bioinformatics and genomics (European Bioinformatics Institute, Cambridge, UK)

Advanced confocal laser scanning microscopy and live cell imaging (University of Bonn, Bonn, Germany).

Jyvaskyla Summer School dedicated to Basic Fluorescence Microscopy (Jyvaskyla, Finland).

MUZIC workshop on Cloning, expression and purification of eukaryotic proteins and protein complexes (Karolinska Institutet, Stockholm, Sweden).